Université d'Ottawa · University of Ottawa

Université d'Ottawa • University of Ottawa

FACULTÉ DES ÉTUDES SUPÉRIEURES ET POSTDOCTORALES

FACULTY OF GRADUATE AND POSTDOCTORAL STUDIES

Ferawati GANI

AUTEUR DE LA THÈSE - AUTHOR OF THESIS

M. A. Sc. (Civil Engineering)

GRADE - DEGREE

Department of Civil Engineering

FACULTÉ, ÉCOLE, DÉPARTEMENT - FACULTY, SCHOOL, DEPARTMENT

TITRE DE LA THÈSE - TITLE OF THE THESIS

Parametric Excitation of Stay-Cables

H. Tanaka

DIRECTEUR DE LA THÈSE - THESIS SUPERVISOR

CO-DIRECTEUR DE LA THÈSE - THESIS CO-SUPERVISOR

EXAMINATEURS DE LA THÈSE - THESIS EXAMINERS

D. Lau

M. Mohareb

N. Naumoski

J.-M. De Koninck, Ph.D.

LE DOYEN DE LA FACULTÉ DES ÉTUDES SUPÉRIEURES ET POSTDOCTORALES

DEAN OF THE FACULTY OF GRADUATE AND POSTDOCTORAL STUDIES

PARAMETRIC EXCITATION OF STAY-CABLES

by

Ferawati Gani

A thesis

presented to the University of Ottawa in partial fulfillment of the requirements for

Master of Applied Science in Civil Engineering

Department of Civil Engineering

University of Ottawa

Ottawa, Canada

K1N 6N5

August 2004

The M.A.Sc. in Civil Engineering is a joint program

with Carleton University administered by the

Ottawa-Carleton Institute for Civil Engineering

Your file Votre référence
ISBN: 0-494-01476-8
Our file Notre référence
ISBN: 0-494-01476-8

THE UNIVERSITY OF OTTAWA-FACULTY OF GRADUATE STUDIES

CERTIFICATE OF EXAMINATION

Examining Board

_____ _____

_____ _____

Advisor

_____

The thesis by
Ferawati Gani
entitled
Parametric Excitation of Stay-cables
is accepted in partial fulfillment
of the requirements of the degree of
Master of Applied Science
in the
Department of Civil Engineering

Date: _____ _____

Chairperson of Examining Board

This thesis is dedicated to the loving memory of my mother.

Cette thèse est dédiée à la mémoire de ma mère.

ACKNOWLEDGEMENTS

I want to express my greatest appreciation to my supervisor, Professor Tanaka. He has given an enormous amount of guidance and support throughout the completion of this thesis. I am honoured to be able to work under his supervision.

I am also thankful to my family, especially my father, who has given me the opportunity to continue my study in Canada. I would also like to thank all of my friends, who have given me their encouragement during my study here.

ABSTRACT

The main objective of this thesis is to develop a finite-element-based cable model to study a self-excited phenomenon categorized as "the parametric excitation" of stay-cables, particularly for the cable-stayed bridges. Non-linear numerical methods were adopted and implemented in Matlab programming. When linearized, the cable model can be utilized to obtain the 3D natural frequencies and corresponding mode-shapes.

Using the methodically developed numerical approach, this study was able to realize the existence of parametric excitation of cables under certain conditions and parameters. As more insightful analyses performed, more interesting results were gained, such as the existence of bifurcation and chaotic vibration of cable systems.

The thesis found many possibilities of parametric excitation that stay-cables may encounter. Further study on the topic of parametric excitation of stay-cables is definitely important and there is also a need to extend the study by including the field measurement.

Key words: stay-cable, natural frequency, mode shape, sag-to-span ratio, inclined cable, non-linear analysis, modal interaction, parametric excitation, support excitation, internal resonance, external resonance, in-plane oscillation, out-of-plane oscillation, bifurcation, chaotic vibration

TABLE OF CONTENTS

LIST OF TABLES

LIST OF FIGURES

GLOSSARY

A	= cross-sectional area of cable (m^2)
a_0, a_1	= damping constants for the Rayleigh damping
am(t)	= function of support excitation amplitude (m)
amt	= amplitude of support excitation (m)
B	= strain-displacement transformation matrix
C	= damping matrix (N.s/m)
c_0	= speed of longitudinal wave propagation (m/s)
c_1	= speed of the transverse wave propagation (m/s)
c_d	= dimensionless damping constant
E	= Young's modulus (Pa)
F	= vector of nodal point forces (N)
H	= horizontal cable tension (N)
ΔH	= change in horizontal cable tension (N)
K	= global stiffness matrix (N/m)
$\tilde{K}$	= local stiffness matrix (N/m)
K_0	= initial stiffness of the system (N/m)
L	= length of element (m)
ΔL	= elongation of element (m)
Lc	= length of the cable (m)
lh	= span length of a suspended cable (m)
lv	= vertical height of a suspended cable (m)
M	= mass matrix (kg)
m	= mass per unit length of cable (kg/m)
p_x, p_y, p_z	= external forces in x, y and z axes (N)
$q, \dot{q}, \ddot{q}$	= dimensionless displacement, velocity and acceleration
R	= sag-to-span ratio
R_F	= local externally applied loads (N)
$\tilde{R}_F$	= global externally applied loads (N)
s_e	= coordinate measured along the cable length (m)
t	= time (s)
T	= transformation matrix

T_{el} = tension of cable element (N)

U(t) = excitation amplitude function (m)

u, v, w = displacement of cable in 3D orientation (m)

$U_1(t)$ = dimensionless excitation amplitude function

u_1, u_2, u_3 = displacements defined by the local coordinates (m)

u_x, u_y, u_z = displacements defined by the global coordinates (m)

w_c = weight per unit length of cable (N/m)

x_e, y_e = x and y components of s_e (m)

ξ = damping ratio (%)

Δ = cable sag (m)

ϕ = inclination angle of a suspended at time t

η = vertical deflection of cable (m)

φ = angle between axis x and 1-3 plane

μ = angle of inclination of pylon or deck due to am(t)

δ = logarithmic decrement of damping

γ = angle between axis1 and x-y plane

θ = inclination angle of a suspended cable

θ_{el} = inclination angle of cable element

θ_1 = angle of axis 1 and projection of element position at time t to plane 1-2

θ_2 = angle of plane 1-2 and element position at time t

ω = natural frequency of the cable (rad/s)

Ω = excitation frequency of the cable support (rad/s)

Abbreviation

DOF = degree-of-freedom

FE = finite element

IP = in-plane

MS = mid-span

OP = out-of-plane

PE = parametric excitation

QS = quarter-span

2D = two-dimensional

3D = three-dimensional

CHAPTER 1
INTRODUCTION

1.1 Introduction

Cable-stayed bridge has an appealing and elegant appearance. More advanced technology in constructing this type of structure has made it possible to reach longer span length, which used to be the domain of suspension bridges. As the span grows longer, so do the stay-cables. Longer span makes the structure more flexible and so are the stays. This flexibility makes cables-stayed bridges and stay-cables increasingly prone to vibration problems.

Cable vibration is divided into two major groups. The 1st group is the directly excited vibration. This type of cable vibration is caused mostly by the wind action and therefore is strongly related to aerodynamics of cables. The 2nd group is the indirectly induced vibration. The movement of cable supports at the bridge deck or pylons, due to wind or traffic, could cause this type of cable vibration.

Indirect cable vibration is becoming more prominent because of the increasing flexibility of bridge and stay-cables. This vibration problem is more related to the physical characteristics of the bridge as a whole. The increased span length and cable length cause one very obvious phenomenon: the proximity of the natural frequencies of the bridge and cables.

When the bridge is flexible, its deck or pylon could experience a rhythmic movement due to wind action and cable could oscillate due to this movement. If the frequency of this periodic movement is close to a half of, or equal to, one of the natural frequencies of the cable, parametric excitation can be triggered.

Parametric excitation is a type of self-excited vibration, which relates to the structural instabilities. There have been a number of studies dedicated to this subject. Through experimental studies or analytical formulation, further understanding of this phenomenon has been sought. However, even though these studies have developed better insight

into the problem, there are points neglected in most of these studies. Effects of sag, dynamic tension, axial extensibility, and most importantly the inclusion of out-of-plane (OP) oscillation during analyses were some of the influential points usually overlooked in analytical formulations. The influence of these factors in the analyses would bring better understanding on the phenomenon. For the numerical studies of this topic, there has not been a very successful research work that was able to capture the effects of non-linearity; such as the large amplitude OP oscillations. It is because these studies did not use any specifically tailored cable elements for parametric excitation analysis.

The present study tries to put together the above mentioned factors, which have been previously overlooked or partially neglected, in order to gain better insight into this phenomenon. A customized finite element (FE) cable modelling was developed. By discretizing cable system into the two-node 3D cable elements and applying non-linear numerical methods, various cases of parametric excitation were simulated, observed and analysed.

It should be noted that here are some restrictions applied to this study. The dynamic interaction of global-local structures is of great engineering interest. However, only the local cable system is modeled in the present study. Support excitation is simulated by using a simple assumption that the cable support at the pylon or deck is moving periodically and tension of cable changes due to this movement. The internal damping is taken into this modeling but no artificial damping is included.

The scope of the study is to validate the cases of primary parametric resonance and also to identify the cases where OP oscillation would occur. Some parametric analyses are performed in order to observe the dependency of parametric excitation on the parameters. Cases of instabilities with bifurcation and chaos were also sought.

Comparisons with the results of previous studies are emphasized in terms of qualitative agreement. In most cases of analysis, it was attempted to employ a practical set of physical parameters based on actual bridges but they were only partially available. However, the conclusions and findings from this study are more generally acceptable since the results are in good agreements with the past experiments and theories.

1.2 Outline of the study

The outline of the study is as follows:

- Chapter 2: Review of the theoretical treatment of cable dynamics with an emphasis on the theory of parametric excitation of suspended cables.

- Chapter 3: Mathematical formulations and the development of approaches on the non-linear cable element stiffness matrix, methods of solutions of the equations and concise explanation of the flow of program development in the present study.

- Chapter 4: Analysis and observation of results, that includes: the analysis of natural frequencies and IP and OP oscillations of stay-cables induced by the parametric excitations.

- Chapter 5: Some concluding remarks and suggested further studies are presented.

CHAPTER 2
REVIEW ON CABLE DYNAMICS

2.1 Importance of cable vibration

When a cable-stayed bridge has long spans, the stay-cables tend to be long, too. However, in the early days of cable-stayed bridges, the researchers did not pay too much attention to dynamics of cable itself. One of the earliest works that pointed out the importance of the dynamic aspects of stay-cables was Abdel-Ghaffar and Khalifa (1992).

Stay-cable vibration can take place in the plane of the cable itself (in-plane, IP, vibration), or its displacement can be out of the plane (out-of-plane, OP, vibration). Its amplitude maybe small or large, depending on the excitation. When the amplitude grows large, obviously there would be a serious concern about possible structural damages, though even a small amplitude vibration could eventually develop fatigue failures. Problems of stay-cable vibrations have been reported in many cable-stayed bridges throughout the world and many different causes of these vibrations have been reported. Rain-wind induced vibration covers the majority of them. Wake galloping, vortex shedding excitation and excitation due to vibration of deck and pylons are others. Many of wind-related excitations have been extensively studied for the last two decades and they have been better understood. A comprehensive discussion about these vibrations can be found in Tanaka (2003). However, the structural excitation through deck and/or pylon has not received the same extent of research interest.

2.2 Non-linearity of suspended cables

In this section, some basic definitions of non-linear cable dynamics are outlined. More directly related terms to the present study are introduced in the next sections and the importance of non-linear analysis would become more obvious.

2.2.1 Non-linear vs. linear analysis

The linear theory of cable dynamics has been well developed and accepted as a method of solution for various problems in cable vibration. The main attraction of this method is the separation of OP from IP oscillation.

In linear theory of cable dynamics, displacements are assumed to be small. Therefore, in the equations of motion, the relation between stresses and displacements are constructed based on the undeformed geometry of the system without considering the changes in geometrical position due to elastic displacements. When the displacements are large, there is a significant change in geometrical configuration of the system and linearized method cannot be used to analyse the behaviour of the system.

2.2.2 Non-linear cable dynamics

The general non-linear equations of motion of a suspended cable, which is assumed to be perfectly flexible and elastic in tension, were introduced in the previous studies by Yamaguchi and Ito (1981) and Yamaguchi et al. (1981) and was quoted in the present study from Yamaguchi (1997):

$$\frac{\partial^2 u}{\partial t^2}-\frac{\partial}{\partial s_e}\left\{\left(c_0^2\frac{1}{x'_e}+c_1^2x_e'^2\right)\frac{\partial u}{\partial s_e}+c_1^2x'_ey'_e\frac{\partial v}{\partial s_e}\right\}-c_1^2\frac{\partial}{\partial s_e}\left[\left(x'_e\frac{\partial u}{\partial s_e}+y'_e\frac{\partial v}{\partial s_e}\right)\frac{\partial u}{\partial s_e}\right]$$
$$+c_1^2\frac{\partial}{\partial s_e}\left[\frac{1}{2}\left\{\left(\frac{\partial u}{\partial s_e}\right)^2+\left(\frac{\partial v}{\partial s_e}\right)^2+\left(\frac{\partial w}{\partial s_e}\right)^2\right\}\left(x'_e+\frac{\partial u}{\partial s_e}\right)\right]=\frac{p_x\cos\Omega t}{m} \tag{2.1}$$

$$\frac{\partial^2 v}{\partial t^2}-\frac{\partial}{\partial s_e}\left\{\left(c_0^2\frac{1}{x'_e}+c_1^2x_e'^2\right)\frac{\partial v}{\partial s_e}+c_1^2x'_ey'_e\frac{\partial u}{\partial s_e}\right\}-c_1^2\frac{\partial}{\partial s_e}\left[\left(x'_e\frac{\partial u}{\partial s_e}+y'_e\frac{\partial v}{\partial s_e}\right)\frac{\partial v}{\partial s_e}\right]$$
$$+c_1^2\frac{\partial}{\partial s_e}\left[\frac{1}{2}\left\{\left(\frac{\partial u}{\partial s_e}\right)^2+\left(\frac{\partial v}{\partial s_e}\right)^2+\left(\frac{\partial w}{\partial s_e}\right)^2\right\}\left(y'_e+\frac{\partial v}{\partial s_e}\right)\right]=\frac{p_y\cos\Omega t}{m} \tag{2.2}$$

$$\frac{\partial^2 w}{\partial t^2} - \frac{\partial}{\partial s_e}\left(c_0^2 \frac{1}{x'_e}\frac{\partial w}{\partial s_e}\right) - c_1^2 \frac{\partial}{\partial s_e}\left[\left(x'_e \frac{\partial u}{\partial s_e} + y'_e \frac{\partial v}{\partial s_e}\right)\frac{\partial w}{\partial s_e}\right]$$
$$+ c_1^2 \frac{\partial}{\partial s_e}\left[\frac{1}{2}\left\{\left(\frac{\partial u}{\partial s_e}\right)^2 + \left(\frac{\partial v}{\partial s_e}\right)^2 + \left(\frac{\partial w}{\partial s_e}\right)^2\right\}\frac{\partial w}{\partial s_e}\right] = \frac{p_z \cos \Omega t}{m} \qquad (2.3)$$

where:

u and v = IP displacements, w = OP displacement, s_e = the coordinate measured along the cable length, $\partial s_e^2 = \partial x_e^2 + \partial y_e^2$, t=time, $c_0 = \sqrt{H/m}$ = the speed of the transverse wave propagation, H = the horizontal cable tension, m = cable mass per unit length, $c_1 = \sqrt{EA/m}$ = the speed of longitudinal wave propagation, E = the Young's modulus, A = the cross-sectional area, Ω = the circular frequency of the external force, and p_x, p_y and p_z = the external forces.

The equations (2.1), (2.2) and (2.3) are developed for the forced vibration of a suspended cable. From these three equations, the non-linearity of a suspended cable can be discussed further. The first two equations, (2.1) and (2.2), are for the IP vertical and horizontal motions. The third equation, (2.3) is for the OP motion. In these equations, there exist quadratic non-linearity terms and cubic non-linearity terms. The cubic terms exist due to the cable stretch or the axial extensibility. The quadratic terms are introduced because the suspended cable has sag and these terms are the terms that make difference for a cable from a taut string. From (2.1), (2.2) and (2.3), it can also be observed that there are coupled terms of IP and OP motions.

For small amplitude vibrations, non-linear terms can be neglected. The linear IP and OP vibrations can be thus separated, uncoupling the equations. However, this is not true in the non-linear case. For purely IP forcing, IP response can be obtained from (2.1) and (2.2). Since IP terms also exist in (2.3) as coefficients of OP motion, w, OP response occurs through bifurcation in a particular frequency range (Takahashi and Konishi, 1987a).

2.4 Parametric excitation

2.4.1 Theory of parametric excitation

Parametric excitation is a type of self-excited or autonomous vibration. The term "self-excited" means that there is a reason of exciting the system in itself and the system is excited further because of its own accord and increases its amplitude until non-linearity limits the growth of the amplitude (Nafyeh and Mook, 1979). This phenomenon could happen to any physical system and is closely related to the stability of the system about its equilibrium position. The nature of the self-excited vibration compared to forced vibration can be briefly stated as follows: "In a self-excited vibration, the alternating force that sustains the motion is created or controlled by the motion itself, when the motion stops, the alternating force disappears. In a forced vibration, the sustaining alternating force exists independent of the motion and persists when the vibratory motion is stopped, "(by Ehrich in Harris and Piersol, 2002).

It is then necessary to define the fundamental difference in mathematical treatment between external excitation and the parametric excitation. In external excitation, the excitation terms appear as in-homogeneities in the governing differential equations. In parametric excitation, on the other hand, the excitation terms appear as the coefficients in the governing differential equations; thus in mathematical terms, the differential equations will have time varying coefficients. The name of "parametric excitation" comes from this understanding, as the excitation terms, when they are time independent, appear as parameters in the governing equations. (Nafyeh and Mook, 1979)

Another distinctive difference between the external excitation and parametric excitation is its relation between a possibility of large response and the system's linear natural frequencies. For external excitation, even a small excitation will result in a large response when the excitation frequency is close to one of the natural frequencies. In the parametric excitation, however, a large response can happen even when the excitation frequency is away from the natural frequencies of the system. There are numerous characteristics of relationships between the excitation frequency and natural frequencies in the case of parametric excitation but the most common ones are the cases when the excitation frequency is approximately twice or equal to the first natural frequency of the system.

2.4.2 Parametric excitation of stay-cables

Kovacs et al. (1982) highlighted the possibility of parametric excitation of stay-cables for the first time. The primary cause of why this became an issue was the extended span of the cable-stayed bridges. The relationship between the natural frequencies of a bridge as the global structure and of the stay-cables as the local structures is unique, in which parametric excitation could be triggered when the global structure is lightly excited at certain frequencies.

The deck or pylon of a cable-stayed bridge could have a periodical movement due to the effect of wind or traffic. The characteristics of a cable-stayed bridge are such that the main contribution to the overall structural stiffness is from its pre-tensioned stay-cables that are connected to the deck and the pylon. When the deck and/or the pylon experiences a periodical movement, the stay-cables would also experience this motion as a form of support excitation. This is called the indirect vibration of cable-stays.

Stay-cables individually are stretched inclined suspended cables. The stretch is caused by the initial tension of the stay-cable. When the support of the suspended cable is harmonically moved, the tension of the cable is changed periodically, too. For each change of cable tension, the overall axial stiffness of the stay-cable also changes. Since the parametric excitation may result in a large amplitude cable response, OP vibration could occur through bifurcation and coupling between IP and OP modes cannot be ruled out.

In Figure 2.1, an illustration of the parametric excitation phenomena of a cable-stayed bridge is shown. This figure shows a simplified diagram of pylon or deck excitation, where Ω_{py} is the excitation frequency by the pylon, Ω_{dc} is the excitation frequency by the deck and ω_1 is the 1st natural frequency of the cable being excited. In this figure, Ω_{py} or Ω_{dc} is assumed to be 2 ω_1, for example.

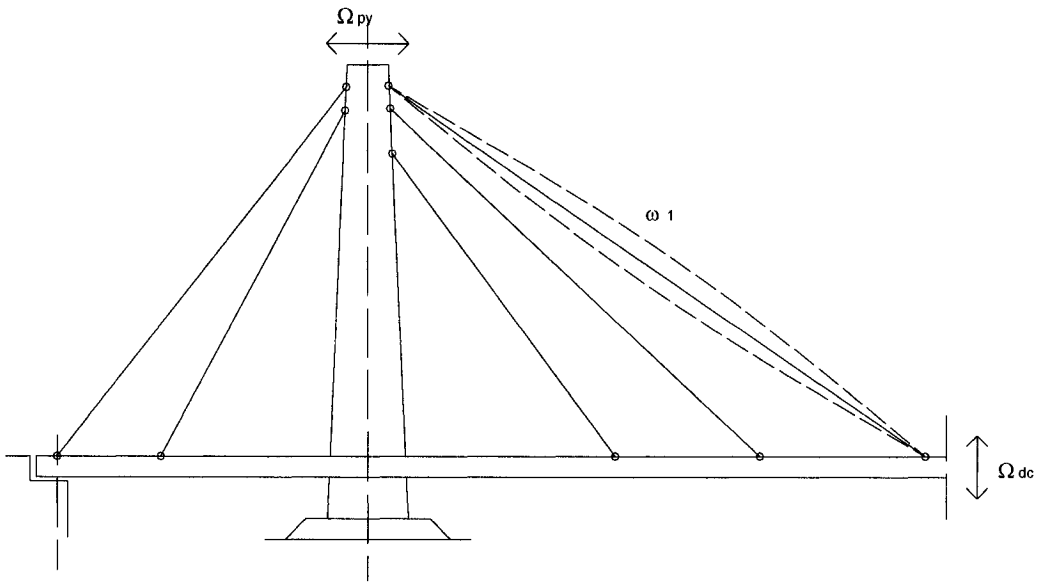

Figure 2.1: Schematic diagram of the parametric excitation of a cable-stayed bridge (redrawn from Kovacs, 1982)

2.4.3 Primary zones of instabilities

The combination of physical parameters, where the system becomes unstable under parametric excitation, can be conveniently expressed by the instability zones defined non-dimensionally using a linearized equation of motion. By defining these zones, the existence of parametric excitation can be easily predicted.

In linear theory, there are two distinct zones in terms of the excitation frequency, where the instability is triggered: when the excitation frequency is close to twice of the first natural frequency of the system and when the excitation frequency is about the same as the first natural frequency of the system. Theoretically, there are many more instability zones. However, it is very unlikely to have actual instability phenomena observed at zones other than the two principal ones

The location of instability zones can be derived from the stability condition of solutions to the Mathieu's differential equation. This approach was first discussed in detail by Bolotin (1964) for the parametric excitation in general.

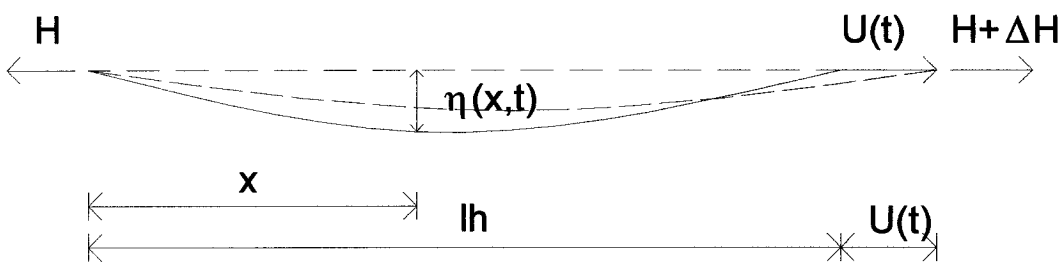

Figure 2.2: Schematic diagram of support excitation of a suspended cable

For a suspended cable, the equation of motion with the end motion along the cable axis without the damping term, is Figure 2.2:

$$m\frac{\partial^2\eta}{\partial t^2} - (H+\Delta H)\frac{\partial^2\eta}{\partial x^2} = 0 \qquad (2.4)$$

where:

m = the cable mass per unit length

H = the cable tension

ΔH = the change in tension

U(t) = the end displacement along the cable axis

$\eta(x,t) = \sum_r q_r(t)\cdot f_r(x)$ = the deflection function

where:

$q_r(t)$ = r-th mode response

$f_r(x)$ = r-th mode shape function, which is generally given by $\sin(r\pi x/lh)$

The equation of motion in (2.4) is typical for a suspended cable and should be expressed in the form of Mathieu's equation to obtain the instability zones. The formulae used in determining the instability zones for the present study were taken from Clement and Cremona (1996) in accordance with Bolotin (1964) and Tanaka (2000).

The fundamental equation of motion is as follows:

$$\ddot{q} + c_d\dot{q} + \omega_1^2(1 - 2a \cdot \cos\Omega t)q = 0 \tag{2.5}$$

where:

$q, \dot{q}, \ddot{q}$ = dimensionless displacement, velocity and acceleration

c_d = damping constant = $\omega_1 \delta/\pi$, where δ = logarithmic decrement

ω_1 = the first natural circular frequency

Ω = the excitation circular frequency

$$a = -\frac{EA}{2H}U_1 = \frac{\Delta H}{2H} \tag{2.6}$$

H = the horizontal cable tension

ΔH = the change in cable tension due to vibration

U_1 = dimensionless excitation amplitude function

"a" defined by (2.6) is an important parameter, which defines the magnitude of fluctuating cable tension. The first part of the definition (2.6) was by Clement and Cremona (1996) and Tanaka (2000) introduced the second part, this is equivalent to the first part but is more relevant to the present study.

Suppose that equation (2.5) has a periodic solution, which can be developed in Fourier series, the solution in trigonometric series is available. The solution for period $2T=4\pi/\Omega$ can be written in the form as follows:

$$q(t) = \sum_{k=1,3,5}^{\infty}\left(a_k \sin\frac{k\Omega t}{2} + b_k \cos\frac{k\Omega t}{2}\right) \tag{2.7}$$

Similarly, for period T, the solution is:

$$q(t) = b_0 + \sum_{k=2,4,6}^{\infty}\left(a_k \sin\frac{k\Omega t}{2} + b_k \cos\frac{k\Omega t}{2}\right) \tag{2.8}$$

By substituting (2.7) to (2.5), the boundaries for the first instability zone can be obtained. For the second instability zone, substitute (2.8) to (2.5). These equations can be solved for a non-trivial solution, if the determinant of the coefficient matrix is equal to zero. Actually, for the solution of Mathieu's equations, substitution is done by mode by mode,

for example, only the first term of the series in (2.7). Details of solving the equations are summarized in the Appendix A.

Instability zones without damping

1st instability zone:

$$\begin{vmatrix} 1 \pm a - \frac{\Omega^2}{4\omega_1^2} & -a \\ -a & 1 - \frac{9\Omega^2}{4\omega_1^2} \end{vmatrix} = 0 \tag{2.9}$$

By solving equation (2.9), boundaries of the 1st instability zone can be obtained as:

$$\frac{\Omega}{2\omega_1} = \frac{\sqrt{5 \pm \frac{9a}{2} + \frac{\sqrt{64 \pm 144a + 117a^2}}{2}}}{3} \tag{2.10}$$

2nd instability zone:

$$\begin{vmatrix} 1 - \frac{\Omega^2}{\omega_1^2} & -a \\ -a & 1 - \frac{4\Omega^2}{\omega_1^2} \end{vmatrix} = 0 \tag{2.11}$$

$$\begin{vmatrix} 1 & -a \\ -2a & 1 - \frac{\Omega^2}{2\omega_1^2} \end{vmatrix} = 0 \tag{2.12}$$

By solving equations (2.11) and (2.12), boundaries for the 2nd instability zone are:

$$\frac{\Omega}{2\omega_1} = \frac{1}{2}\sqrt{\frac{5 + \sqrt{9 + 16a^2}}{8}} \tag{2.13}$$

$$\frac{\Omega}{2\omega_1} = \frac{\sqrt{1 - 2a^2}}{2} \tag{2.14}$$

Instability zones with damping

1st instability zone with damping:

$$\begin{vmatrix} a+1-\dfrac{\Omega^2}{4\omega_1^2} & -c_d\dfrac{\Omega}{2\omega_1^2} \\ c_d\dfrac{\Omega}{2\omega_1^2} & -a+1-\dfrac{\Omega^2}{4\omega_1^2} \end{vmatrix} = 0 \tag{2.15}$$

By solving equation (2.15), the following equation can be obtained:

$$\frac{\Omega}{2\omega_1} = \sqrt{1-\frac{1}{2}\left(\frac{\delta}{\pi}\right)^2 \pm \sqrt{\left(\frac{\delta}{\pi}\right)^4 - \left(\frac{\delta}{\pi}\right)^2 + a^2}} \tag{2.16}$$

In most cases, c_1 is small, therefore, a simplified form of the above equation is:

$$\frac{\Omega}{2\omega_1} = \sqrt{1 \pm \sqrt{a^2 - \left(\frac{\delta}{\pi}\right)^2}} \tag{2.17}$$

2nd instability zone with damping:

$$\begin{vmatrix} 1 & 0 & -a \\ 0 & 1-\dfrac{\Omega^2}{\omega_1^2} & -c_d\dfrac{\Omega}{\omega_1^2} \\ -2a & c_d\dfrac{\Omega}{\omega_1^2} & 1-\dfrac{\Omega^2}{\omega_1^2} \end{vmatrix} = 0 \tag{2.18}$$

By solving equation (2.18), boundaries of damped 2nd instability zone is:

$$\frac{\Omega}{\omega_1} = \sqrt{1-a^2 \pm \sqrt{a^4 + \left(\frac{\delta}{\pi}\right)^2\left(a^2-1\right)}} \tag{2.19}$$

Using equations (2.10), (2.13) and (2.14), the undamped instability zones can be obtained and the damped instability zones can be obtained from (2.17) and (2.19).

From Figure 2.3, one can see that the 1st instability zone is much wider than the 2nd instability zone. Damping has the effect of increasing the limit of a. This means higher excitation amplitude is needed to trigger the parametric excitation. The areas of instabilities for the damped system are only slightly reduced compared to the undamped case.

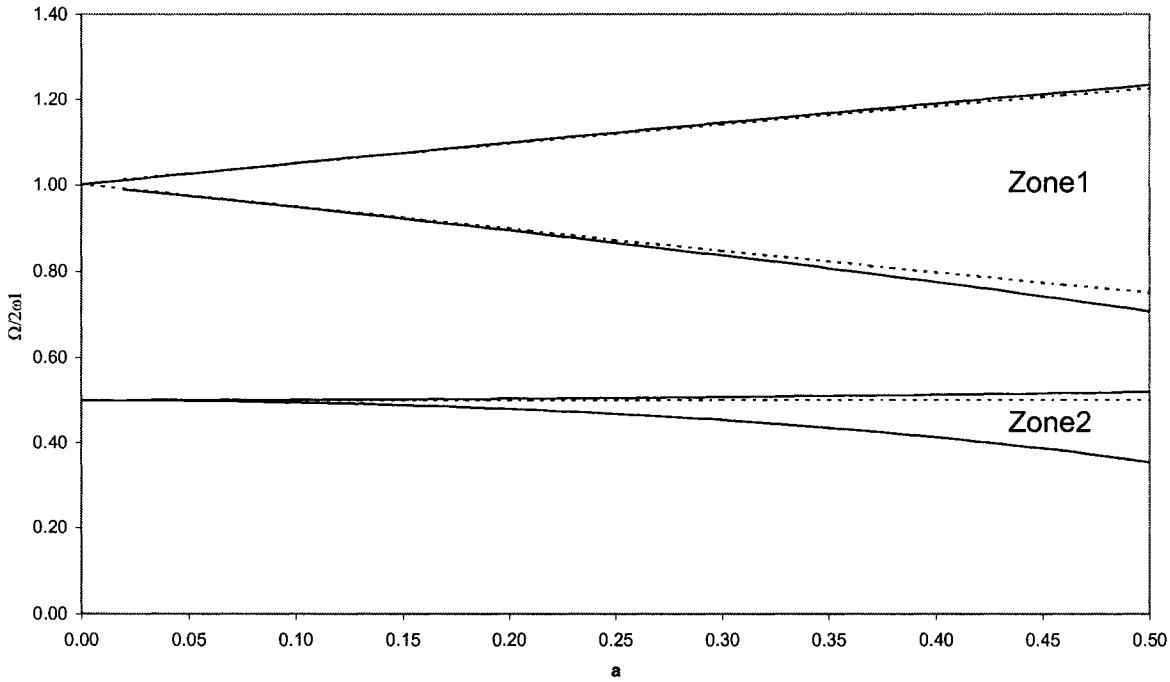

Figure 2.3: Primary zones of instabilities

Note that solid lines represent the undamped instability zones and the dotted lines represent the damped instability zones (ξ=0.6%)

2.4.4 Possibility of parametric excitation with actual cable-stayed bridges

After some definitions in the non-linear dynamics of suspended cables and theoretical aspects of parametric excitation are presented, it is now the time to define their relations to the behaviour of bridge stay-cables.

The earliest work that mentioned the possibility of parametric excitation of stay-cables was by Kovacs et al. (1982). To develop better understanding about parametric excitation on stay-cables, an example is presented to show how this phenomenon could possibly happen on bridge stay-cables considering their physical characteristics is presented.

Pinto da Costa et al. (1994) studied four different cable-stayed bridges and analysed possibilities of parametric excitation by looking at the observed natural frequencies of the bridge and the cables.

Table 2.1: Possibility of occurrence of parametric excitation on actual cable-stayed bridges (Pinto da Costa et al., 1994)

Bridge	Instability zones	Pair of stay-cables and global bridge mode
Arade	1st region	N/A
(256m; 16)	2nd region	29-9; 24-10; 22-12; 20-14
Guadiana	1st region	16-14,15; 15-16; 14-19,20; 11-22; 7-27,28
(324m; 16)	2nd region	16-4; 12-6; 6-13 to 17; 5-18; 4-21
Ikuchi	1st region	27,28-5; 23 to 26-6; 21-8
(490m; 28)	2nd region	28-2; 20 to 22-4,9; 19-5,13; 18-6,10;17-15
Normandie	1st region	(C): 22,23-6,7; 21,22-8; 17-9; 14-10 (F): 23-10
(856m; 23)	2nd region	(C): 17-3; 14-4; 9-6,7 (F): 18-4; 17-5; 16-6; 11-8

Note: N/A means not applicable

Table 2.1 is quoted from the original paper by Pinto da Costa et al. (1994). The available data are from four cable-stayed bridges of different dimensions: Arade (main span: 256 meter; a half of the pairs of stay-cables at mid-span: 16), Guadiana (324m; 16), Ikuchi (490m; 28), Normandie (856m; 23). Table 2.1 indicates the stay-cables that might be parametrically excited in the 1st region (1st instability zone) and the 2nd region (2nd instability zone), in each case by the number of the associated bridge oscillation mode. In each bridge, cable 1 is the shortest of the cables. For instance, in Ikuchi Bridge, the stay-cables 27 and 28 might be parametrically excited in the 1st region by the 5th bridge mode. The number of the natural frequencies available for this study in each case is not the same, and in the last case, the Normandie Bridge, both the data for the construction phase (C) and for the final structure (F) are presented.

From data in Table 2.1, it can be observed that for the Ikuchi Bridge and the Normandie Bridge, which have longer spans, the parametric excitation in the 1st instability zone could be triggered by the 5th to 10th modes, for example, of the bridge. For the Arade Bridge, the risk of parametric excitation in 1st region is non-existent and even for the 2nd region, the risk is quite remote, since it comes only from much higher modes.

Therefore, the cable-stayed bridges with longer span will raise the possibility of parametric excitation due to the global-local structures relationship in their natural frequencies. When a cable-stayed bridge has a long span, it is possible that the first few lowest natural frequencies of the bridge as the global structure are about twice of or equal to the first few natural frequencies of one of the longer stay-cables as the local structure.

Further to this, some characteristics of the stay-cables should be defined in more detail. If one looks at the stay-cables of the Ikuchi Bridge and the Normandie Bridge in Table 2.1, in which the parametric excitation could be triggered, it is obvious that they are at the long or the longest stay-cables of the bridge. For example, for the case of the Ikuchi Bridge, for the 1st instability zone, the 27th and 28th stay-cables, which are the longest stays, could have parametric excitations with the 5th frequency of the bridge. For the Normandie Bridge stays, for the 1st instability zone, the 23rd cable, which is also the longest stay, could have parametric excitation with the 10th frequency of the bridge.

The bridge stay-cables are axially loaded members. Due to its self-weight, a stay-cable has the sag that reduces the effective stiffness of the member. The longer cables tend to have greater deflection due to self-weight and this in turn, causes a larger sag-to-span ratio (R).

In order to make stay-cables more effective as the tension members, it would be desirable to decrease the sag of a long stay-cable by increasing its axial stiffness. "However, stated Gimsing (1997), it should be emphasized that the increased axial stiffness, that could be achieved by choosing a lower stress level, generally leads to a more expensive structure due to the quantity of cable steel. Only if the lower stress level makes it possible to use less expensive steels for the cables will it be economically

sound to increase the stiffness by enlarging the cross section." Hence, it is difficult to avoid having a considerably large sag for a long stay-cable.

The existence of sag in a stay-cable introduces a curved geometric configuration. The implication of this to a stay-cable, which has a constant cross section, is that the design stress is only reached at the upper supporting point whereas all other cable cross-sections have smaller stresses (Gimsing, 1997). This is the physical meaning of the quadratic non-linearity of a suspended cable.

The above descriptions are more based on the physical characteristics of the cable-stayed bridges and stay-cables. Then it would come to a question if parametric excitation ever happened in real bridges or if there are any field observations. Several studies found parametric excitation of stay-cables. Fujino and Kimura (1997) mentioned about the parametric excitation of stay-cables of the Hitshuisijima Bridge and the Yohkura Bridge. These parametric excitations were found during the forced excitation experiments of the bridge deck to measure the natural frequencies of the bridge. However, the cable response amplitude was not large and the excitation amplitude needed was quite high. Macdonald (2001) mentioned that the deck of the Second Severn Crossing Bridge was found to be excited at twice the cable frequency during the forced cable vibration tests, but there was no direct evidence of parametric excitation of the cables by the deck.

Based on the available field observations on the parametric excitation of stay-cables, it can be said that its existence has not yet been fully verified. Nevertheless, from the physical characteristics, the stay-cables of a long-span cable-stayed bridge are certainly prone to experience this phenomenon.

2.5 Previous works on parametric excitation of stay-cables

Before outlining previous works related to parametric excitation of stay-cables, a short summary of previous sections is presented.

The parametric excitation is a non-linear phenomenon that concerns with possibility of large amplitude response (IP and OP) and relates to instability of the system. This

phenomenon is possible for long stay-cables of long-span cable-stayed bridges. The physical characteristics of a long stay-cable are such that it has quadratic non-linearity. When a large amplitude response is possible and the quadratic non-linearity exists, a non-linear analysis is required to find the behaviour of the cable.

In relation to the non-linearity due to geometric configuration of stay cables, the free vibration of the suspended cables has been studied quite thoroughly. Hagedorn and Schäfer (1980) made one of the earliest contributions in the planar free vibration of cables with large sags. Later on Rega et al. (1984) also studied the planar free vibration of cables with large sags and highlighted the importance of geometrical and mechanical properties of the cables. Similar studies were conducted by Luongo et al. (1984) and Takahashi and Konishi (1987a). All of these studies emphasized on the effects of cubic and quadratic non-linearity of the suspended cables.

The parametric excitation of stay-cables has been studied in the last decade. Uhrig (1993) developed his analysis using the Mathieu's equation. Lilien and Pinto da Costa (1994) did similar things in defining the instability zones. They extended the study by including the taut cables subjected to small excitation along the cable chord and in this study. However, no specific mention was made about OP vibration. Cai and Chen (1994) developed an analysis combined with a numerical method of IP vibration based on the experiments of a stack supported with guy wires. They emphasized the importance of numerical analysis in parametric excitation. Clement and Cremona (1996) studied in detail about the instability zones of stay-cables with emphasis on the importance of cubic and quadratic non-linearity, particularly for one IP mode and using the Galerkin method. Pinto da Costa et al. (1996) developed analytical and numerical formulation for the taut stay-cables subjected to small support excitation. They did not include OP oscillations since there was no significant findings of OP vibration during their experiments for validating the analytical formulation. Sun et al. (2003) studied this phenomenon with their emphasis on the effectiveness of the tuned-mass damper to eliminate the vibration.

The existence of OP vibration is one of the most characteristic issues in cable vibrations and it should be considered during any experimental or numerical modeling or analytical formulations. Some of the studies have found the existence of OP oscillation associated

with IP vibrations. Perkins (1992) developed an analytical approach using one IP mode and one OP mode to describe possibilities of the development of OP out of IP oscillation due to mode interaction, in order to explain a significant OP oscillation observed during his experiment of a horizontally suspended cable with large R. Fujino et al. (1993) observed the OP oscillation during an experiment of cable-stayed beam and developed an analytical approach that agreed very well with the experimental results. Lorenzo and Macdonald (2003) found OP oscillation using FE approach and validated the result with experiment. The studies by Fujino et al. (1993) and Lorenzo and Macdonald (2003) are of great interest since they found OP oscillation during experimental observation of suspended inclined cable. Nevertheless, what they focused upon was the interaction between global and local structures. Also the characteristics of time history record of the cable response that they found from the study did not really represent clear characteristics of parametric excitation, in which the response amplitude should increase until the non-linearity of the system limits the amplitude growth of it. What they found were quite similar, that is more like the existence of two steady-state solutions with the indication of the existence of bifurcation.

From this quick review, it can be said that, with the exception of studies by Fujino et al. and Lorenzo and Macdonald (2003), most of the previous studies on the parametric excitation of inclined suspended cables did not find any development of significant OP oscillations. This is because of the following assumptions and observation: a) they assumed the cable as a taut cable with no geometric non-linearity; b) they did not observe OP oscillation during the experiment; c) they did not develop multi-mode analysis and considered only uncoupled OP and IP modes, even though cubic and quadratic non-linearities are included. The only study that was successful in finding OP oscillation was by Perkins (1992) that did consider multi-mode and geometric non-linearity. The study by Perkins (1992) was, by the way, of horizontally suspended cables.

2.6 Importance of the present study

It is now of a great interest to develop a research into the parametric excitation of inclined cables by including all the necessary non-linear terms. The first task is to include the coupling effect between the modes. It is important because by doing so, any possibility of IP and OP coupling can be included. The second task is to have the cubic and quadratic non-linearity that means the inclusion of axial extensibility and the effect of cable mass. By incorporating these terms, the effect of dynamic tension of the cable can be represented properly. The third is to develop an analysis that can adapt the term of parametric excitation. This means the change of the coefficient of the equations of motion for each time step. By considering these non-linear effects, an analysis that would result in better understanding of the mechanism of the parametric excitation of stay-cables would be developed.

2.7 Summary of Chapter 2

The fundamental theory of non-linear cable dynamics and the understanding on its parametric excitation have been reviewed. The mechanism of parametric excitation of stay-cables of cable-stayed bridges and a possibility of occurrence of this phenomenon have been briefly outlined. The related previous works on this topic have been reviewed. The importance of pursuing the present study was stated following them.

CHAPTER 3
MATHEMATICAL FORMULATION

3.1 Static configuration of a suspended cable

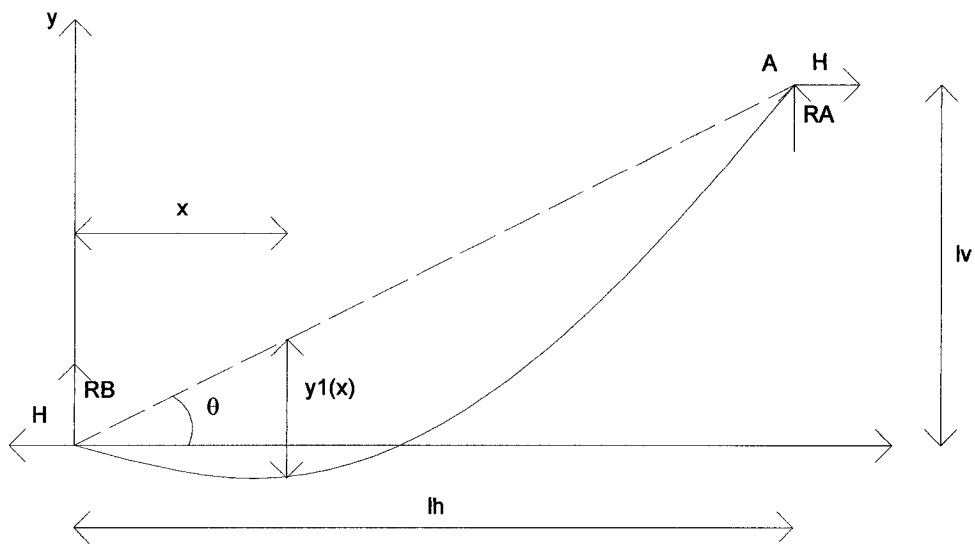

Figure 3.1: Catenary configuration of cable

The static equilibrium position of a perfectly flexible uniform cable, suspended between two supports A and B (Figure 3.1) in the gravitational field is given by the following expression (Tanaka, 2000):

$$y(x) = \frac{H}{w_c} \cdot \left\{ \cosh\left(\frac{w_c \cdot x}{H} + C_1 \right) - \cosh(C_1) \right\} \qquad (3.1)$$

where:

H = the horizontal cable tension

w_c = weight per unit length of the cable.

$$C_1 = \sinh^{-1}\left(\frac{\alpha \cdot \tan(\theta)}{\sinh(\alpha)}\right) - \alpha \tag{3.2}$$

$$\alpha = \frac{w_c \cdot lh}{2 \cdot H} \tag{3.3}$$

where lh = the span length

Since the slope of the cable is given by:

$$y'(x) = \sinh\left(\frac{w_c \cdot x}{H} + C_1\right) \tag{3.4}$$

the total length of the cable between two supports is given by:

$$Lc = \int_0^{lh} \sqrt{1 + (y')^2}\, dx = \frac{lh}{\alpha} \sinh(\alpha) \cdot \cosh(\alpha + C_1) \tag{3.5}$$

or, it can also be written as:

$$Lc = lh \cdot \sqrt{\left(\frac{\sinh(\alpha)}{\alpha}\right)^2 + \tan^2(\theta)} \tag{3.6}$$

where Lc = length of the cable.

The sag of a cable, Δ, is defined as maximum value of $y_1(x)$ in Figure 3.1. Since:

$$y_1(x) = x \cdot \tan(\theta) - y(x) = x \cdot \tan(\theta) - \frac{H}{w_c}\left\{\cosh\left(\frac{w_c}{H} \cdot x + C_1\right) - \cosh(C_1)\right\} \tag{3.7}$$

the sag-to-span ratio defined by $R = \Delta/lh$, is given by:

$$R = \frac{\Delta}{lh} = \frac{H}{w_c \cdot lh}\left\{\tan(\theta) \cdot \left[\sinh^{-1}(\tan(\theta) - C_1)\right] - \sec(\theta) + \cosh(C_1)\right\} \tag{3.8}$$

For the FE approach that is used in this study, it is useful to derive a secondary equation from equation (3.5) to calculate x coordinates and the corresponding y coordinates, where the same element length is to be obtained. This secondary equation provides convenience in cable analyses later on, for the transformation between the local and the global coordinate system and vice versa.

If Lc is taken as a small segment lx, then equation (3.5) takes the form of:

$$lx = \int_{x_1}^{x_2} \sqrt{1+(y')^2}\,dx = \frac{H}{w_c} \cdot \left[\sinh\left(\frac{w_c \cdot x_2}{H} + C_1 \right) - \sinh\left(\frac{w_c \cdot x_1}{H} + C_1 \right) \right] \qquad (3.9)$$

Therefore, if lx is set to be a certain length with one end of the element at a known point, the other end of the element can be calculated using:

$$x_2 = \frac{H}{w_c} \cdot \left(\sinh^{-1}\left(\frac{w_c}{H} \cdot lx + \sinh\left(\frac{w_c \cdot x_1}{H} + C_1 \right) \right) - C_1 \right) \qquad (3.10)$$

With the calculated x coordinates, y(x) can be obtained by using (3.1). The result is a set of x and y coordinates with each cable segment having the same length.

For example, if the cable system has 20 elements and the total cable length is Lc, for the first element, first node coordinates are x_1 and y_1, second node coordinates are x_2 and y_2, $dx=x_2-x_1$ and $dy=y_2-y_1$, and the same procedure applies for the other elements. Then, the length of each element is: $l_{el} = \sqrt{dx^2 + dy^2} = 1/20\,Lc$.

3.2 Concept of non-linear stiffness

Application of non-linear analysis in the present study rooted from the concept of axial extension of the cable in relation to the tension change caused by the motion of the cable supports. The static configuration of a stay-cable is decided by the initial cable tension. When a stay-cable is excited by its support motion, in each time step, the tension of the cable changes and this in turn changes the general stiffness term.

The present study focuses its attention only on the change of stiffness and the cable mass is kept unchanged. The internal damping is also assumed to remain the same. The tangent stiffness approach is adopted to account for the change in the stiffness matrix for each time step. This approach is an approximate method. A more precise method would be a secant stiffness approach, that is the stiffness based on the present displaced configuration to find the displacement for the next time step, which is not known yet. The tangent stiffness approach was developed based on displacements

from the previous time step, which are already known. By using a small enough time step, the error introduced by using this approach can be minimized.

3.3 Discretization

3.3.1 Total Lagrangian formulation

Stay-cables as structural members are always considered to be tension members. They are assumed to be perfectly flexible and hence the bending stress does not exist theoretically. In reality, of course, the cables are not perfectly flexible and the effect of cable bending stiffness may not be entirely negligible. Inclusion of the effective bending stiffness into the cable analysis has been discussed elsewhere, for example in Tanaka (2000).

In the present study, the non-linear analysis of cables are developed with an assumption that the displacement can be large but strains due to displacement are small. Typical formulation used is the Total Lagrangian (TL) scheme with the Second Piola-Kirchoff stresses and the Green-Lagrange strains. TL formulation for dynamic analysis with time implicit integration is given by:

$$M^{t+\Delta t}\ddot{U} + ({}_0^tK_L + {}_0^tK_{NL})U = {}^{t+\Delta t}R - {}_0^tF \qquad (3.11)$$

where:

M = time-independent mass matrix

${}_0^tK_L$ = linear strain incremental stiffness matrix

${}_0^tK_{NL}$ = non-linear strain (geometric or initial stress) incremental stiffness matrix

U = vector of increments in the nodal point displacements

${}^{t+\Delta t}\ddot{U}$ = vectors of nodal points accelerations at times $t+\Delta t$

${}^{t+\Delta t}R$ = vector of externally applied nodal point loads at time $t+\Delta t$

${}_0^tF$ = vector of nodal point forces equivalent to the element stresses at time t

${}_0^tK_L + {}_0^tK_{NL}$ = tangent stiffness matrix

Damping effect is assumed to be negligible or can be modeled in the non-linear constitutive relationships.

$$ {}_0^tK_L\hat{u} = \left(\int_{0_V} {}_0^tB_L^T \, {}_0C_0^tB_L d^0V \right)\hat{u} \tag{3.12} $$

$$ {}_0^tK_{NL}\hat{u} = \left(\int_{0_V} {}_0^tB_{NL}^T \, {}_0^tS_0^tB_{NL} d^0V \right)\hat{u} \tag{3.13} $$

$$ {}_0^tF = \int_{0_V} {}_0^tB_L^T \, {}_0^t\hat{S} d^0V \tag{3.14} $$

where:

${}_0^tB_L^T$ = linear strain-displacement transformation matrices

${}_0^tB_{NL}^T$ = non-linear strain-displacement transformation matrices

${}_0C$ = incremental stress-strain material property matrices (equal to E=modulus of elasticity)

${}_0^tS, {}_0^t\hat{S}$ = matrix and vector of second Piola-Kirchoff stresses (equal to cable tension)

3.3.2 Stress-strain principles

It is of considerable importance to describe further the principles of stress and strain measures taken in the present study; namely, the Green-Langrange strain tensor based all derivatives on initial coordinates of an element. It should also be noted that, this is a complete strain tensor, higher order terms are not neglected during derivation, (Bathe, 1996).

The Green-Langrange strain tensor and the second Piola-Kirchhoff stress tensor do not change when the material is subjected only to the rigid body translation or rotation, because such motion does not change the deformation gradient.

These two approaches are found to be suitable for analyses of the cable systems for the present study, because, even though the non-linear analyses are to be carried out, the cable material is assumed to remain linearly elastic and the cable system principally is allowed to have large displacements while the element strain remains small. Related to

this principle, for the parametric excitation that is to be studied further, Bolotin (1964) mentioned that an elastic system would have small changes in terms of lengths, volumes and sectional areas. Nevertheless, the important changes to be considered are the displacements experienced by the system.

3.3.3 Derivation of stiffness matrix of 2-node cable element

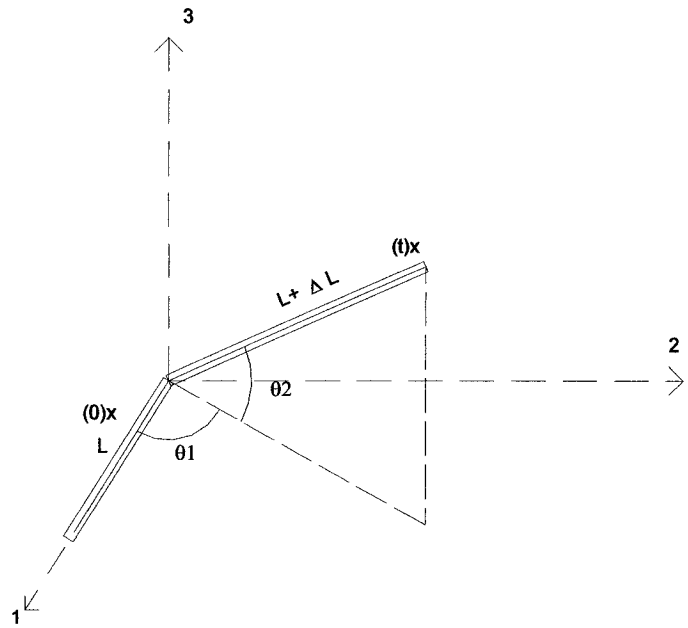

Figure 3.2: Two-node, 3D cable element at time=0 and time=t

A non-linear two-node cable element with 3D orientation will be developed based on the formulations by Bathe (1996):

$$ {}^{0}\hat{x}^{T} = \left[{}^{0}x_1^1 \quad {}^{0}x_2^1 \quad {}^{0}x_3^1 \quad {}^{0}x_1^2 \quad {}^{0}x_2^2 \quad {}^{0}x_3^2 \right] \tag{3.15} $$

$$ {}^{t}\hat{u}^{T} = \left[{}^{t}u_1^1 \quad {}^{t}u_2^1 \quad {}^{t}u_3^1 \quad {}^{t}u_1^2 \quad {}^{t}u_2^2 \quad {}^{t}u_3^2 \right] \tag{3.16} $$

$$ \hat{u}^{T} = \left[u_1^1 \quad u_2^1 \quad u_3^1 \quad u_1^2 \quad u_2^2 \quad u_3^2 \right] \tag{3.17} $$

$$ H_m = \left[h_1 I_3 \quad h_2 I_3 \right] \tag{3.18} $$

$$ h_1 = \frac{1}{2}(1-r) $$

$$ h_2 = \frac{1}{2}(1+r) \tag{3.19} $$

$$I_3 = \begin{bmatrix} 1 & 0 & 0 \\ 0 & 1 & 0 \\ 0 & 0 & 1 \end{bmatrix} \tag{3.20}$$

$${}^{t}_{0}B_L = \left({}^{0}J^{-1}\right)^2 \left({}^{0}\hat{x}^T H_r^T H_r + {}^{t}\hat{u}^T H_r^T H_r\right) \tag{3.21}$$

$${}^{t}_{0}B_{NL} = {}^{0}J^{-1} H_r \tag{3.22}$$

$${}^{0}J^{-1} = dr/d^{0}s \tag{3.23}$$

$$H_r = \frac{1}{2} \cdot \begin{bmatrix} -1 & 0 & 0 & 1 & 0 & 0 \\ 0 & -1 & 0 & 0 & 1 & 0 \\ 0 & 0 & -1 & 0 & 0 & 1 \end{bmatrix} \tag{3.24}$$

where:

${}^{0}\hat{x}^T$ = coordinate of the cable element at initial condition, at (3.15) on the right side: the subscripts indicate axis and superscripts indicates number of nodes of the element, on the left side: the superscripts indicate initial condition

${}^{t}\hat{u}^T$ = displacement at time t

H_m = volume-displacement interpolation matrix

h = interpolation function

r = relation between actual global coordinates and a natural coordinate system ($-1 \le r \le 1$)

H_r = derivatives of H_m with respect to r

${}^{0}J$ = Jacobian matrix at initial condition, for 2-node cable element, the value is ${}^{0}L/2$

By substituting equations (3.15), (3.16), (3.17) and (3.18) into (3.21), see Figure 3.2, the following equation can be obtained:

$${}^{t}_{0}B_L = \frac{\left({}^{0}L + \Delta L\right)}{{}^{0}L^2} \times \left[-C_1 \cdot C_2 \quad -S_1 \cdot C_2 \quad -S_2 \quad C_1 \cdot C_2 \quad S_1 \cdot C_2 \quad S_2\right] \tag{3.25}$$

where:

θ_1 = angle between axis 1 and projection of element's position at time t to plane 1-2

θ_2 = angle between plane 1-2 and element's position at time t

${}^0L={}^0x_1^2-{}^0x_1^1$

ΔL = element's elongation at time t

$C_1 = \cos(\theta_1)$

$S_1 = \sin(\theta_1)$

$C_2 = \cos(\theta_2)$

$S_2 = \sin(\theta_2)$

By substituting (3.22) and (3.23) into (3.24):

$$ {}^t_0B_{NL} = \frac{1}{{}^0L}\begin{bmatrix} -1 & 0 & 0 & 1 & 0 & 0 \\ 0 & -1 & 0 & 0 & 1 & 0 \\ 0 & 0 & -1 & 0 & 0 & 1 \end{bmatrix} \tag{3.26} $$

By substituting (3.25) into (3.12) and integrate it, the linear part of the stiffness matrix is:

$$ {}^t_0K_L = \frac{({}^0L+\Delta L)^2}{({}^0L)^3}\cdot EA\cdot\begin{bmatrix} (C_1\cdot C_2)^2 & S_1\cdot C_1\cdot(C_2)^2 & C_1\cdot S_2\cdot C_2 & -(C_1\cdot C_2)^2 & -S_1\cdot C_1\cdot(C_2)^2 & -C_1\cdot S_2\cdot C_2 \\ S_1\cdot C_1\cdot(C_2)^2 & (S_1\cdot C_2)^2 & S_1\cdot S_2\cdot C_2 & -S_1\cdot C_1\cdot(C_2)^2 & -(S_1\cdot C_2)^2 & -S_1\cdot S_2\cdot C_2 \\ C_1\cdot S_2\cdot C_2 & S_1\cdot S_2\cdot C_2 & (S_2)^2 & -C_1\cdot S_2\cdot C_2 & -S_1\cdot S_2\cdot C_2 & -(S_2)^2 \\ -(C_1\cdot C_2)^2 & -S_1\cdot C_1\cdot(C_2)^2 & -C_1\cdot S_2\cdot C_2 & (C_1\cdot C_2)^2 & S_1\cdot C_1\cdot(C_2)^2 & C_1\cdot S_2\cdot C_2 \\ -S_1\cdot C_1\cdot(C_2)^2 & -(S_1\cdot C_2)^2 & -S_1\cdot S_2\cdot C_2 & S_1\cdot C_1\cdot(C_2)^2 & (S_1\cdot C_2)^2 & S_1\cdot S_2\cdot C_2 \\ -C_1\cdot S_2\cdot C_2 & -S_1\cdot S_2\cdot C_2 & -(S_2)^2 & C_1\cdot S_2\cdot C_2 & S_1\cdot S_2\cdot C_2 & (S_2)^2 \end{bmatrix} $$

(3.27)

By substituting (3.26) into (3.13) and integrate it, the non-linear part of the stiffness matrix is obtained:

$$ {}_0^tK_{NL} = \frac{{}^tT_{el}}{\left({}^0L + \Delta L\right)} \begin{bmatrix} 1 & 0 & 0 & -1 & 0 & 0 \\ 0 & 1 & 0 & 0 & -1 & 0 \\ 0 & 0 & 1 & 0 & 0 & -1 \\ -1 & 0 & 0 & 1 & 0 & 0 \\ 0 & -1 & 0 & 0 & 1 & 0 \\ 0 & 0 & -1 & 0 & 0 & 1 \end{bmatrix} \tag{3.28} $$

By substituting (3.25) to (3.14) and integrate it:

$$ {}_0^tF = {}^tT_{el} \cdot \begin{bmatrix} -C_1 \cdot C_2 \\ -S_1 \cdot C_2 \\ -S_2 \\ C_1 \cdot C_2 \\ S_1 \cdot C_2 \\ S_2 \end{bmatrix} \tag{3.29} $$

where T_{el} = tension of a cable element.

Because of the geometric configuration, which is catenary, the distribution of tension along the cable is not uniform. This characteristic can easily be represented in FE method. Each element has slightly different angle of inclination, which is defined from the cable's geometric configuration. Therefore, for each element, $T_{el} = H \cdot \sec\theta_{el}$, where θ_{el}=inclination angle of an element.

3.3.4 Transformation matrix of a cable element from local to global axes

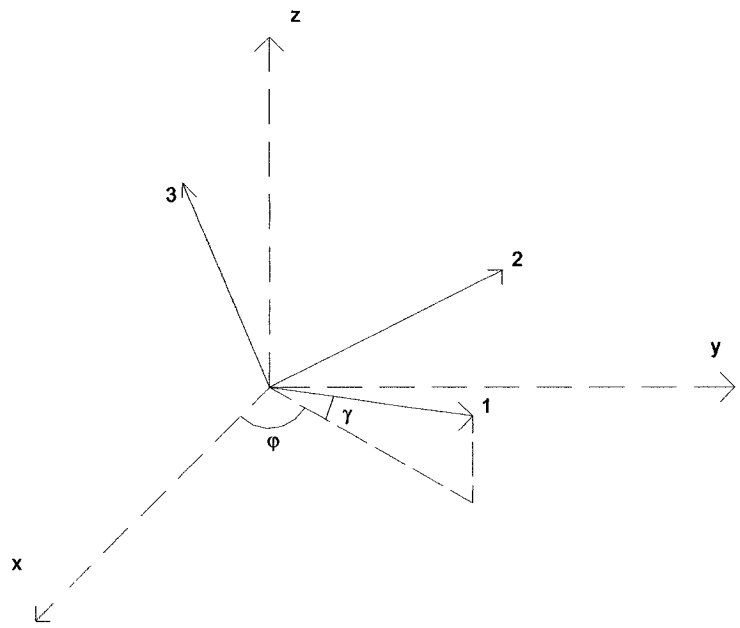

Figure 3.3: Transformation from local to global axes

The stiffness matrix derived in the previous section is given in the 3D local coordinates. For the convenience of the analysis and computation, it is important to transform these local coordinates to the global coordinates. Here, the local coordinate axes are given by 1,2 and 3, whereas global coordinate axes are called x, y and z.

The relationship between the local and global coordinates is:

$$\begin{bmatrix} u_1 \\ u_2 \\ u_3 \end{bmatrix} = \begin{bmatrix} \cos(\varphi)\cdot\cos(\gamma) & \sin(\varphi)\cdot\cos(\gamma) & \sin(\gamma) \\ -\sin(\varphi) & \cos(\varphi) & 0 \\ -\cos(\varphi)\cdot\sin(\gamma) & -\sin(\varphi)\cdot\sin(\gamma) & \cos(\gamma) \end{bmatrix} \cdot \begin{bmatrix} u_x \\ u_y \\ u_z \end{bmatrix} \qquad (3.30)$$

where:

u_1, u_2, u_3 = displacements defined by the local coordinates

u_x, u_y, u_z = displacements defined by the global coordinates

γ = angle between axis 1 and x-y plane

φ = angle between axis x and 1-3 plane

If the cable configuration is defined in 2D orientation, γ is the inclination angle of the cable element.

Therefore, transformation matrix is:

$$T = \begin{bmatrix} \cos(\varphi)\cdot\cos(\gamma) & \sin(\varphi)\cdot\cos(\gamma) & \sin(\gamma) & 0 & 0 & 0 \\ -\sin(\varphi) & \cos(\varphi) & 0 & 0 & 0 & 0 \\ -\cos(\varphi)\cdot\sin(\gamma) & -\sin(\varphi)\cdot\sin(\gamma) & \cos(\gamma) & 0 & 0 & 0 \\ 0 & 0 & 0 & \cos(\varphi)\cdot\cos(\gamma) & \sin(\varphi)\cdot\cos(\gamma) & \sin(\gamma) \\ 0 & 0 & 0 & -\sin(\varphi) & \cos(\varphi) & 0 \\ 0 & 0 & 0 & -\cos(\varphi)\cdot\sin(\gamma) & -\sin(\varphi)\cdot\sin(\gamma) & \cos(\gamma) \end{bmatrix} \tag{3.31}$$

Transformation from the local to global matrix is:

$$K = T^T \cdot \tilde{K} \cdot T \tag{3.32}$$

$$R_F = T^T \tilde{R}_F \tag{3.33}$$

where:

T = transformation matrix

K = global stiffness matrix

$\tilde{K}$ = local stiffness matrix

R_F = global externally applied point loads

$\tilde{R}_F$ = local externally applied loads

In this study, φ is taken as 0.25π rad. or 45°. The reason of this choice is mainly because of the speed of convergence in calculation. In fact, any angle φ can be taken, for example, φ=0. However, this will result in a much longer iteration period; twice as much.

For the case of φ = 0°, in fact, there is a very clear explanation. At this angle, the global x-axis would be along cable element's normal axis, which means that any displacement along this axis is a pure axial extension, while any displacement recorded at global y-axis represents the pure out-of-plane oscillations. As stated before, the cable would only have small dynamic strains. Therefore, the axial extension is very small. As a result, it

takes longer time to achieve the convergence for each time step. When φ=0.25πrad., the iteration process will be faster since the distribution of displacements are more even.

After the stiffness matrices of each element are defined based on the formulations described in sections 3.3.1 to 3.3.4, they are ready to be assembled. This method of forming the total stiffness matrix is called the direct stiffness method. By using this method, the stiffness of the system is represented by a summation of the stiffness of its elements.

3.3.5 Mass and Damping

3.3.5.1 Mass matrix

The lumped mass method is applied for this study. Given the mass per unit length, the element's length and the cross sectional area, the global mass matrix will be assembled according to the number of elements. Since the mass matrix is a diagonal matrix, the transformation from local to global is not needed. The use of the lumped mass assumption has the advantage of forming a diagonal matrix, which would result in faster and simpler analysis.

3.3.5.2 Damping matrix

It is well known that the cables have very low internal damping. Abdel-Ghaffar and Khalifa (1992) reported that the damping ratio of the stay-cables is between 0.05%-4%, though the upper limit is rather high for most stay-cables. Virlogeux (1998) reported that it is in the range of 0.01%-0.2%. Also, in Humar, 2002, it is mentioned that, since damping characteristics cannot, in any case, be defined with certainty, it is not unreasonable to assume that they also remain constant with time.

Based on these assumptions, though the present study is basically on the non-linear principles, the internal damping is assumed to remain constant. The Rayleigh damping is adopted here. After forming the mass matrix of cable system, the stiffness matrix with zero displacements is formed.

From Chopra (1995):

$$C = a_0 \cdot M + a_1 \cdot K_0 \qquad (3.34)$$

The damping ratio for the n-th mode of such system is:

$$\xi_n = \frac{a_0}{2} \cdot \frac{1}{\omega_n} + \frac{a_1}{2} \cdot \omega_n \tag{3.35}$$

The coefficients a_0 and a_1 can be determined from the specified damping ratios ξ_i and ξ_j for the i^{th} and j^{th} modes, respectively. Expressing equation (3.35) for these two modes in a matrix form leads to:

$$\frac{1}{2} \cdot \begin{bmatrix} 1/\omega_i & \omega_i \\ 1/\omega_j & \omega_j \end{bmatrix} \cdot \begin{Bmatrix} a_0 \\ a_1 \end{Bmatrix} = \begin{Bmatrix} \xi_i \\ \xi_j \end{Bmatrix} \tag{3.36}$$

These two algebraic equations can be solved to determine the coefficients a_0 and a_1. If both modes are assumed to have the same damping ratio ξ, which is a reasonable assumption, based on experimental data, then:

$$a_0 = \xi \cdot \frac{2 \cdot \omega_i \omega_j}{\omega_i + \omega_j} \tag{3.37}$$

$$a_1 = \xi \cdot \frac{2}{\omega_i + \omega_j} \tag{3.38}$$

where:

C = damping matrix of the system

M = mass matrix of the system

K_0 = initial stiffness of the system

ω_i, ω_j = natural frequencies of the system

a_0, a_1 = damping constants

ξ = damping ratio

3.4 Methods of solution

After defining the tangent stiffness matrix and knowing other necessary terms like M, R, F, and initial conditions, equation (3.11) can be solved using numerical step-by-step procedure or the direct integration method. The method that is used here is the Newmark method and is added with the iterative procedure of modified Newton-Raphson method to minimize error due to the use of tangent stiffness.

The principle of this non-linear method is the same as a linear solution method, where equations of motion should be in equilibrium. The difference is, instead of satisfying

equilibrium for each time step, this non-linear method will try to satisfy equilibrium for each incremental time step. Table 3.1 summarizes the Newmark's average acceleration method and Table 3.2 summarizes the Newton-Raphson iterative procedure (Chopra, 1995).

Table 3.1: Average acceleration method for Non-linear systems

1.0 Initial calculations

1.1 Solve: $M^0\ddot{U} = R - C^0\dot{U} - K^0U$ to obtain $^0\ddot{U}$

1.2 Select time step = dt

1.3 a=4/dt*M; b=2M

2.0 Calculations for each time step i

2.1 $\Delta\hat{R}_i = \Delta R + a\dot{u}_i + b\ddot{u}_i$

2.2 Determine tangent stiffness matrix K_i

2.3 $\hat{K}_i = K_i + \frac{2}{dt}C + \frac{4}{dt^2}M$

2.4 Solve for Δu_i from $\hat{K}_i$ and $\Delta\hat{R}_i$ using the iterative procedure of Table 3.2

2.5 $\Delta\dot{u}_i = \frac{2}{dt}\Delta u_i - 2\dot{u}_i$

2.6 $\Delta\ddot{u}_i = \frac{4}{dt^2}\Delta u_i - \frac{4}{dt}\dot{u}_i - 2\ddot{u}_i$

2.7 $u_{i+1} = u_i + \Delta u_i;\quad \dot{u}_{i+1} = \dot{u}_i + \Delta\dot{u}_i;\quad \ddot{u}_{i+1} = \ddot{u}_i + \Delta\ddot{u}_i$

3.0 Repetition for the next time step: replace *i* by *i+1* and implement steps 2.1 until 2.6 for the next time step.

where:

Δ = incremental value, (e.g. ΔR is incremental value of R)

$u, \dot{u}, \ddot{u}$ = displacement, velocity and acceleration of the system

The use of the average acceleration method has a draw back. It provides no numerical damping, as stated by Chopra (1995). This is a disadvantage, because it is important to sort out the response contribution from higher modes. The higher modes and their

frequencies, which have been calculated from an idealization of the structure, are usually not accurate relative to the actual properties of the structure. A damping matrix that is consistent with increased damping ratio for modes higher than the desired important modes (e.g. the first 10 modes) should be formed to obtain only the desirable range of results.

Table 3.2: Modified Newton-Raphson iteration method

1.0 Initialize data

$$u_{i+1}^{(0)} = u_i \quad f_S^{(0)} = (f_S)_i \quad \Delta R^{(1)} = \Delta \hat{p}_i \quad \hat{K}_T = \hat{K}_i$$

2.0 Calculations for each iteration, j=1,2,3...

2.1 Solve $\hat{K}_T \Delta u^{(j)} = \Delta R^{(j)}$ to obtain $\Delta u^{(j)}$

2.2 $u_{i+1}^{(j)} = u_{i+1}^{(j-1)} + \Delta u^{(j)}$

2.3 $\Delta f^{(j)} = f_S^{(j)} - f_S^{(j-1)} + (\hat{K}_T - K_i)\Delta u^{(j)}$

2.4 $\Delta R^{(j+1)} = \Delta R^{(j)} - \Delta f^{(j)}$

3.0 Repetition for the next iteration: replace *j* by *j+1* and repeat calculation steps from 2.1 to 2.4

The iterative process is terminated after m iterations when the incremental displacement vector $\Delta u^{(m)}$ becomes small enough, say smaller than ε.

Convergence criterion is:

$$\frac{\left[\Delta R^{(j)}\right]^T \Delta u^{(j)}}{\left[\Delta \hat{R}_i\right]^T \Delta u} < \varepsilon \qquad (3.37)$$

After implementing these two methods, u_{i+1} is found. The next step is finding the tangent stiffness for this time step, using the equation of motion, for calculating displacement of the next time step.

3.5 Support excitation

When the pylon or deck is periodically moved, which may be caused by different reasons, (e.g. traffic or wind), cable could experience vibration due to this indirect excitation. This is likely to happen, if it ever happens, to long-span cable-stayed bridges, as it was discussed in Chapter 2.

Lilien and Pinto da Costa (1994) applied a periodic end movement along the cable chord, not specifically as either deck or pylon movement. Their study was more focused on the cables with very small R and therefore the cable's angle of inclination was not considered important. When R is no longer small, the angle of inclination starts taking an important role. The support excitation not only causes changes in tension, it also introduces change in the angle of inclination in small magnitude.

The present study tries to simulate this type of excitation by considering a function of tension changes as the effect of support movement. There is no inclusion of global-local structure interaction in the present study. This interaction is of course important but its importance falls beyond the scope of the present study.

Support excitation is simulated as a pure IP movement. During the support excitation, the deck or pylon may sway and, of course, this will cause the OP oscillation for cables. However, this is not the case for parametric excitation. For studying the possibility of OP oscillation in the case of the parametric excitation, it is important that only the IP excitation and initial movement are considered.

3.5.1 Excitation by the pylon

When a pylon of the bridge vibrates, the tension of the cables attached to the pylon changes. This change will be formulated based on the assumption that pylon itself does not bend due to this excitation and the pylon has only a small periodic rotation around its base.

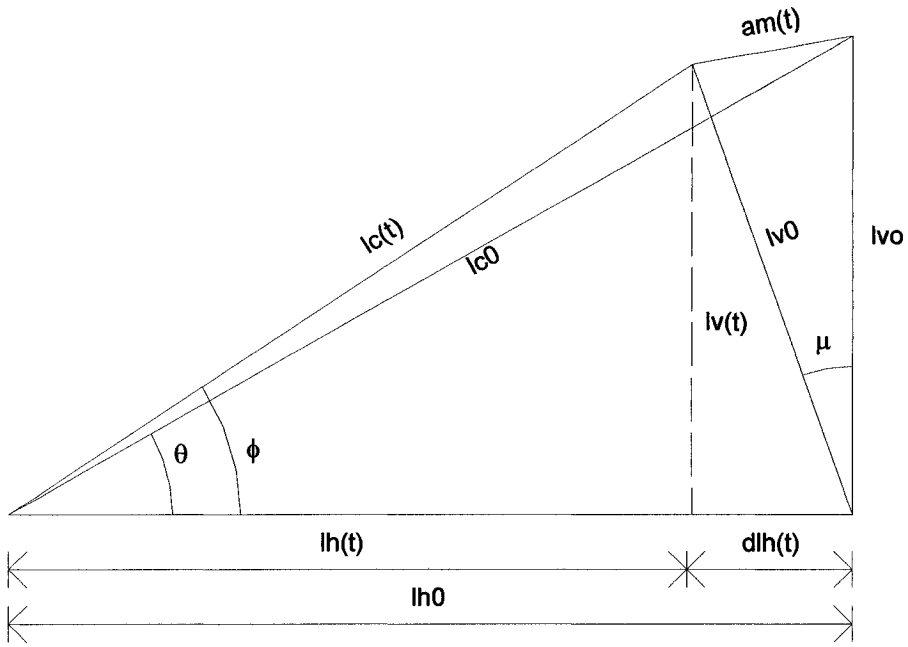

Figure 3.4: Schematic diagram to show the excitation of pylon

$$\mu = 2 \cdot \sin^{-1}\left(\frac{0.5 \cdot am}{lv_0}\right) \tag{3.38}$$

$$lv = lv_0 \cdot \cos(\mu) \tag{3.39}$$

$$dlh = lv_0 \cdot \sin(\mu) \tag{3.40}$$

$$lh = lh_0 - dlh \tag{3.41}$$

$$\phi = \tan^{-1}\left(lv/lh\right) \tag{3.42}$$

where:

am(t) = function of pylon excitation amplitude

θ = initial inclination angle of the cable system

ϕ = inclination angle of the cable system at time t

μ = angle of inclination of pylon due to am(t)

lh0 = initial span length

lv0 = initial vertical height

lc0 = initial chord length

lh(t) = function of span length due to am(t)

lv(t) = function of vertical height due to am(t)

lc(t) = function of chord length due to am(t)

3.5.2 Excitation by the deck

When the bridge deck vibrates, the tension of cables anchored to the deck changes. This change will be formulated based on the assumption that the deck itself does not deflect due to this excitation and the deck has small periodic rotation around the pylon base.

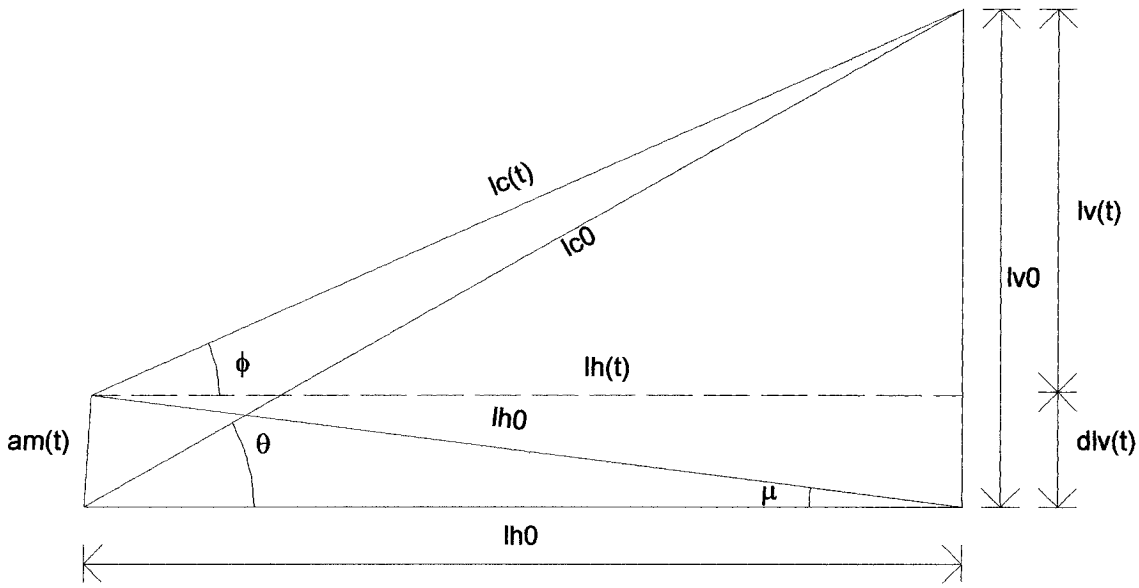

Figure 3.5: Diagram of excitation of deck

$$\mu = 2 \cdot \sin^{-1}\left(\frac{0.5 \cdot am}{lh_0}\right) \tag{3.43}$$

$$lh = lh_0 \cdot \cos(\mu) \tag{3.44}$$

$$dlv = lh_0 \cdot \sin(\mu) \tag{3.45}$$

$$lv = lv_0 - dlv \tag{3.46}$$

$$\phi = \tan^{-1}\left(lv/lh\right) \tag{3.47}$$

where:

am(t) = function of deck excitation amplitude

μ = angle of inclination of deck due to am(t)

Other terms are the same as in section 3.5.1.

3.6 Development of solution

Previous sections have discussed mathematical backgrounds that are needed for formulating the solution procedure of the parametric excitation of suspended cables. Using Matlab, a specifically tailored non-linear FE modeling of cable systems, according to sections 3.2.3 to 3.2.5, was developed in forms of mathematical functions. Numerical solution procedures as defined in section 3.2.6 were also formulated in functions.

The FE modeling can be adjusted to any number of elements. However, for the convenience of analyses, the number of elements were made to be dividable by four. By having this number of elements, the response for the 1st quarter-span of the cable (1st QS), mid-span of the cable (MS) and 2nd quarter-span of the cable (2nd QS) can be obtained. These three locations along the cable span are the most commonly observed locations for a cable dynamic analysis. From these locations, the general behaviour of the cable can be observed. This approach is also for the convenience of plotting the time history and graphics.

Elements generation are developed automatically and so are the numbering of nodes and DOFs numbering once the number of elements for the cable system is known. For example, for a given set of cable data and a number of elements (n), the cable system would have the elements numbered automatically as 1st, 2nd, 3rd ...n-th element. This is the convenience obtained of analysing a continuous system. For the system that is not continuous, (e.g. truss frame), a specific numbering system, which can be much more complicated, must be developed.

Functions of support excitation are developed as an extension of cable's initial conditions. Using the relation between the deck or pylon excitation amplitude given in section 3.5, the new tension and element's configuration can be obtained for each time step.

To illustrate the assembled cable elements, Figure 3.6 shows the discretized suspended cable. The hatched area is the cable plane. The thick curved line represents the suspended cable in 3D orientation, with θ=cable inclination angle, φ=angle between cable plane and x-axis, n=number of elements and H=the horizontal cable tension.

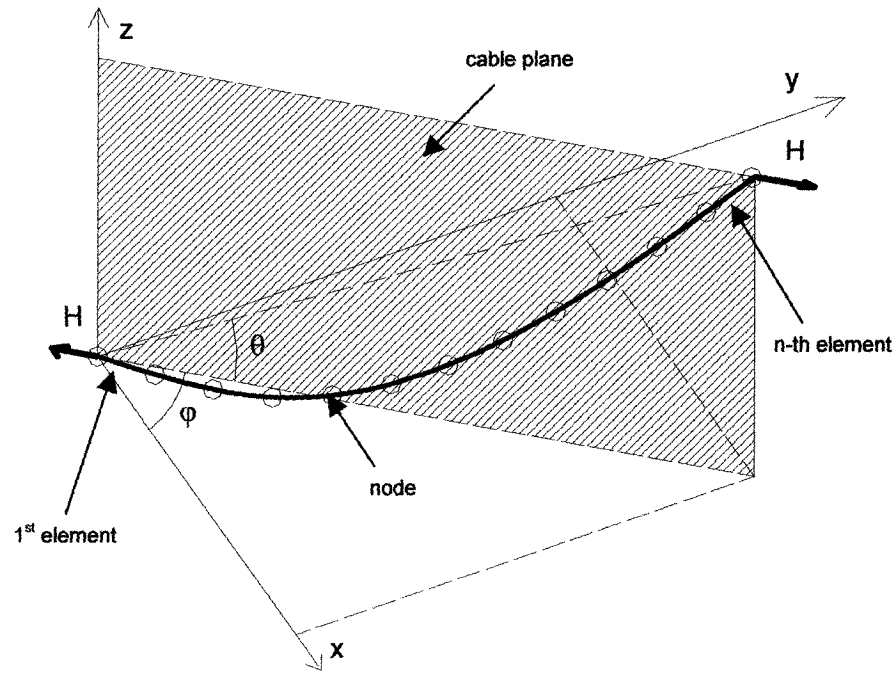

Figure 3.6: The assembled cable elements in 3D global coordinates

To help understanding the flow of calculation to obtain the solution, Figures 3.7 and 3.8 provide concise procedures of the combined functions. Details on the creation of functions or the element numbering system will not be presented here for brevity. However, detailed Matlab functions are available in the Appendix C.

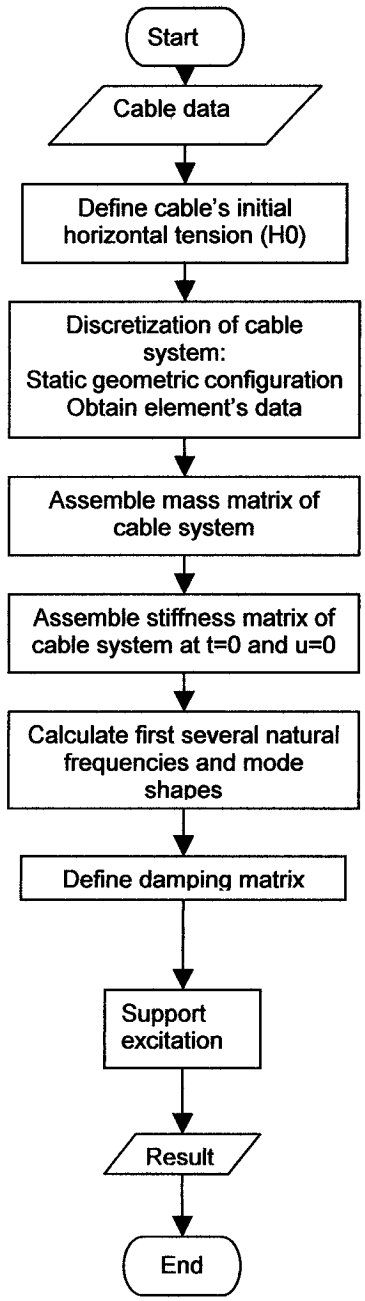

Figure 3.7: Flowchart of cable analyses

The last part of the flowchart in Figure 3.7 should be defined in another flowchart as in Figure 3.8.

Support excitation:

For this type of vibration, the formation of the tangent stiffness for each time step is determined by more factors. On top of the displacements, the change of cable tension of each element at each time step is considered.

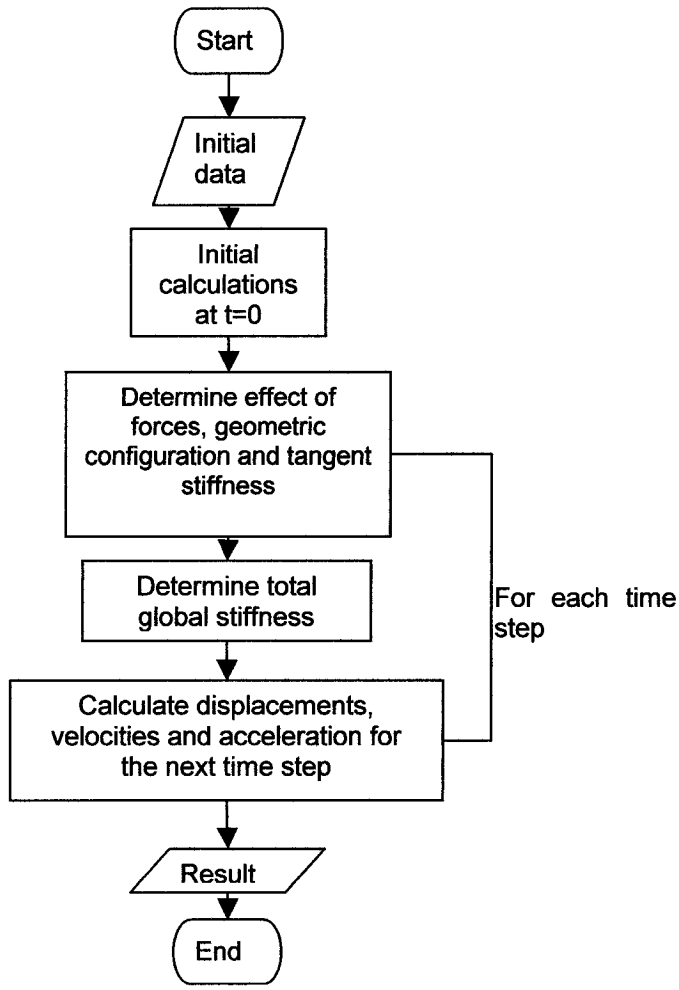

Figure 3.8: Flowchart of dynamic analyses of cable

Geometric configuration of the cable changes during oscillation of cable and this in turn changes transformation matrix from local to global coordinates for each time step. For cases of support excitation, it is very important to account any changes in cable configuration due to support excitation plus the displacements. This is to ensure the numerical analyses to capture any possibilities of OP oscillations.

3.7 Summary of Chapter 3

In this chapter, the non-linear two-node cable elements with 3D orientation were developed. The stiffness matrix of the element is adaptable towards large displacements and the change in element tension. The configuration and distribution of element tension are determined from the catenary shape of the cable. The parametric excitation is simulated by a function of support excitation that changes the tension of the cable for each time step. The solution of this non-linear problem was obtained by applying the Newmark method with an addition of Newton-Raphson iterative procedure.

CHAPTER 4
RESULTS AND DISCUSSION

4.1 Parameters as input data

The structural cable data assumed for the analyses throughout the present study were taken from Clement and Cremona (1996). They are the data of a long stay-cable of the Normandy Bridge. This set of data was chosen because the Normandy Bridge is a typical of the contemporary cable-stayed bridges, which was designed with advanced technology, and also many of the parameters were readily available to a great extent. Various calculations are performed throughout this Chapter. Some of the parameters are changed during the analyses, depending upon their purposes.

The standard set of cable parameters for the analyses is as follows:

Cross section, $A=15.30\times10^{-3}m^2$
Cable length, $Lc=440m$
Mass per unit length, $m=133kg/m$
Young's modulus, $E=190GPa$

With the cable's original configuration, $\theta=17.50°$, the initial horizontal tension is $H_0=8.00MN$, initial sag is 3.76 m, with the initial sag-to-span ratio, $R_0=0.008969$. The sag value agrees well with the value calculated by Lilien and Pinto da Costa which is 3.84 m. The first IP natural frequency, $\omega_2=1.89rad/s$, agrees well with the calculation by Clement and Cremona, that is $\omega_2=1.87rad/s$.

4.2 Results of the analyses

The analytical examinations of parametric excitation involved in the present study are summarized in this section. The physical parameters used for the analyses are as given in 4.1, unless they are stated otherwise.

4.2.1 Horizontal cables (θ=0°)

Tangential support excitation was given to the horizontally suspended cable. The cable was discretized in 12 elements and damping ratio, ξ=0.6%.

1. Changing the value of R with support excitation amplitude, amt=0.1m.
   a. R_0=0.008969 at $\Omega=2.05\omega_1$. In-plane (IP) parametric excitation (PE) observed. Peak amplitude existed. Beating followed.
   b. R_0=0.010 at $\Omega=2.18\omega_1\approx2\omega_2$. PE(IP) observed
   c. R_0=0.015 at $\Omega=2.7\omega_1\approx2\omega_2$. Out-of-plane (OP) PE observed. At first the oscillation was IP, then as the IP amplitude reached certain magnitude, OP oscillation started to occur.
   d. R_0=0.018 at $\Omega=3.08\omega_1\approx2\omega_2$. PE(OP) observed.
   e. R_0=0.020 at $\Omega=3.4\omega_1\approx2\omega_2$. PE(OP) observed.
   f. R_0=0.024 at $\Omega=4\omega_1\approx2w_2$. PE(IP) observed.
2. Changing Ω from $3.2\omega_1$ to $3.6\omega_1$ with R_0=0.02. ω_1=1.1701rad/s (1st OP), ω_2=1.9002rad/s (1st IP), ω_3=2.3159rad/s (2nd OP), ω_4=2.3195rad/s (2nd IP) and amt=0.1m. PE(OP) observed at $\Omega\approx3.4\omega_1$. When the frequency sweep was refined, the PE(OP) has the highest peak amplitudes at $\Omega=3.38\omega_1$. To illustrate the difference in the cable response between PE occurred and not occurred, in Figures 4.1 to 4.3, the time history records of the mid-span (MS) point response produced from the numerical simulation are shown.
3. Changing the excitation amplitude from 0.05m to 0.15m, with R_0=0.02 and $\Omega=3.38\omega_1=2.08\omega_2$.
   a. amt=0.050m. No PE observed.
   b. amt=0.075m to 0.125m. PE(OP) observed. As amt was increased, the OP oscillation became less.
   c. amt=0.150m. PE(IP) observed but OP was not.

4.2.2 Inclined cable (θ=17.5°)

In this analysis, R_0 was kept constant and the support excitation (amt) was given by the motion of the deck. The inclined cable was discretized in 12 elements and ξ=0.6%, unless otherwise stated. The natural frequencies are: ω_1=1.7883rad/s (1st OP), ω_2=1.8929rad/s (1st IP), ω_3=3.5448rad/s (2nd OP) and ω_4=3.5458rad/s (2nd IP).

1. Changing the value of excitation frequency (Ω).
   a. The first instability zone; $1.96\omega_1 \leq \Omega \leq 2.10\omega_1$ with amt=0.1m:
      i) $\Omega=1.96\omega_1$ to $1.99\omega_1$. No PE observed. The beating were observed and the higher Ω was increased, the less the beating became.
      ii) $\Omega=2.00\omega_1$ to $2.06\omega_1$. PE(IP) observed. As Ω was increased, the highest transient peaks grew larger, beating observed.
      iii) $\Omega=2.07\omega_1$ to $2.10\omega_1$. No PE observed, more beating observed at higher Ω.

      To illustrate points 1.a.i) to 1.a.iii), Figures 4.4 to 4.6 show the time history records of the response at the MS point.
   b. The second instability zone; $0.96\omega_1, \leq \Omega \leq 1.04\omega_1$ with amt=0.5m:
      i) $\Omega=0.96\omega_1$ to $0.98\omega_1$. No PE observed.
      ii) $\Omega=0.99\omega_1$ to $1.01\omega_1$. PE(IP) observed.
      iii) $\Omega=1.02\omega_1$ to $1.04\omega_1$. No PE observed.
   c. Possibility of PE(OP); $1.80\omega_1 \leq \Omega \leq 1.94\omega_1$ with amt=0.1m:
      i) $\Omega=1.80\omega_1$ to $1.82\omega_1$. No PE observed.
      ii) $\Omega=1.83\omega_1$ to $1.90\omega_1$. PE(OP) observed. No large IP amplitude was observed before the development of OP oscillation.
      iii) $\Omega=1.92\omega_1$ to $1.94\omega_1$. No PE observed.

      To illustrate points 1.c.i) to 1.c.iii), Figures 4.7 to 4.9 show the time history records of the response at the MS point.
2. Changing the deck excitation amplitude for a range of frequency:
   a. $1.96\omega_1 \leq \Omega \leq 2.06\omega_1$ with amt=0.05m to 0.40m with an increment of 0.025m, for a time span of t=100s. A more refined analysis with longer time span, t=1000s, was done for amt=0.05m to 0.75m at $\Omega=2\omega_1$:
      i) amt=0.05m. No PE observed.
      ii) amt=0.10m to 0.25m. PE(IP) observed. As the excitation amplitude was increased, the highest transient peaks became higher and more beating phenomena observed.
      iii) amt=0.50m to 0.75m. No PE observed.
   b. $\Omega=\omega_1$ with amt=0.40m to 0.80m, for a time span of 100s. PE(IP) observed at 0.40m≤amt<0.80m. No PE observed at amt=0.80m
3. Changing the damping ratio to compare with $\xi=0.6\%$ at $\Omega=2\omega_1$, amt=0.1m and time span=1000s

a. ξ=0.3%, PE(IP) observed. The highest transient peaks occurred at earlier time and were 2 times larger than at ξ=0.6%. More beating phenomenon was observed.
b. ξ=1.0%, PE(IP) observed. The amplitude gradually increased for the whole time span. The highest transient peak was about 30% of the case of ξ=0.6%.

4.2.3 Discretization using more elements

The cable was discretized into 48 elements. The support excitation was performed at Ω=1.85ω1, amt=0.1m. The MS point response was compared with the results from the analysis using 12 elements. With 48 elements, the analysis took 10 times longer than that with 12 elements. However, the response amplitude differs less than 4.3% compared to the 12-element analysis. The vibration characteristics were identical in both cases. The time when highest transient peaks were reached was 10 to 20 seconds longer, for the case of 12-element analysis.

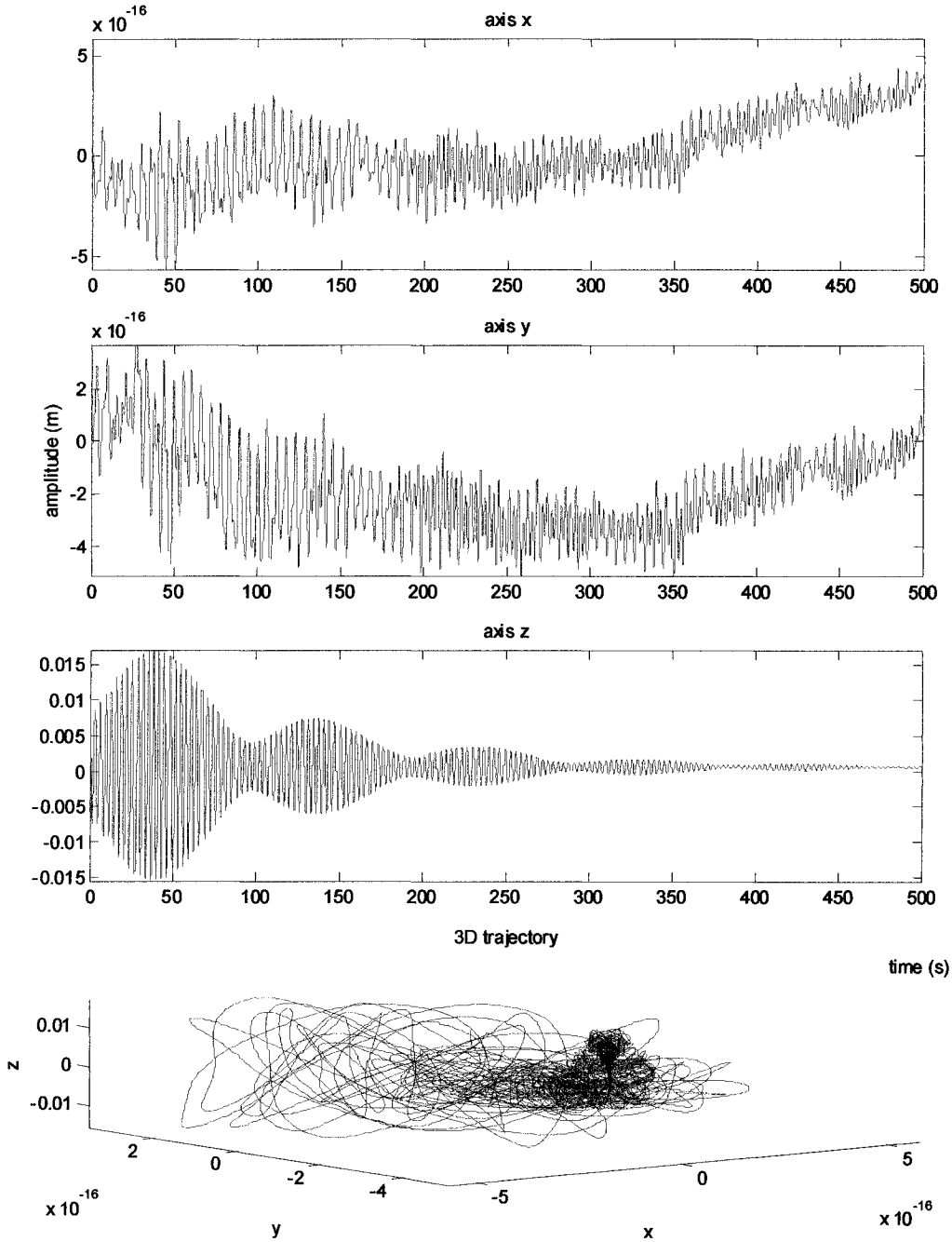

Figure 4.1: Mid-span point response of a horizontal cable, R_0=0.02, amt=0.1m, Ω=3.3ω_1

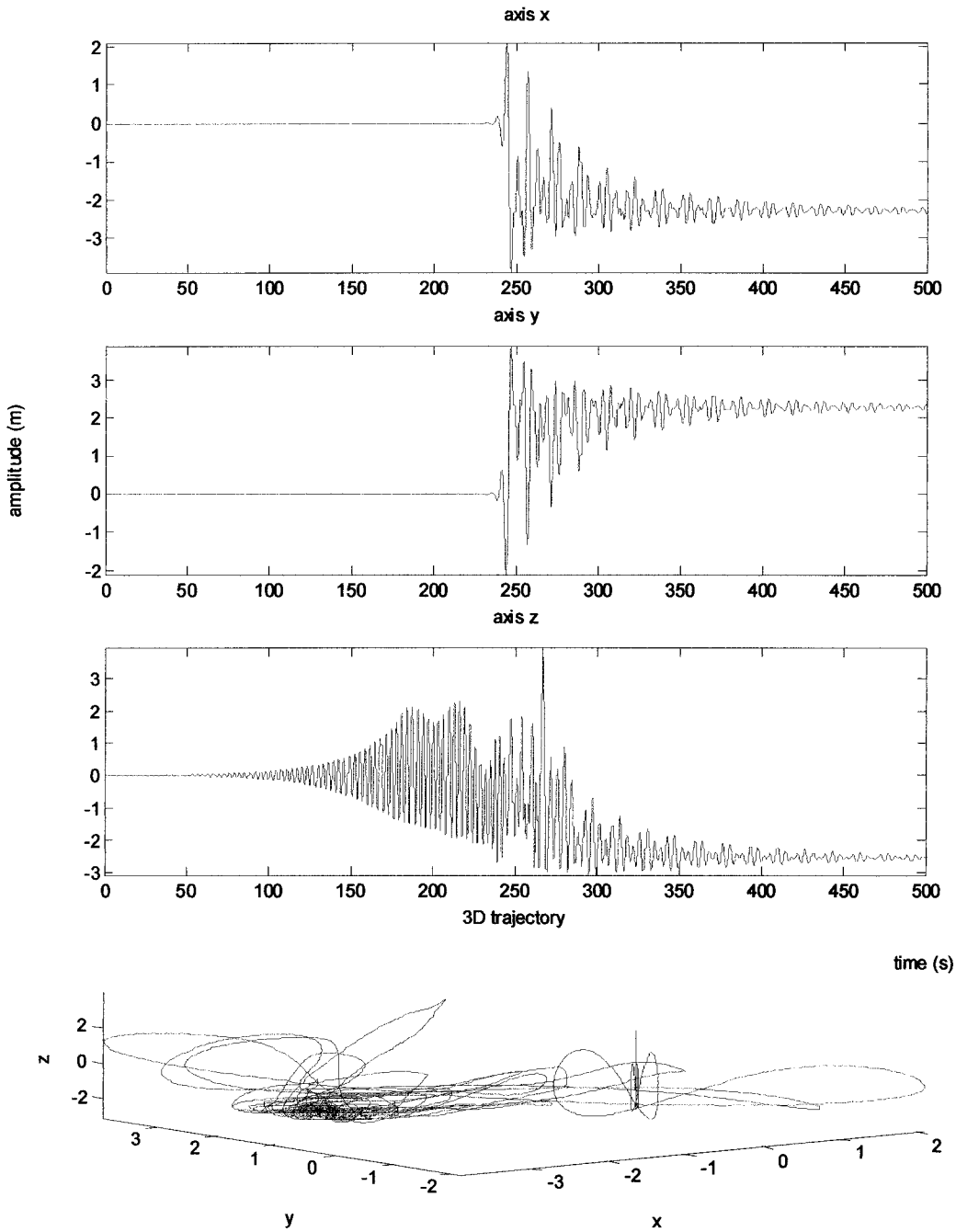

Figure 4.2: Mid-span point response of a horizontal cable, R_0=0.02, amt=0.1m, Ω=3.38ω_1

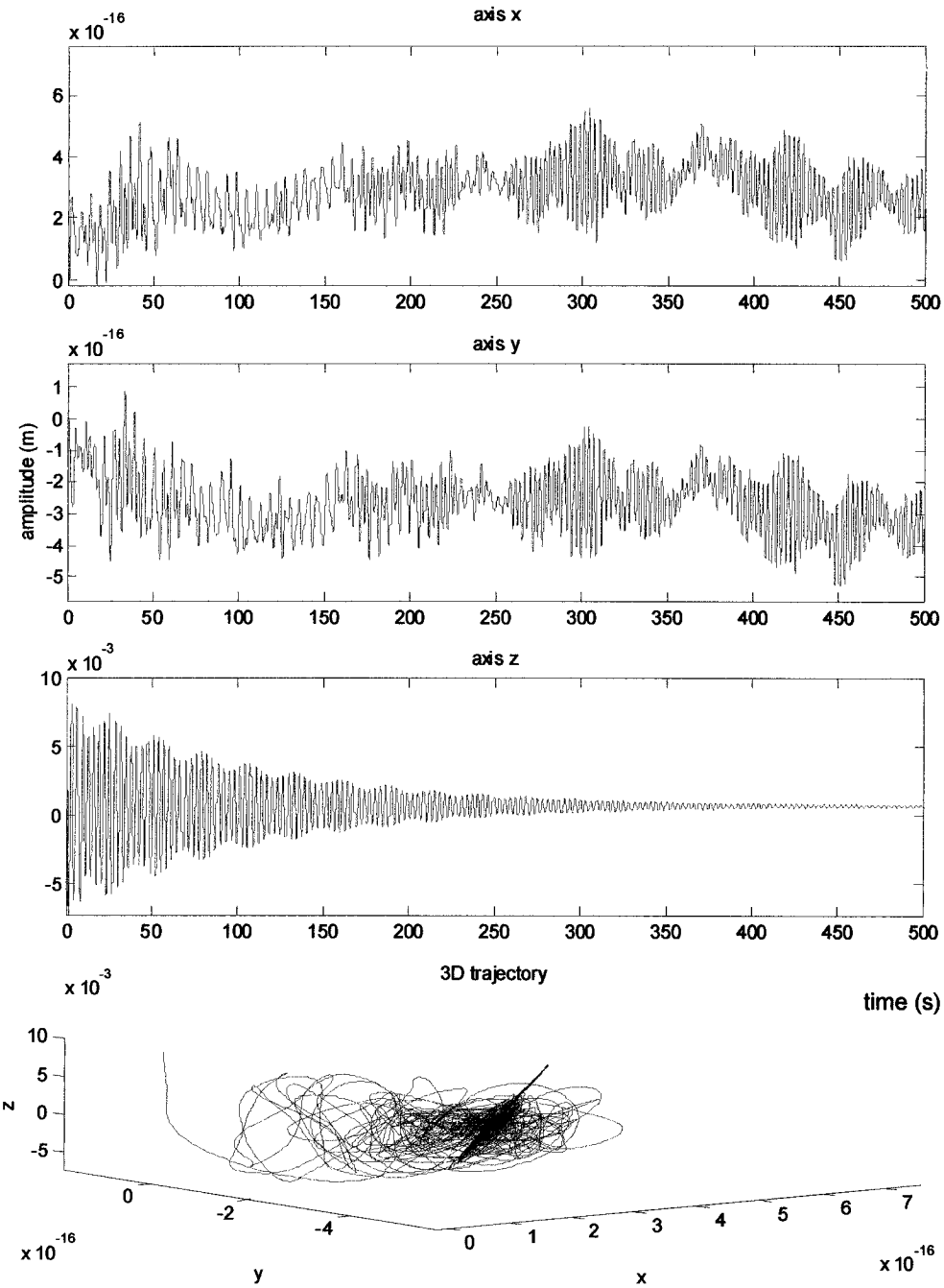

Figure 4.3: Mid-span point response of a horizontal cable, R_0=0.02, amt=0.1m, Ω=3.6ω_1

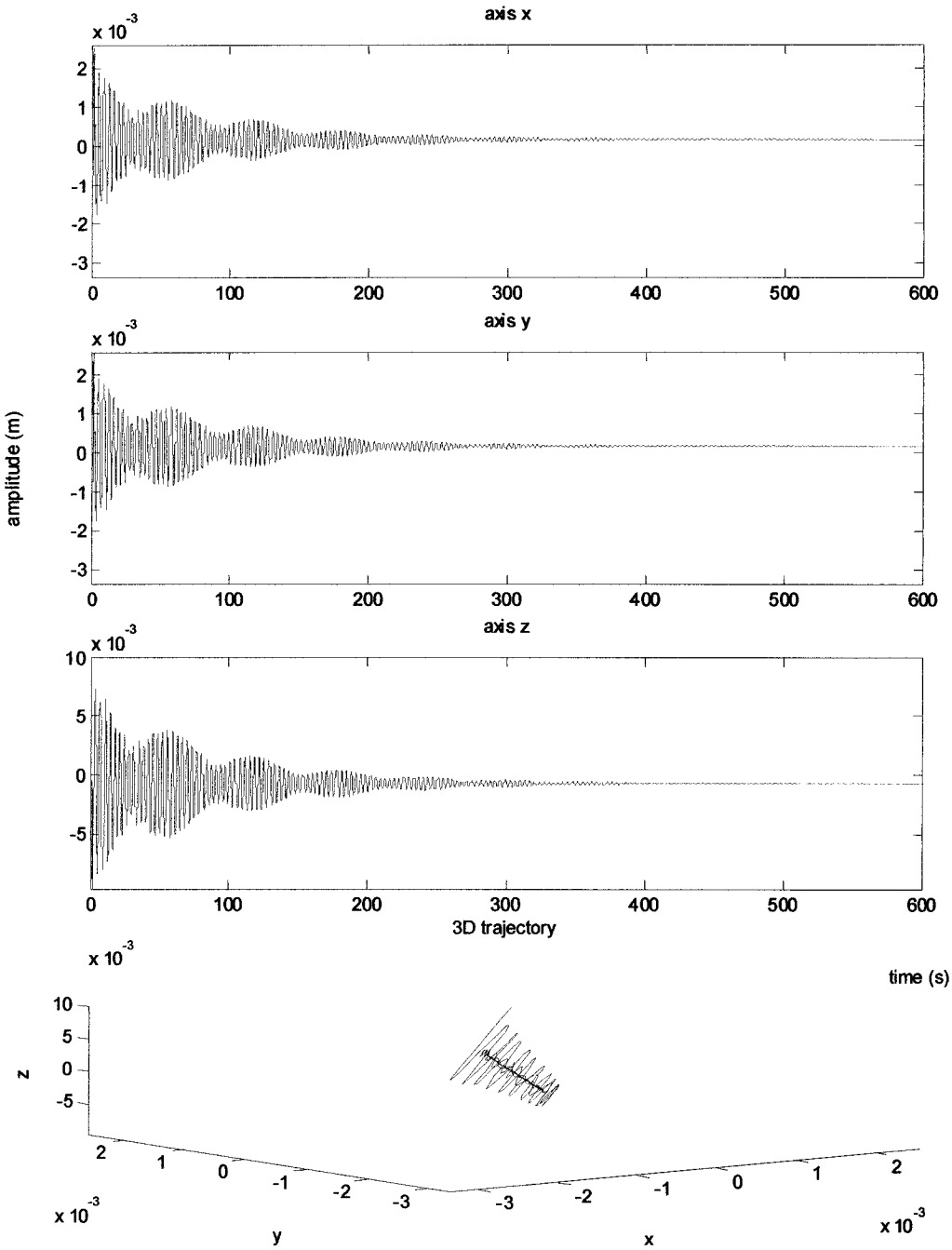

Figure 4.4: Mid-span point response of an inclined cable, R_0=0.008969, amt=0.1m, Ω=1.96ω_1

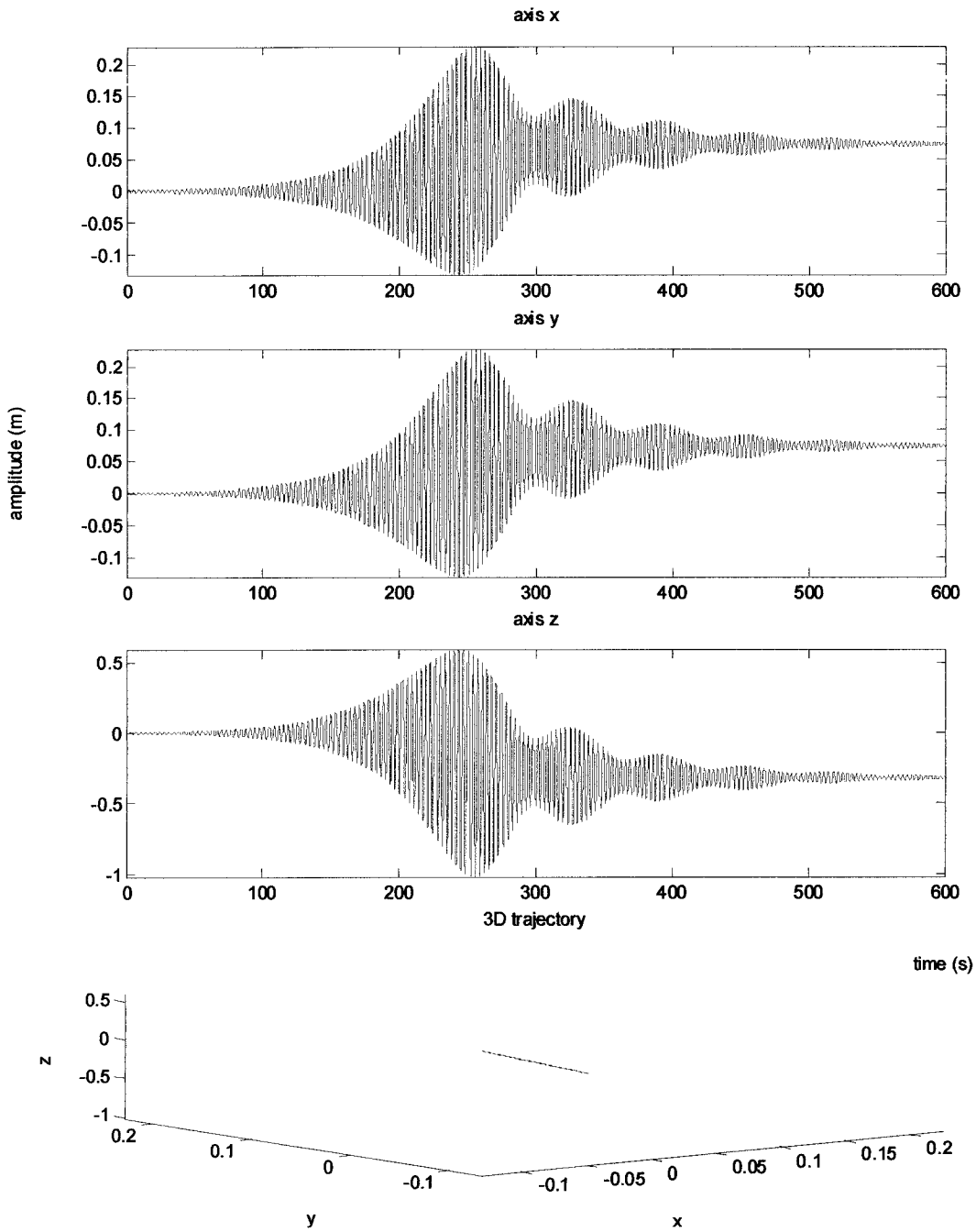

Figure 4.5: Mid-span point response of an inclined cable, R_0=0.008969, amt=0.1m, $\Omega=2.02\omega_1$

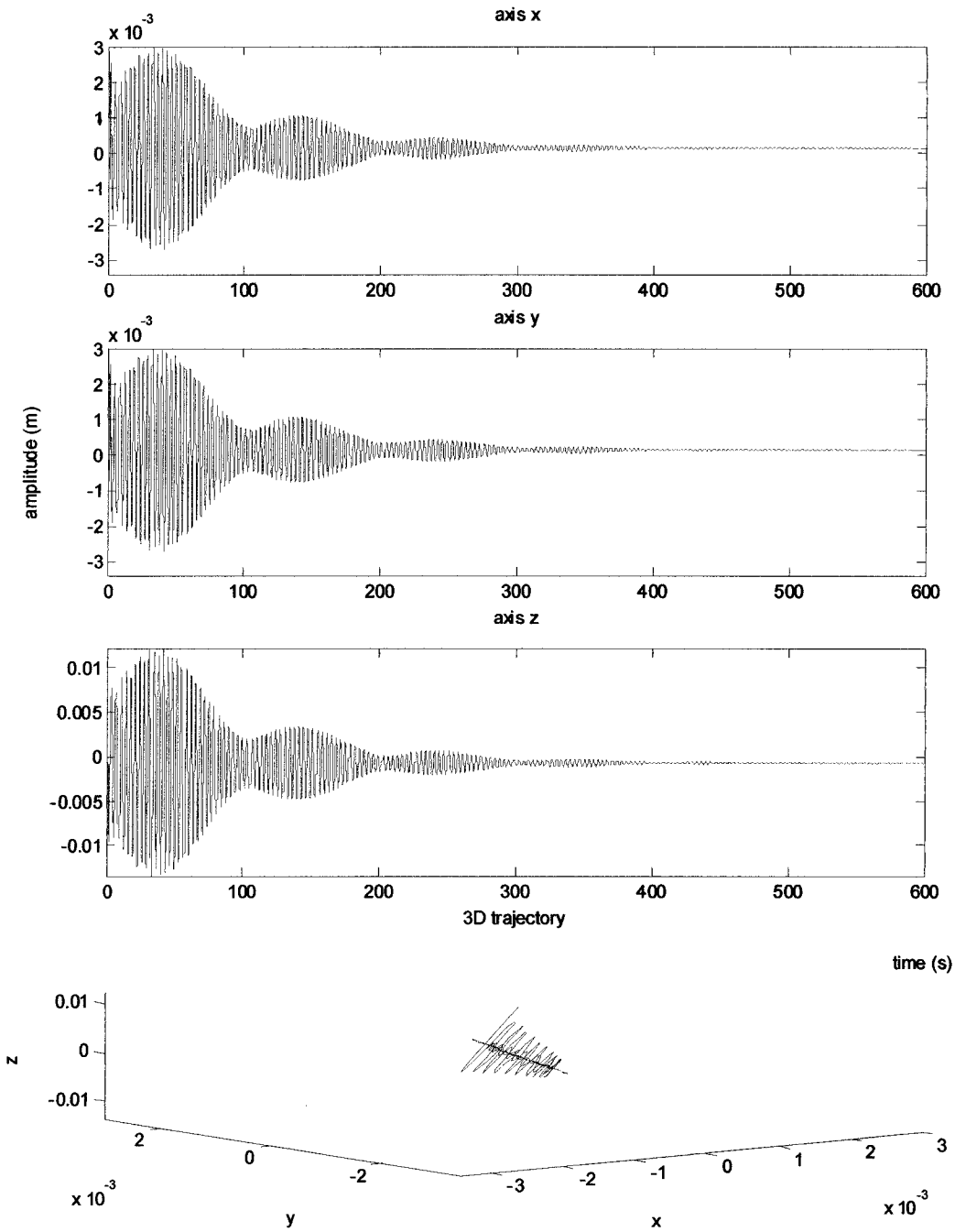

Figure 4.6: Mid-span point response of an inclined cable, R_0=0.008969, amt=0.1m, Ω=2.08ω_1

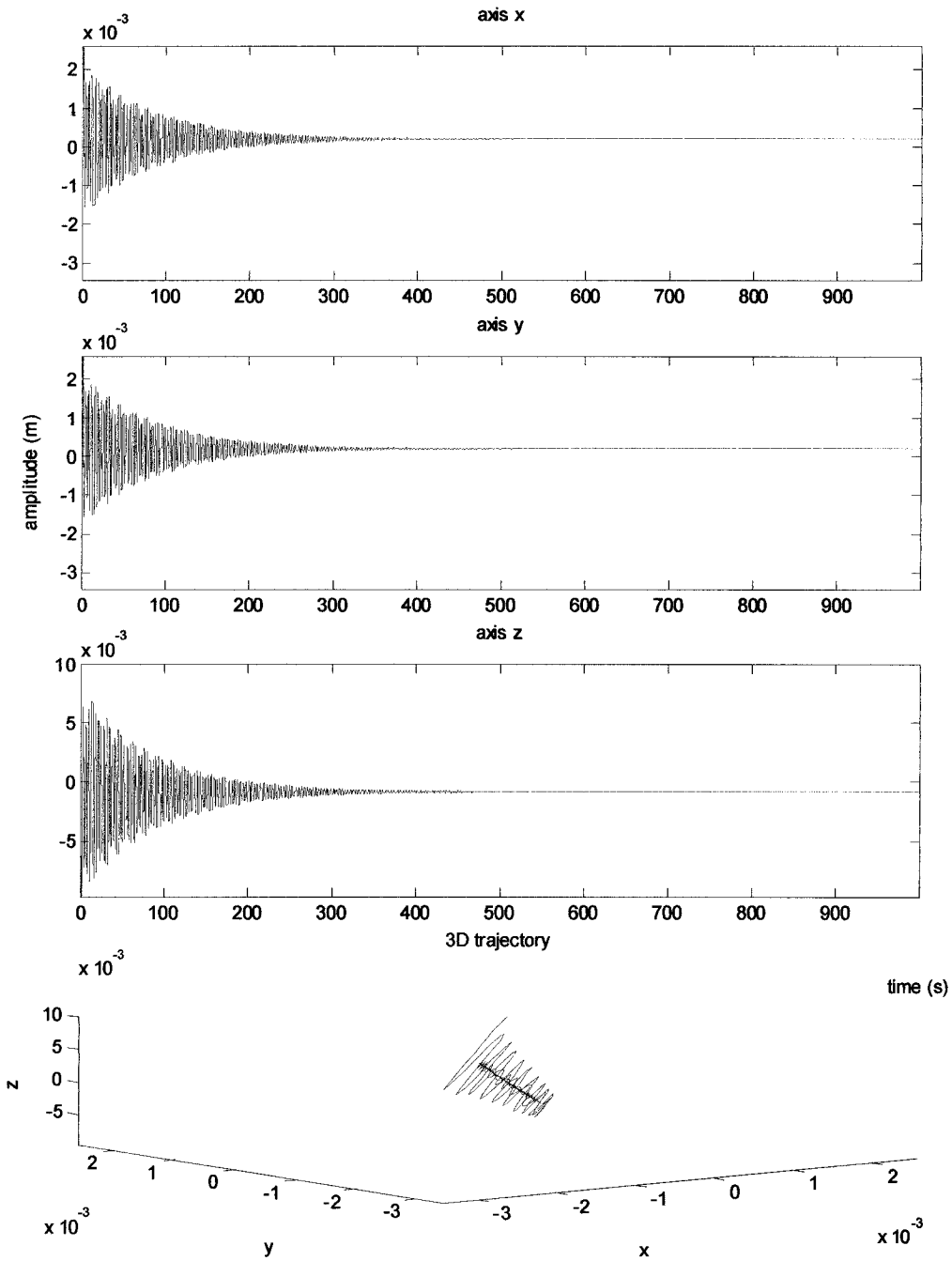

Figure 4.7: Mid-span point response of an inclined cable, R_0=0.008969, amt=0.1m, $\Omega=1.8\omega_1$

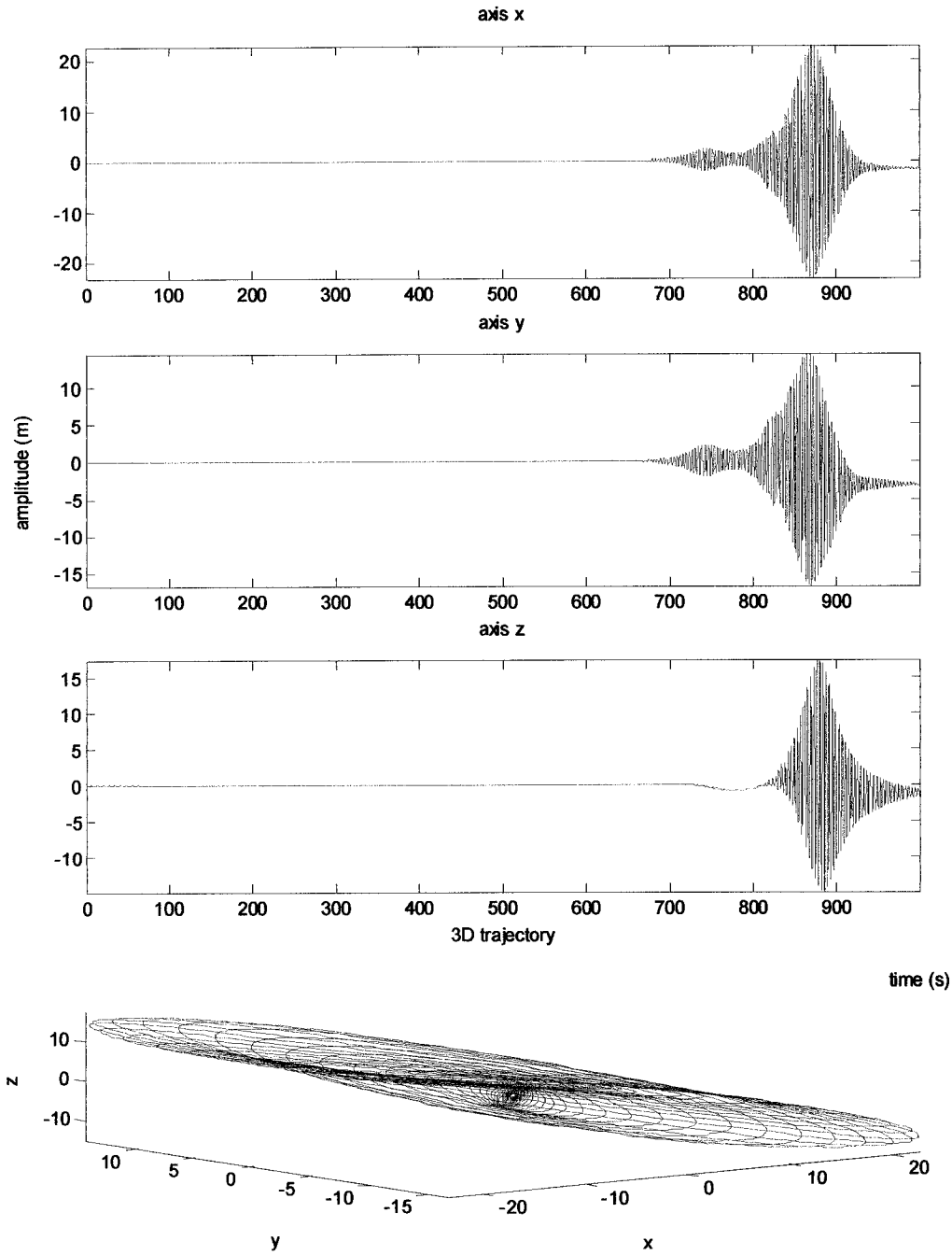

Figure 4.8: Mid-span point response for an inclined cable, R_0=0.008969, amt=0.1m, Ω=1.85ω_1

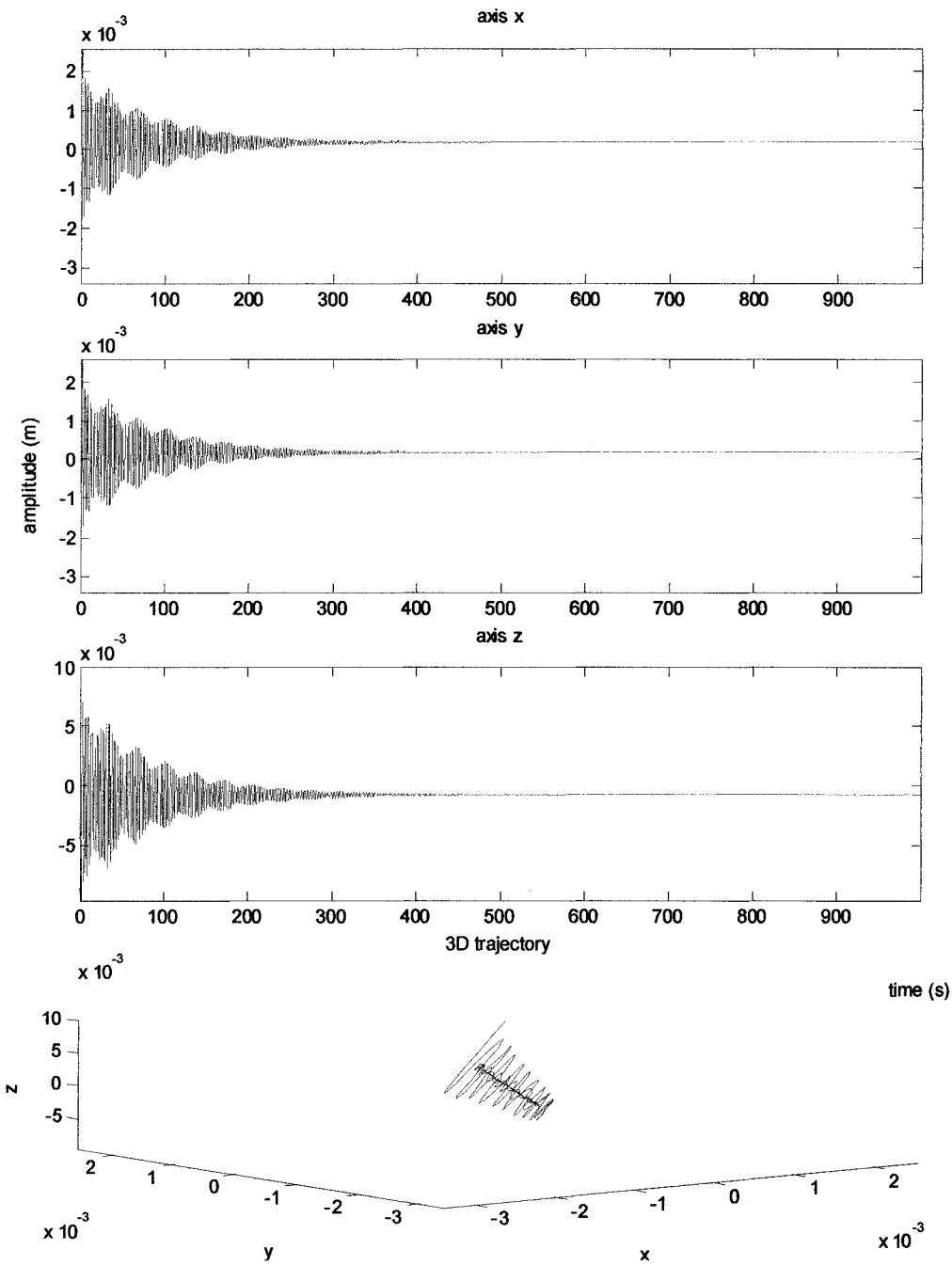

Figure 4.9: Mid-span point response of an inclined cable, R_0=0.008969, amt=0.1m, Ω=1.92ω_1

4.3 Natural frequencies and mode shapes of suspended cables

By linearizing the cable equations, the natural frequencies and corresponding mode shapes of the suspended cable model can be numerically obtained by solving the eigenvalue problem. These data are useful to further understand the characteristics of cable oscillations and provide some background information on interrelation between the modes.

The natural frequencies and mode shapes of the inclined and horizontal cables that were obtained in the present study, agreed well with numerous previous works. Not only limited to 2D analyses, the present study revealed the relations between the OP and IP modes, which agreed very well with Yamaguchi and Fujino (1998). Even though the cable data were not the same, the dynamic characteristics of the cable system in general, including the mode shapes, were in very good agreement.

4.3.1 Natural frequencies and mode shapes of the inclined cable

Using the cable data defined in 4.1, with constant cable inclination angle, θ=17.5° and the number of elements=12, various sag-to-span ratio (R) are analysed for their static initial geometric configurations to get the first four natural frequencies and the corresponding mode-shapes.

Figure 4.10 shows the relationships between R and the first four natural frequencies. One can observe that for R<0.01, $\omega_1 \approx \omega_2$, which is typical as the characteristics of natural frequencies of stay-cables according to Nielsen and Kirkegaard (2002). Before the transition zones, the values of ω_3 are almost equal to ω_4, while after the transition, the values of ω_2 are very close to those of ω_3. Inside the transition zone, at a very narrow range of R, it can be seen that $\omega_2 \approx \omega_4$. This is the range where the 1st IP mode shape changes gradually to 2nd IP mode shape. The transition of the 1st IP mode to 2nd IP mode, and vice-versa, can be observed from Figures 4.11 and 4.12.

For the case of θ=17.5° and using a 12 elements model, the mode transitions happened at around R=0.026 to 0.027. At this range of R, the 1st symmetric IP mode starts to change to an asymmetric IP mode and the 2nd IP asymmetric mode starts to change to a symmetric mode (Figures 4.11 and 4.12). The 1st OP and 2nd OP mode shapes remain

the same throughout the total range of R. Even if more elements were used, the nature of the relation between natural frequencies and R does not change and values of transition R become only slightly higher.

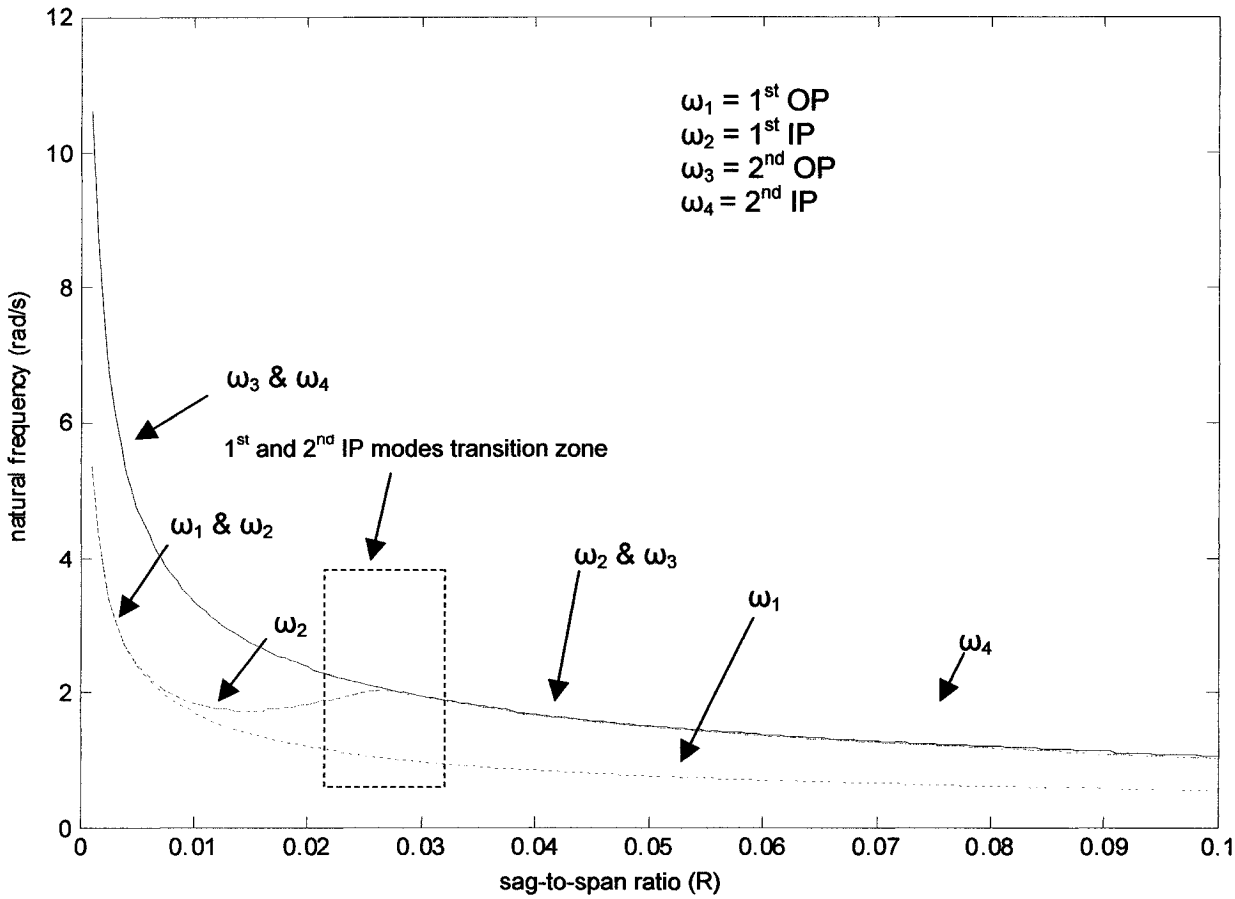

Figure 4.10: Natural frequencies vs. R for an inclined cable, θ=17.5°

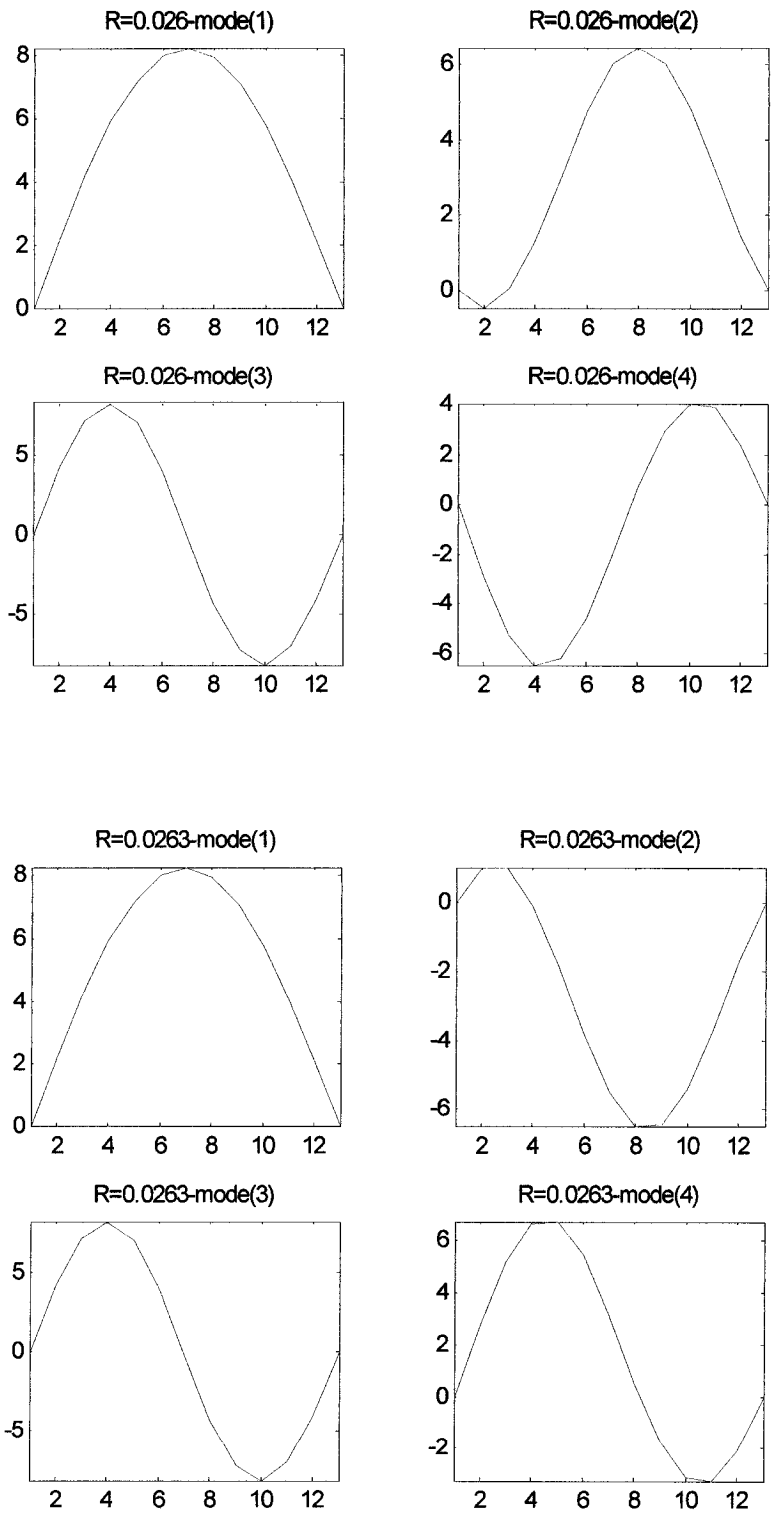

Figure 4.11: Mode shapes at R=0.026 and R=0.0263 for an inclined cable, θ=17.5°

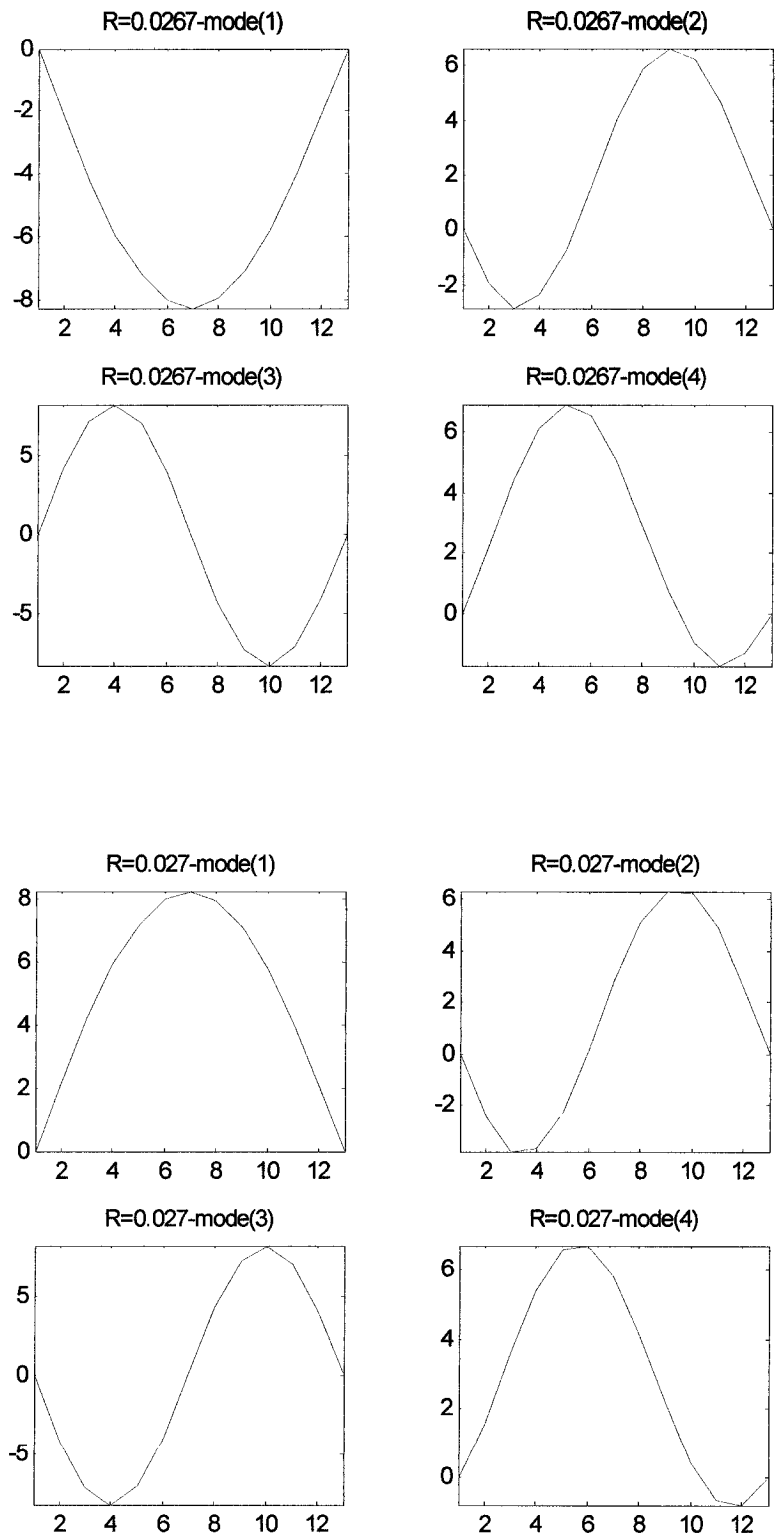

Figure 4.12: Mode shapes at R=0.0267 and R=0.027 for an inclined cable, θ=17.5°

4.3.2 Natural frequencies and mode shapes of the horizontal cable

Using the cable data defined in 4.1, a horizontally suspended cable with the number of elements=12 and with various R, is analysed to obtain the first four natural frequencies and the corresponding mode-shapes.

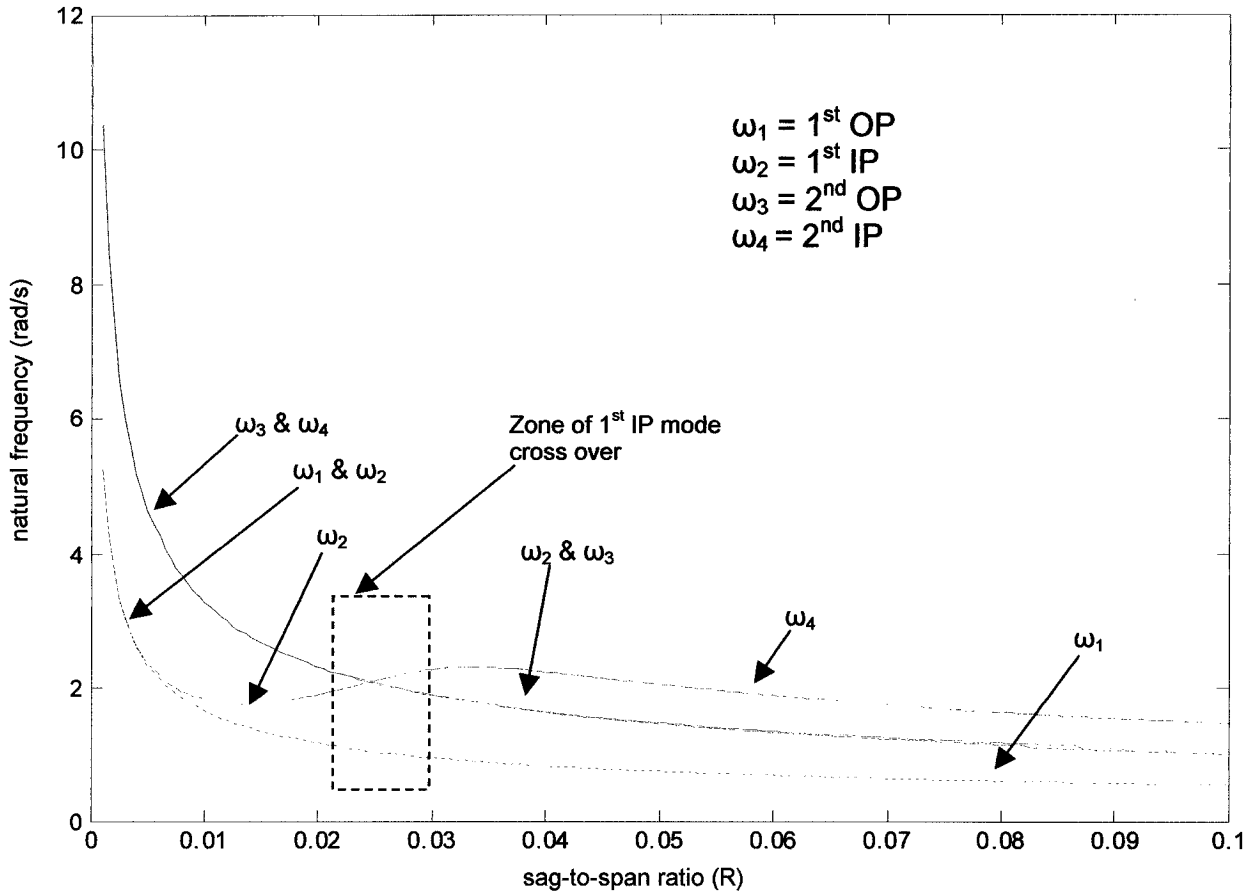

Figure 4.13: Natural frequencies vs. R for a horizontal cable

The change of the first four natural frequencies against R for a horizontal cable is shown in Figure 4.13 and it can be seen that the relationships between R and the natural frequencies are quite similar as the inclined cable. A horizontal cable exhibits rather different behaviour in modal changes, well known as the modal cross-over. From Figures 4.14 and 4.15, it is observed that the 1st IP mode changes to asymmetric mode and 2nd IP mode changes to symmetric mode at R=0.0246. The change in the IP mode shapes is sudden and it is not gradual like the one found for the inclined cable. For OP modes, the same characteristics are maintained for different R.

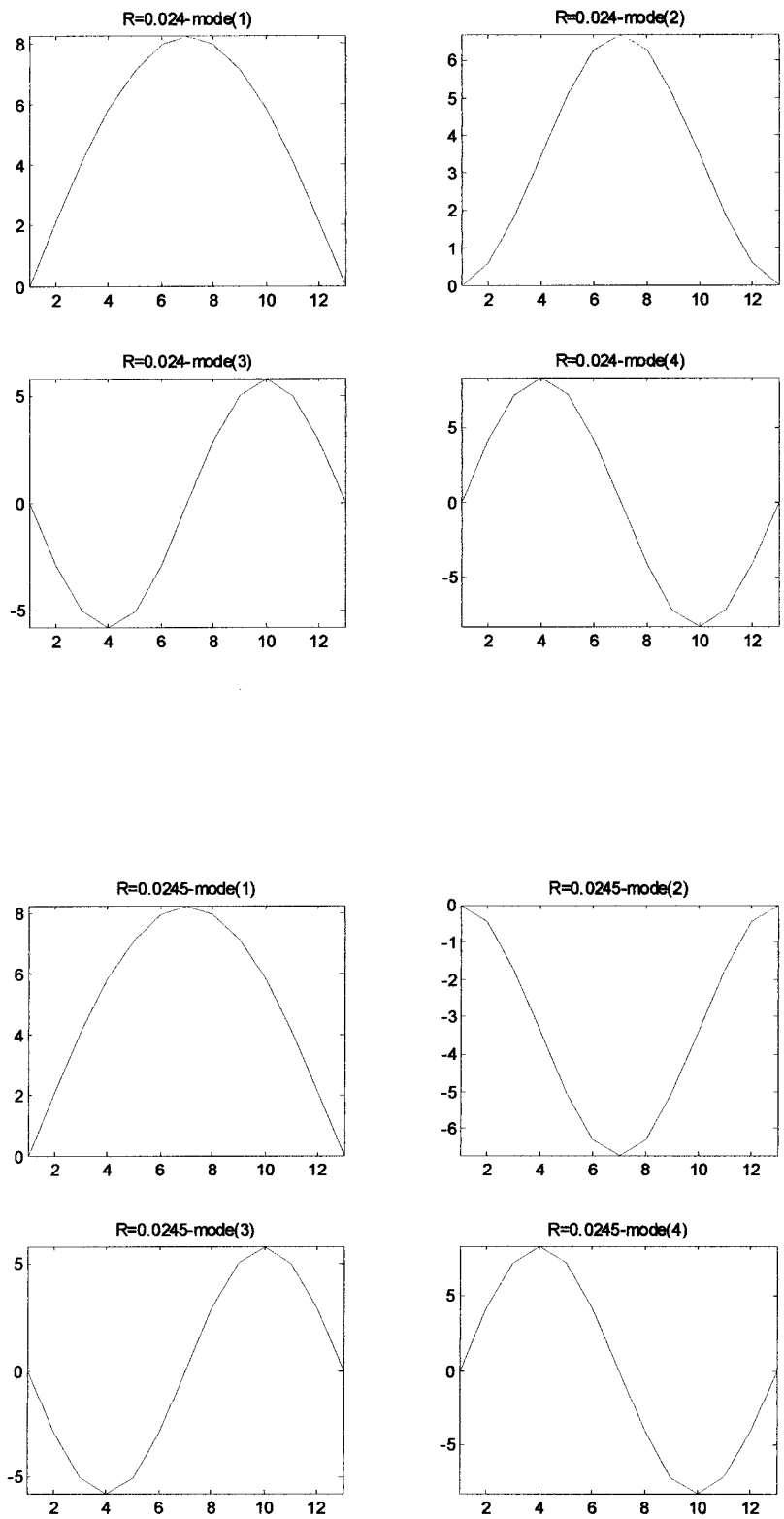

Figure 4.14: Mode shapes at R=0.024 and R=0.0245 for a horizontal cable

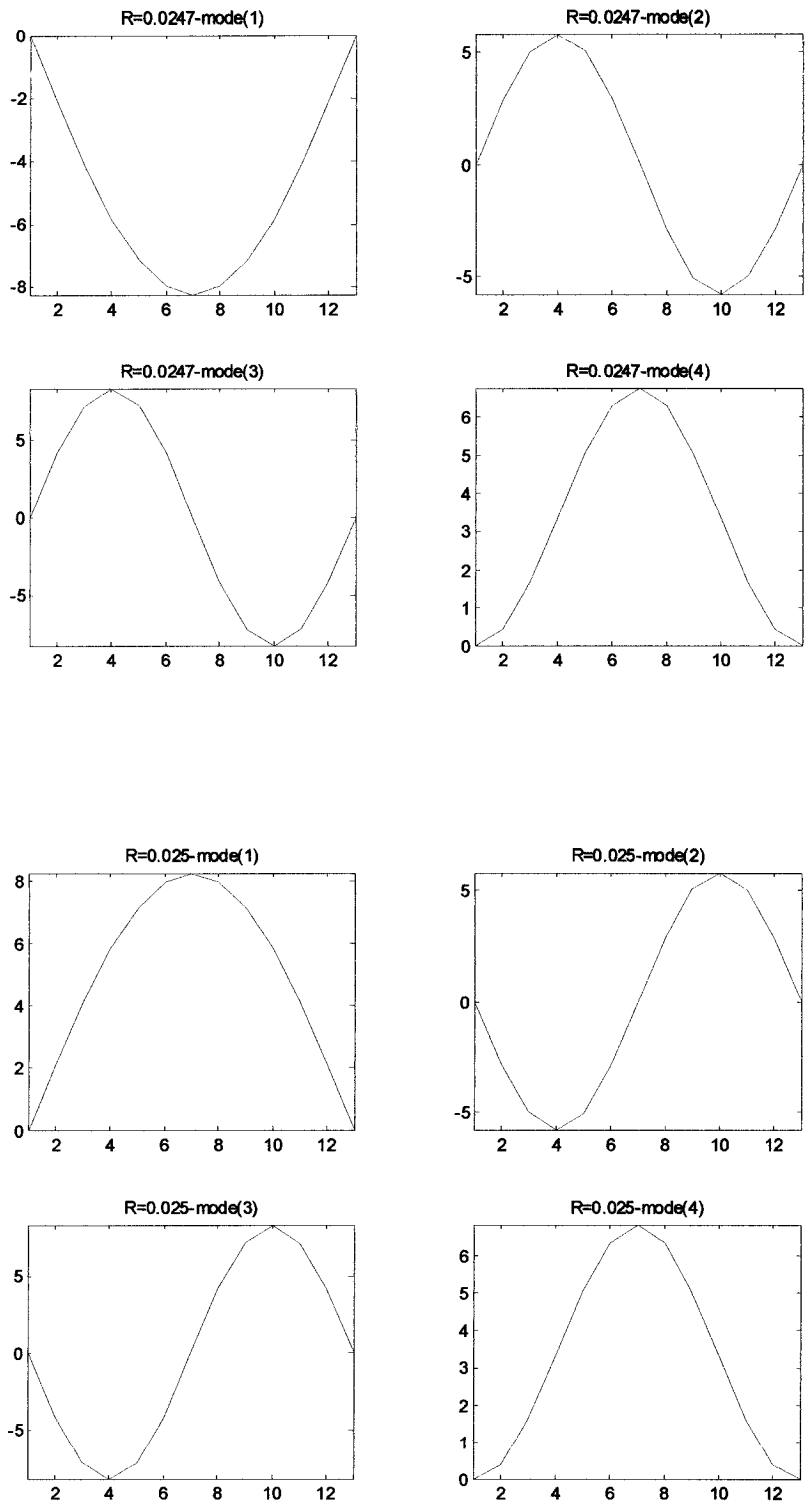

Figure 4.15: Mode shapes at R=0.0247 and R=0.025 for a horizontal cable

4.4 IP parametric excitation

The present study was able to validate the existence of the primary and secondary parametric excitation. These two instability zones indicate the range of excitation frequency that induces IP parametric excitation response. The agreement between observations of simulated parametric excitation with theoretical prediction was very good. The significant OP response was observed at Ω outside of those zones. There is a certain range of amplitude of support excitation that triggers the parametric excitation. The amplitude needed to trigger the parametric excitation is higher for the secondary parametric excitation.

There were new finding in the present study; there is a limit of support excitation amplitude that can trigger parametric excitation. Previous works have mentioned that oscillation amplitude becomes greater when support excitation amplitude is higher, (Perkins, 1992). This statement is true only up to a certain limit, depending on the parameters interaction. After certain amplitude is reached, the parametric excitation ceased to happen.

Regarding the non-linearity of suspended cables, this study has shown that there is peak amplitude during oscillation. This is what the use of non-linear theory makes difference from the linear analysis in the parametric excitation study. Linear theory would not be able to predict the limit of amplitude and the oscillations would grow into infinity. Nevertheless, Bolotin (1964) mentioned that the non-linearity of the system would limit the growth of displacements.

4.4.1 Characteristics of parametric resonance at the 1st instability zone

To analyse cases of IP parametric excitation further in the 1st instability zone, several different cases defined in section 4.2.2 point 1.a are discussed here.

The result produced in this numerical analysis is the cable amplitude induced by the support excitation. To give better visualization of the response produced during each simulation, Figure 4.16 shows the time history response in the cable plane and trajectory at the MS point during parametric excitation. In order to clearly show that there is no

cable response for different excitation frequency, even if there is a support motion, Figure 4.17 is presented.

From Figures 4.16 and 4.17, it is clearly observed that parametric excitation occurred when $\Omega=2\omega_1$, for 0.1m of deck excitation amplitude (2.7% of the initial sag). However, for the same excitation amplitude with only 0.5% less value of excitation frequency, at $\Omega=1.99\omega_1$, there is no parametric excitation. This finding states that the occurrence of parametric excitation is highly dependent on its excitation frequency.

It is clear from Figure 4.16(a) that the developed parametric excitation is an IP motion. At first, the cable response increases exponentially, then the non-linearity of the cable starts restricting the growth of the response amplitude and the response reaches its highest peak. After that, the cable response shows a beating phenomenon. Beating phenomenon usually takes place when the excitation frequency and the natural frequency of the system are close to each other. For this particular case, the beating was observed when the excitation frequency is two times greater compared to the 1st natural frequency and it occurs following the transient state.

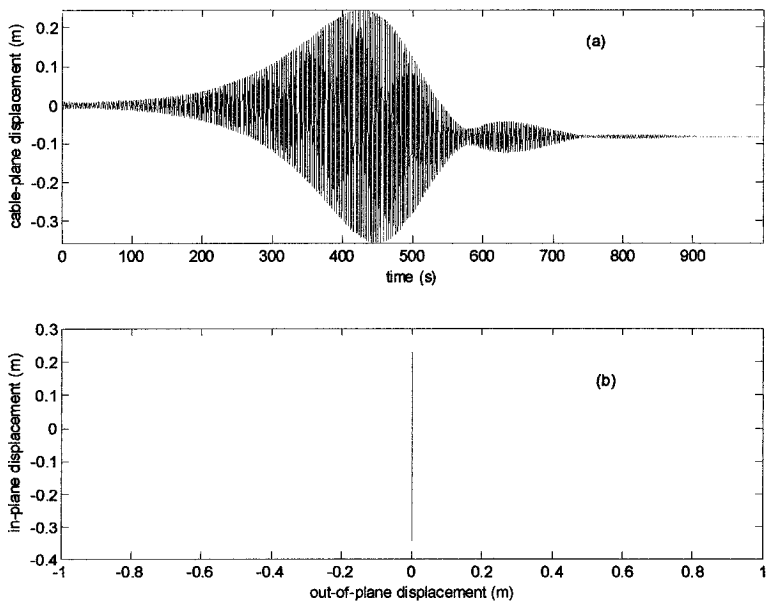

Figure 4.16: MS point response for $\Omega=2\omega_1$, (a) time history response in the cable plane; (b) trajectory of the response

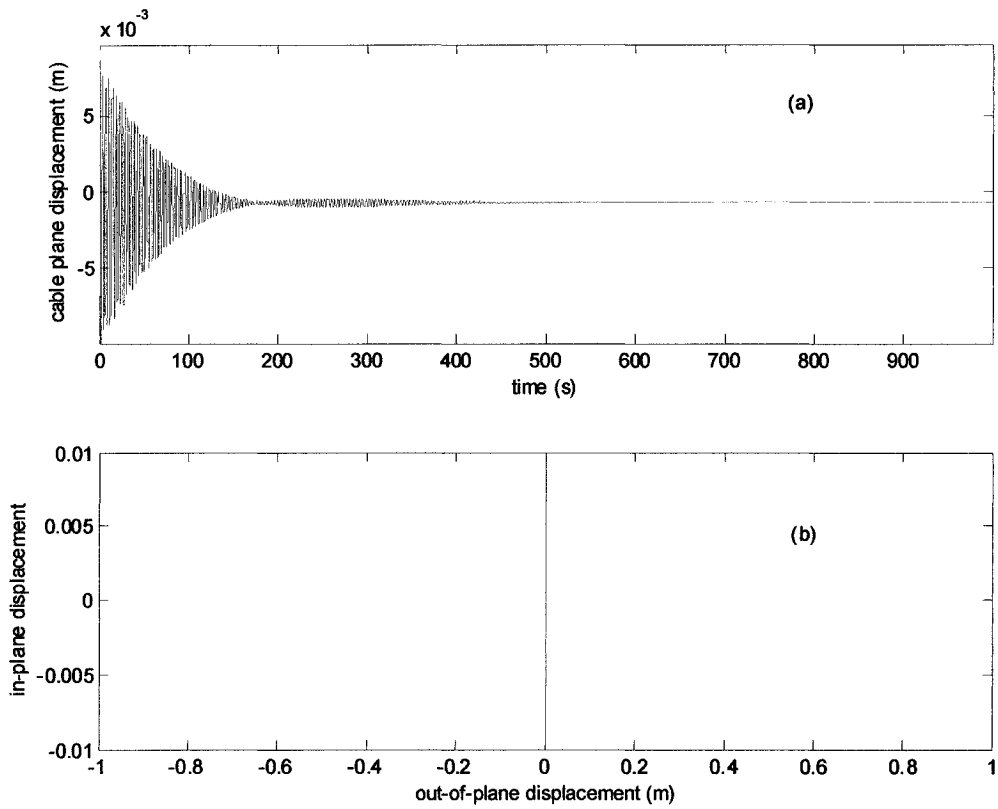

Figure 4.17: Mid-span response for $\Omega=1.99\omega_1$, (a) time history response in the cable plane; (b) trajectory of the response

When the parametric excitation is not triggered, even if there is a support excitation, see Figure 4.17(a), the cable response simply dies down and is accompanied by a light beating phenomenon. The vibration is also purely IP, look at Figure 4.17(b).

4.4.1.1 Transient period

For the analyses of data from section 4.2.2 point 1.a, parametric excitations occurred at the excitation frequencies of $\Omega=2\omega_1$ to $\Omega=2.06\omega_1$. Based on these data, the transient responses of the cable systems were analysed. The highest peak-to-peak amplitudes of MS point during transient periods were plotted in Figure 4.18. It can be observed in Figure 4.18 that for the case of IP parametric excitation with $\Omega=2\omega_1$ up to $2.06\omega_1$ and 0.1m of deck excitation amplitude, the highest peak-to peak amplitude is around 2.5 m. After $\Omega=2.06\omega1$, at Ω higher than that ($2.07\omega1\leq\Omega\leq2.10\omega1$), parametric excitation did not occur and highest transient peaks were not measured.

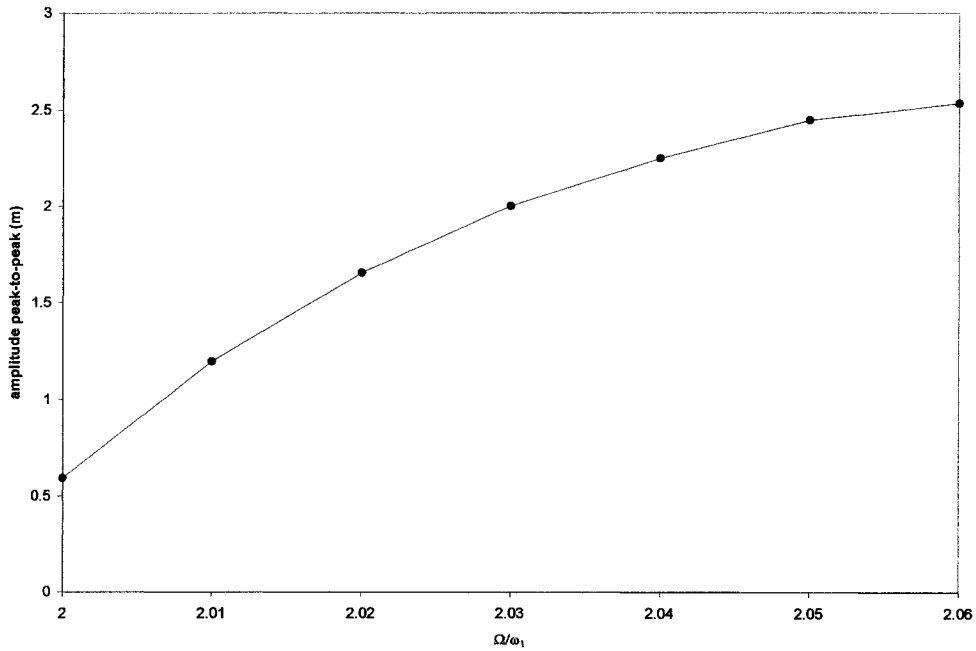

Figure 4.18: Maximum peak-to-peak amplitude during transient period of 1st instability zone

4.4.2 Characteristic of parametric resonance at the 2nd instability zone

In this section, a brief discussion on analysis from section 4.2.2 point 1.b is presented. It was obvious that much higher amplitude of support excitation is needed to trigger parametric excitation at 2nd instability zone. In this example, the excitation amplitude is five times higher than the one for the 1st instability zone. Another important point to notice is the width of the secondary instability zone which was much narrower than the 1st zone.

4.4.2.1 Transient period

For this analysis, parametric excitation occurred at the excitation frequency of $\Omega=0.99\omega_1$ to $\Omega=1.01\omega_1$. Based on these data, the transient response of the cable systems was analysed.

The highest transient peak-to-peak amplitudes of MS points were plotted in Figure 4.19, it can be seen that the highest transient peaks are lower than the ones from the 1st

instability zone, yet the deck excitation amplitude needed to trigger the parametric excitation was much higher.

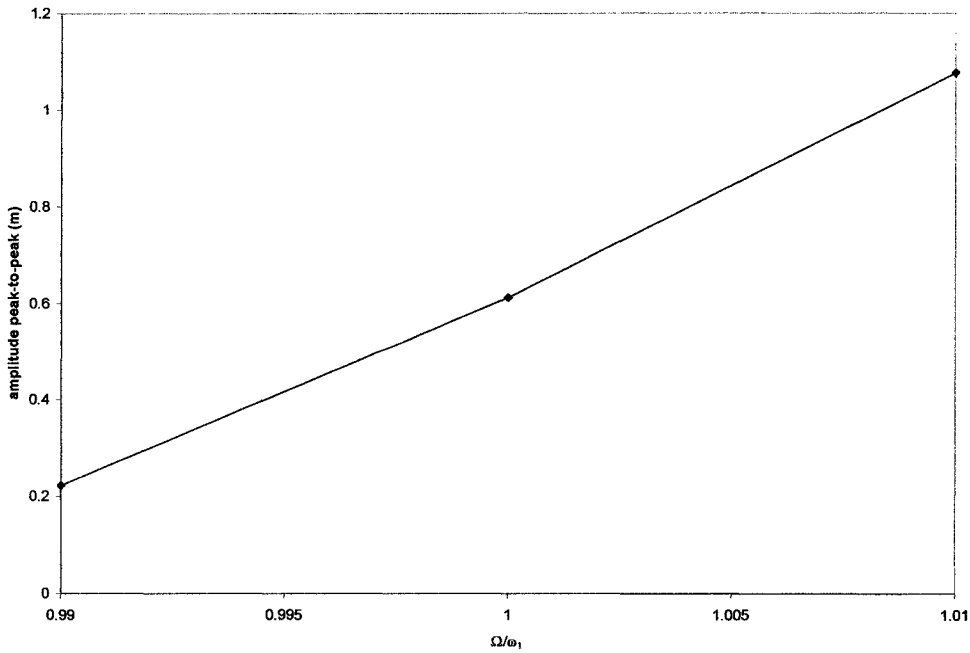

Figure 4.19: Maximum peak-to-peak amplitude during transient period, 2nd instability zone

4.4.3 Zones of instabilities

It is important to examine whether results of numerical non-linear analyses on parametric excitation found in this study were within the zones of instabilities previously found from other studies and have been briefly discussed in section 2.4.3. This study is emphasizing a numerical approach to investigate the general characteristic of the cable behaviour under parametric excitation.

A series of numerical calculations were performed as defined in section 4.2.2 point 2.a. Analyses for the 1st instability zone were performed. The range of excitation frequencies when parametric excitation was observed is in the range of $1.96\omega_1 \leq \Omega \leq 2.06\omega_1$. The different deck excitation amplitudes, between 0.05m and 0.40m was given, this is equivalent to the change of horizontal cable tension (ΔH) in the range of $0.150H_0 \leq \Delta H \leq 0.505H_0$.

The 2nd instability zone was captured only with one excitation frequency ($\Omega=\omega_1$) with different deck excitation amplitudes, between 0.40 and 0.70m. This is the result of section 4.2.2 point 2.b. This range of excitation amplitude corresponds to ΔH between 0.505 and 0.604 of H_0.

Figure 4.20 shows the results of these numerical analyses. The solid lines represent instability zones for undamped systems. The dotted lines represent those with damping. The circular bullets represent the results of the present analysis in the 1st instability zone, and the triangular bullets represent results in the 2nd instability zone.

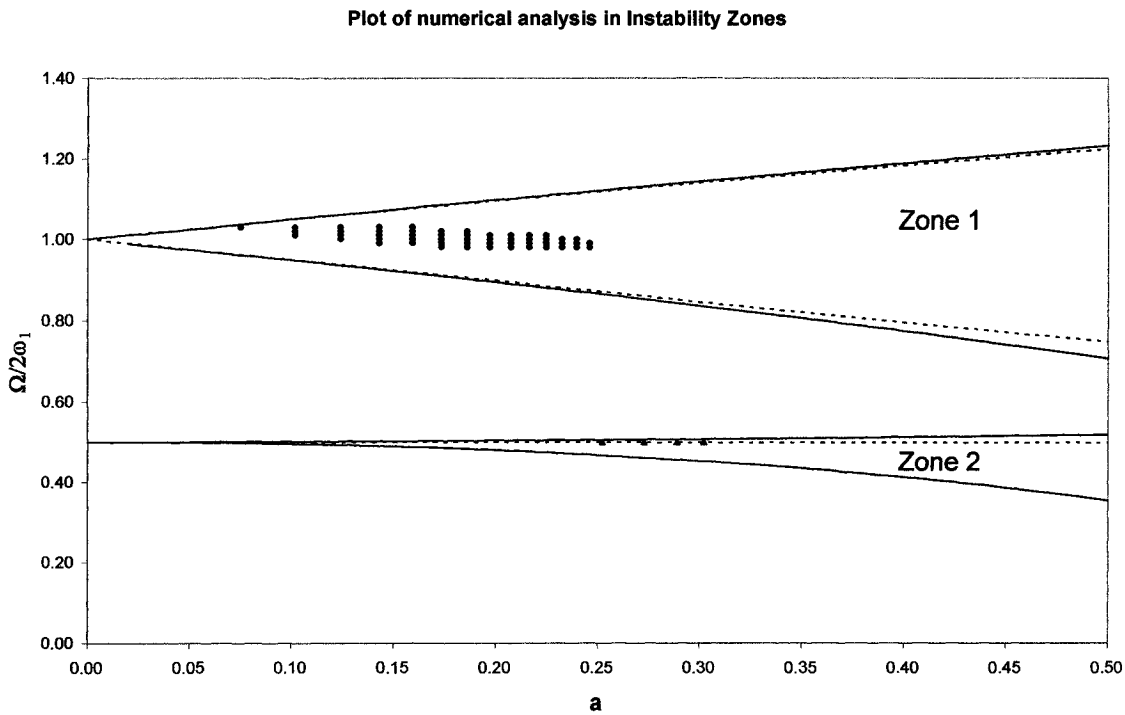

Figure 4.20: The result of the present analysis with the expected instability zones

Figure 4.20 shows that the results of the non-linear numerical analyses for parametric excitation of the cable performed in this study agreed well with the instability zones theoretically predicted. This result agrees with the statement by Bolotin (1964), which mentioned that even though instability zones were determined based on linear theory, it would be applicable to the non-linear systems.

However, there are several points that would be missing if one only looks at the plotting above as the only result. Magnitude of cable oscillation, duration of transient oscillation, duration of beating phenomena and interaction between modes are several of the most important points. They cannot be predicted by looking at those scattered points in the instability zones unless the time history records of the response are examined.

For the 1st instability zone, it was found that when Ω is higher than $2\omega_1$, parametric excitation would happen at lower deck excitation amplitude than the cases where Ω is smaller than $2\omega_1$. For example, at Ω=2.06 ω_1, at the deck excitation amplitude near 0.05 m, parametric excitation already exists. However, for Ω=1.96 ω_1, the deck excitation amplitude needed to trigger the parametric excitation is around 0.175 m.

Another important finding was the fact that there is a limit of deck excitation amplitude with which the parametric excitation would be triggered. For example, when Ω=2.06 ω_1, though the deck excitation amplitude needed to trigger parametric excitation was quite low, when the excitation amplitude was increased gradually, at the amplitude near 0.175 m, parametric excitation no longer exists and the cable oscillation was found to be decreasing with time. The same thing happened for other excitation frequencies. There is always the amplitude of deck excitation where the parametric excitation ceases to exist.

In linear theory, it was predicted that, as long as the excitation amplitude is increased, the magnitude of oscillation would also increase. However, in non-linear case, this does not happen. One of the very likely explanations of this phenomenon is a coupling between modes and changes in the characteristics of mode shapes, which may not be revealed by the linear theory.

4.5 OP parametric excitation

Three-dimensional analysis of cable system requires non-linear methods of solution. The linear analysis of cable system, which allows separation of IP and OP modes, has been well developed and accepted as a method of solution for cable oscillation. However, the main concern of parametric excitation is the occurrence of large amplitude OP oscillations. It is then important to include the OP modes during analyses in the

case of parametric excitation. A very short and yet clear discussion about relationship between the IP and OP oscillations can be found in Luongo et al. (1987); it states that the non-linear coupling terms between IP and OP modes are such that the IP oscillation can exist by itself, while the OP oscillation is always coupled with the IP oscillation.

4.5.1 OP oscillation of the horizontal cable

There have been a few successful studies in revealing OP parametric excitation of horizontally suspended cables, namely by Perkins (1992) and Lee and Perkins (1992). Therefore, it was considered necessary for the present study to validate those previous works.

The possibility of the OP oscillations as the result of parametric excitation of a horizontal cable is very dependent on the value of R. Rao and Iyengar (1991) and Perkins (1992) brought in the importance of internal resonance and coupling between OP and IP modes in reducing the IP stability and enhancing the possibility of OP oscillation. These studies found that when the 1st IP frequency is nearly twice the 1st OP frequency (R is between 0.01 and 0.024), there is a strong possibility of occurrence of the OP oscillations due to a coupling between OP and IP modes. Further to this, Perkins (1992) stated that the 1st IP mode is symmetric, which means that even though the 1st IP is almost twice of 1st OP, R should be in the range where the modal crossover does not occur. This paper stated that during the parametric excitation, there should be an internal resonance between 1st OP symmetric mode and 2nd IP asymmetric mode.

When a MDOF system has the natural frequencies that have certain ratios within each other and if during excitation, this system responds with large amplitude for small excitation amplitude, then the system is said to have an internal resonance. This phenomenon shows the importance of non-linear analysis because it could only happen when the modes are coupled. The existence of internal resonance is more pronounced when accompanied with an external resonance.

Nafyeh and Balachandran (1989) discussed various possibilities of internal resonance for various physical systems. The internal resonance can occur in a system with the cubic non-linearity, if ω_n is approximately equal to ω_m, $|\pm 2\,\omega_m \pm \omega_k|$, or $|\pm\,\omega_m \pm \omega_k \pm \omega_l|$. For a system with the quadratic non-linearity, other than the terms defined above,

the internal resonance could occur when $\omega_n \approx 2\,\omega_m$ or $\omega_m \pm \omega_k$, where the subscripts m, n, k and l of ω indicate the number of modes. Modal interactions from these internal resonances can lead to interesting phenomena, such as the quasi-periodic and chaotic motions. They also stated that for a system with quadratic non-linearity, there are two possibilities of primary parametric resonance, $\Omega=2\omega_1$ and $\Omega=2\omega_2$. An external resonance happens when $\Omega\approx\omega_n$. For example, for a system where $\omega_2=2\omega_1$, and parametric excitation happen at $\Omega=2\omega_1$, then the system is said to have the primary parametric resonance with ω_1 and has an external resonance with ω_2 since $\Omega=\omega_2$.

From the results of the previous research works, the value of R was decided with which the 1st IP frequency becomes nearly twice of the 1st OP frequency and yet it is still in the symmetric mode (e.g. $R_0=0.015$ to $R_0=0.024$). A number of analyses were carried out to obtain the range of excitation frequency that could trigger OP parametric excitation, see section 4.2.1 point 1.c to 1.f. It was found that the OP oscillation is triggered when the excitation frequency is two times the first IP frequency. This finding is rather different from the case of the IP parametric excitation where $\Omega\approx2\omega_1$ (ω_1=1st OP frequency). Nevertheless, it is possible that $\Omega\approx2\omega_2$. Perkins (1992) mentioned the possibility of the occurrence of this condition in relation to the study by Nafyeh and Balachandran (1989). The consequence of this, is the possibility of having a simultaneous principal parametric resonance, because for the specific R near the 1st cross-over, $\omega_2\approx\omega_3\approx\omega_4$. In relation to this, Perkins (1992) stated that the analytical formulation developed in his study was not sufficient to capture the coupling of more than two modes. The present numerical method successfully overcame this difficulty in representing mode coupling for more than two modes.

Finally some distinct OP oscillations were found for a certain range of R near the first cross-over of IP modes, with small amplitude of support excitation. Qualitatively, the results showed very good agreements with Perkins (1992) and Lee and Perkins (1992). Detailed analyses are presented for one value of R with different support excitation amplitudes to capture the importance of the modal cross-over and existence of OP oscillations during the parametric excitation.

4.5.1.1 Horizontal cable with different support excitation amplitudes

From the analysis in section 4.2.1 point 3, further observation upon the time history records of the response was done. In Figure 4.21, trajectories of the quarter span (QS) point for different deck excitation amplitude are given. Presented figures are as follows: (a) to (e) are for the support excitation amplitude of 0.050m, 0.075m, 0.100m, 0.125m and 0.150m respectively. Figure 4.22 shows the trajectory of mid-span (MS) point with the same index (a) to (e) as Figure 4.21.

From Figures 4.21 and 4.22, it is clear that support excitation amplitude defined the behaviour of cable oscillations for a fixed value of the excitation frequency. For amt=0.050m, there is no occurrence of parametric excitation while at amt=0.15m, the IP parametric excitation existed. Though this fact is not recognized from Figures 4.21 or 4.22, it can be seen from the time history records. One can see that, for amt=0.075m, there is a distinct OP oscillation. Figures 4.21 and 4.22 show that amt=0.075m has larger response than others do at time=375s to 390s. At amt=0.10m, OP oscillation is also distinct even though it happened at different time during the time history record (e.g. at time=250s to 265s, the OP oscillation from amt=0.100m is more distinct than the one from amt=0.075m). As support excitation amplitude is increased, the OP oscillation decreased and eventually became hard to notice.

At R=0.02, the 1st IP vibration is in a symmetric mode. When there is support excitation, R changes with time, at small deck excitation amplitude, the change in R would still be within the range before 1st modal cross-over, between R=0.0200 and R=0.0239 (for 12 elements, modal cross over happened at R=0.0246). As support excitation amplitude is increased, R as a function of time would become greater than the crossover point and therefore the 1st IP mode will no longer be symmetric, and there would be no more internal coupling between the 1st OP and the 2nd IP. For example, if R=0.025, the 1st IP mode is asymmetric and the 2nd IP mode is symmetric. By this configuration of mode shapes, the parametric excitation is less likely to occur. This phenomenon highlighted the influence of modal coupling and internal resonance between the 1st OP and 2nd IP modes of vibration.

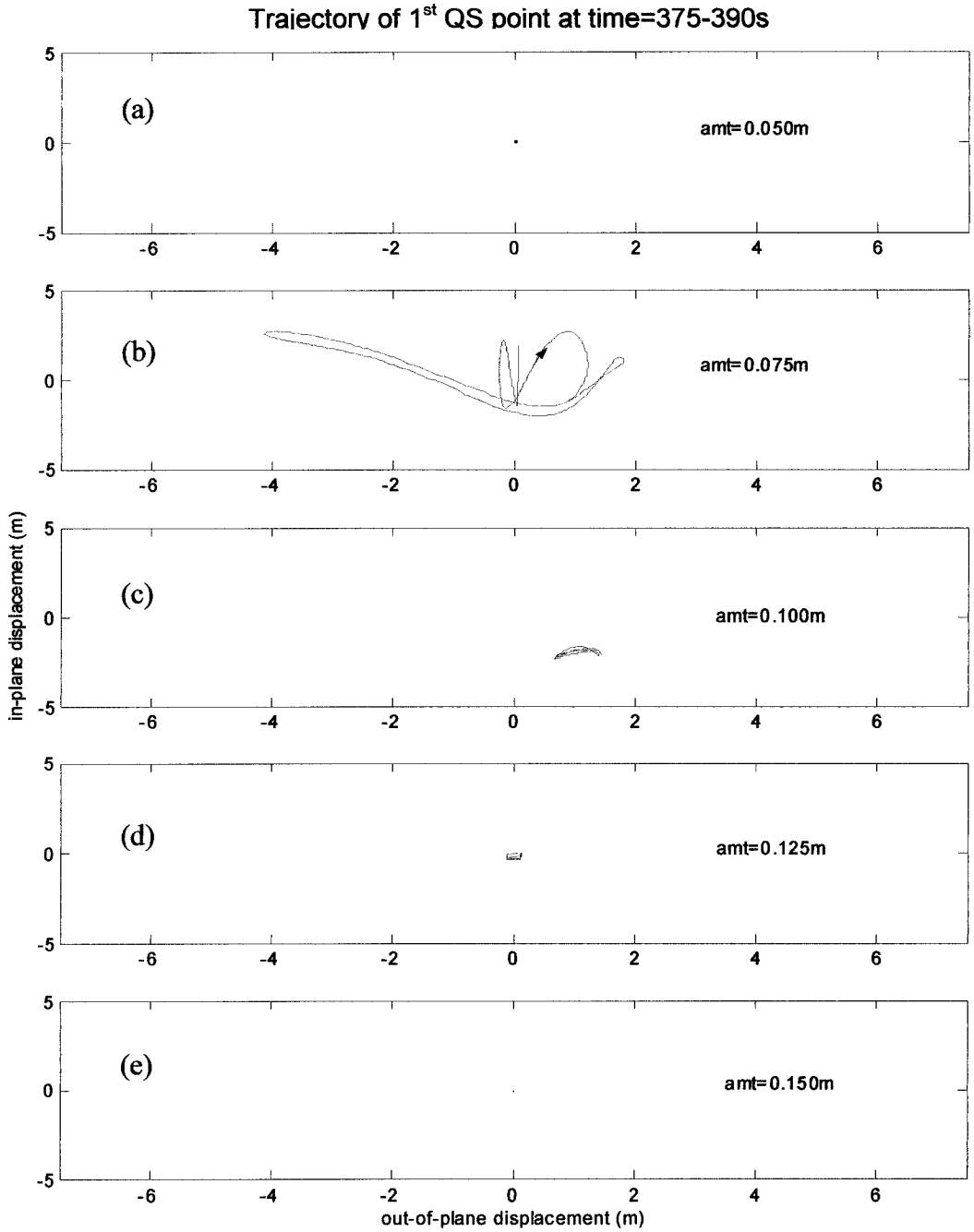

Figure 4.21: Trajectory of 1st QS point of a horizontal cable with $\Omega=2.08\omega_2$

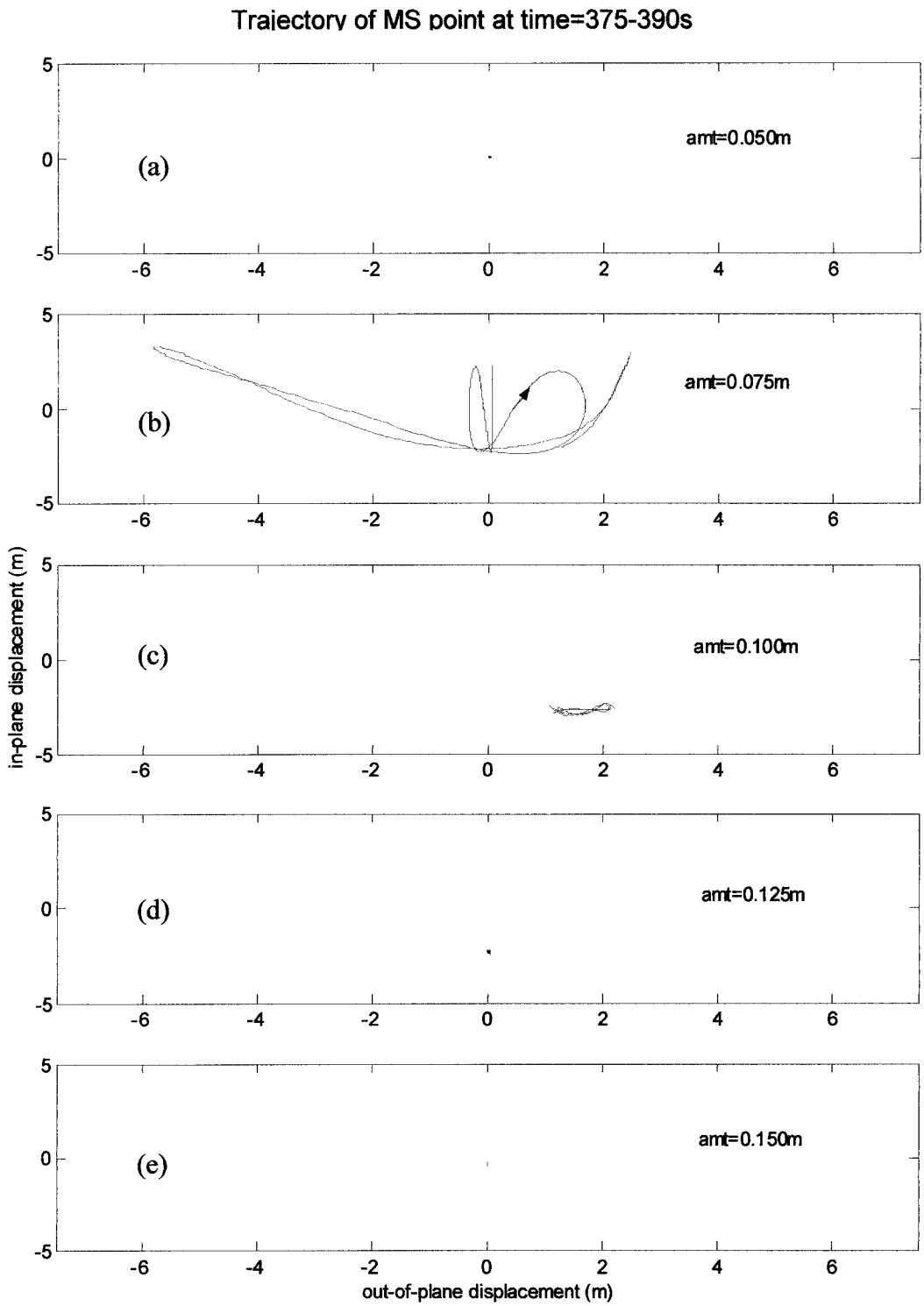

Figure 4.22: Trajectory of MS point of a horizontal cable with $\Omega=2.08\omega_2$

4.5.2 OP oscillation of the inclined cable

A non-planar cable oscillation for inclined cable system was observed coincidentally while the case of IP parametric excitation was investigated. After the finding, to observe this case further, a series of analyses was performed, see section 4.2.2 point 1.c. Unlike the case of a horizontal cable, where all of the parameters were set according to theories from previous works, see section 4.5.1, OP oscillation for the inclined cable was found when support excitation frequency was far from 2 times the 1st OP frequency (e.g. $\Omega=1.83\omega_1$ to $1.90\omega_1$ for deck excitation amplitude of 0.1m), where the linear theory will not predict any instability zone.

The parametric excitations of suspended inclined cables were previously studied by Cai and Chen (1994) and Pinto da Costa (1996). However, they did not find any significant OP oscillations, though they mentioned that under different parameters others than what they studied, strong OP oscillation might occur. Also there is an explanation by Srinil et al. (2003) on the difference of the behaviour of horizontally suspended cable system from the inclined suspended cable, which discussed the much more pronounced contribution of longitudinal amplitudes for the case of inclined cable that render OP oscillations less possible to occur.

Clear explanation on why the OP oscillation occurred when the excitation frequency is far from the primary instability zone is definitely needed. Because if one looks at the change of R with time at, say $\Omega=1.85\omega_1$, for certain support excitation amplitude, say amt=0.1m, is exactly within the same range as the change of R for $\Omega=2\omega_1$. The R is between 0.00897 and 0.01193, this brings tension fluctuation, $\Delta H=0.25H$. Nevertheless, the tension fluctuation happens at different frequency and somehow this condition triggers the OP oscillation.

Further analyses were carried out in order to obtain better understanding on the difference between IP parametric excitation and the large amplitude OP parametric excitation. Both of them were caused by support excitation and there must be a relationship between the pattern of cable oscillation and fluctuation of tension due to support excitation. It was found that for IP parametric excitation, the highest transient peaks coincide with highest peaks of the cable tension. For the case of OP parametric excitation, an opposite tendency occurred; the highest transient peaks coincide with

lowest the tension peaks. Though this finding is rather unique, it will not be the only cause of these phenomena. More detailed analyses about this matter are definitely in need.

4.5.3 Difference in OP oscillation of the horizontal and inclined cable

Characteristics and initiation of growth of OP oscillations for the case of inclined cable are different from those of the horizontal cable. Detailed observation of the growth of oscillations for these two cases in OP modes revealed this difference.

4.5.3.1 The growth of OP oscillation for the horizontal cable

The growth of OP oscillation was observed as an extension of primary parametric excitation for a certain range of R, where 1st IP frequency is nearly twice the 1st OP frequency. As defined before in section 4.5.1, surely, OP parametric excitation finally occurred at R_0 in the neighbourhood of the 1st cross-over, say between R_0=0.015 and R_0=0.020. Therefore, it was obvious that significant OP oscillation of horizontal cable occur after IP oscillation grew to certain high amplitudes.

To analyse further the OP parametric excitation of horizontal cable, an analysis based on the cable response from section 4.2.1 point 3 with support excitation amplitude of 0.1m was carried out. The tendency of OP oscillation growth of horizontal cable can be observed from the trajectories of the 1st quarter-span (QS) point, mid-span (MS) point and the 2nd QS point that are plotted in Figures 4.23 to 4.28. From Figure 4.23, one can see that the oscillation is IP, going up and down. After longer duration of excitation, from Figure 4.24, it can be seen that slight OP oscillation took place. In Figures 4.25 to 4.26, it is observed that after certain IP amplitudes, a swaying motion started and grew larger, see Figures 4.27 and 4.28, until non-linearity of the system limited the growth. The pattern of this oscillation agrees well with Perkins (1992), which showed experimental result of a horizontally suspended cable.

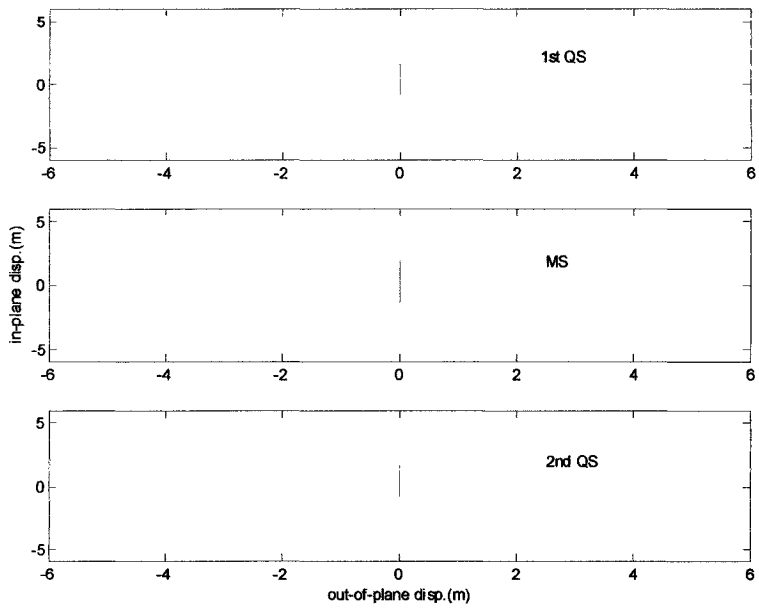

Figure 4.23: Trajectories of 1st quarter span (QS), mid-span (MS) and 2nd QS points of a horizontal cable at $\Omega=2.08\omega_2$, from time=174.76 to 181.12s.

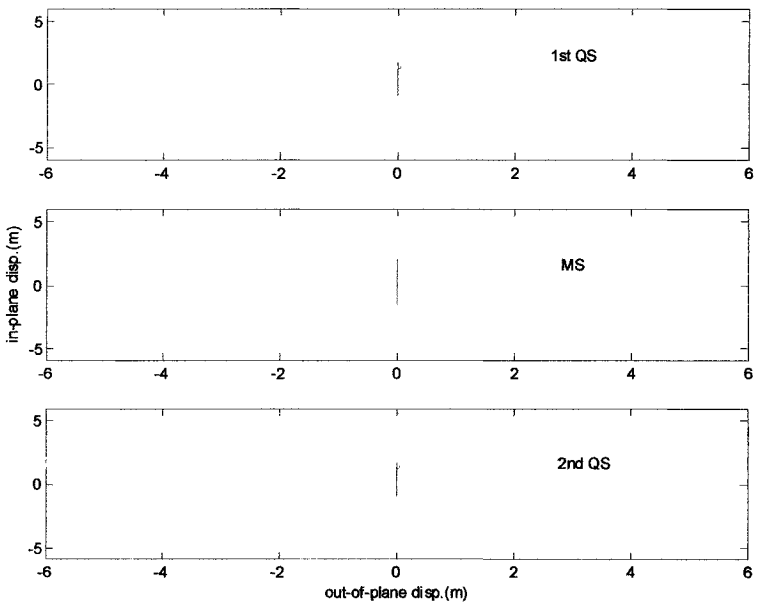

Figure 4.24: Trajectories of 1st QS, MS and 2nd QS points of a horizontal cable at $\Omega=2.08\omega_2$, from time=190.65 to 197.00s.

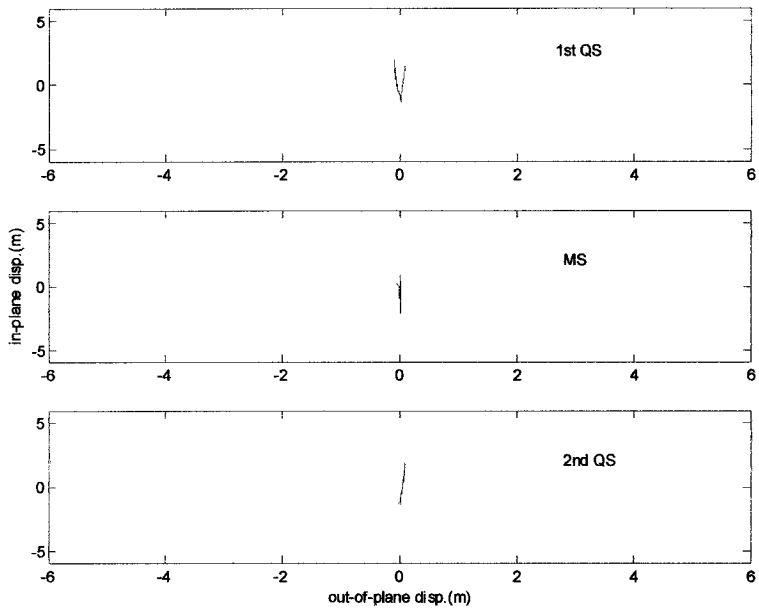

Figure 4.25: Trajectories of 1st QS, MS and 2nd QS points of a horizontal cable at $\Omega=2.08\omega_2$, from time=225.60 to 231.96s.

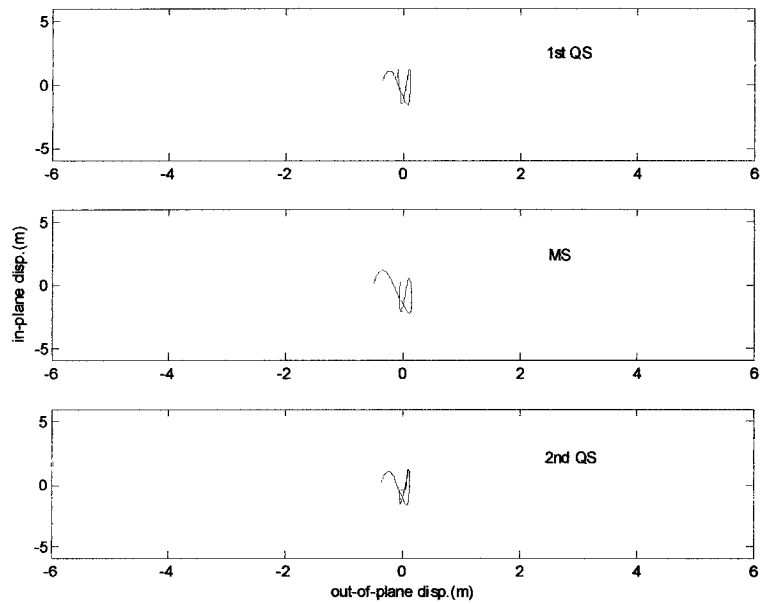

Figure 4.26: Trajectories of 1st QS, MS and 2nd QS points of a horizontal cable at $\Omega=2.08\omega_2$, from time=231.96 to 238.31s.

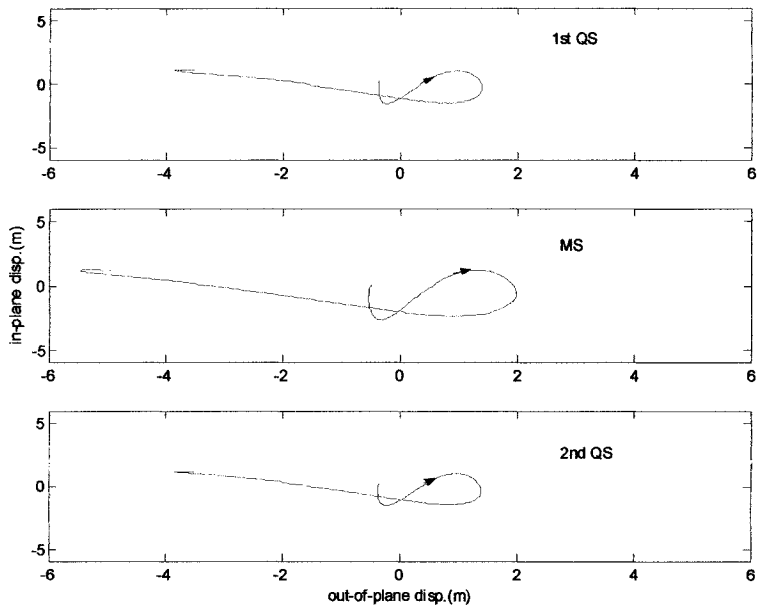

Figure 4.27: Trajectories of 1st QS, MS and 2nd QS points of a horizontal cable at $\Omega=2.08\omega_2$, from time=238.31 to 244.67s.

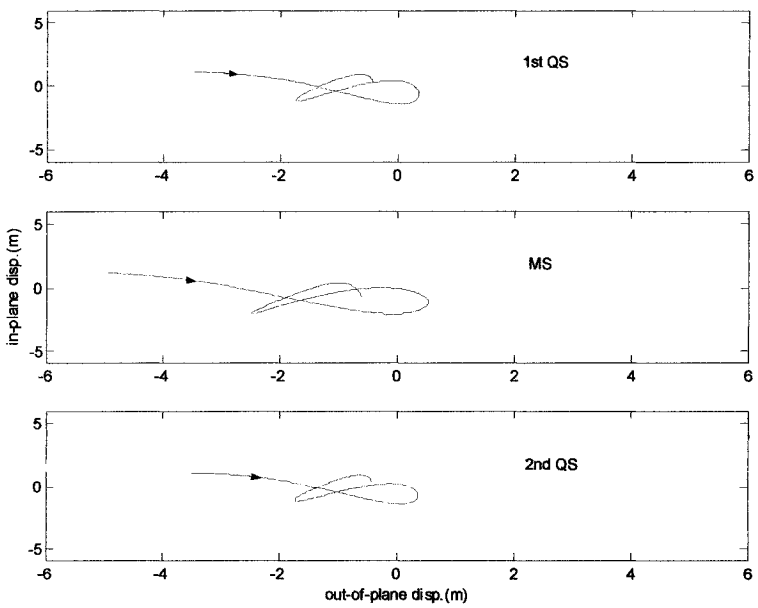

Figure 4.28: Trajectories of 1st QS, MS and 2nd QS points of a horizontal cable at $\Omega=2.08\omega_2$, from time=244.67 to 251.02s.

4.5.3.2 The growth of OP oscillation for the inclined cable

The cable data that are used for this section are taken from section 4.2.2 point 1.c.ii) with $\Omega=1.85\omega_1$. The Figures 4.29 to 4.34 show the growth of large amplitude oscillation of suspended inclined cable from the trajectories of 1st QS, MS and 2nd QS points. The tendency of oscillation growth is completely different from horizontal cable. The occurrence of OP oscillation is rather unique for inclined cable.

At the beginning of analysis, there is no significant in-plane oscillation; in fact, one would think that there is no parametric excitation if simulation was run for a short duration of time. However, after the simulation was run for about 400 cycles of the excitation frequency, in Figure 4.29, OP oscillation occurred. After the OP amplitudes became obvious, IP amplitudes started to grow along with OP, which is more apparent in Figure 4.31. Instead of having a swaying motion like the one found from OP oscillation of horizontal cable, inclined cable has a whirling motion. A clear pattern of this oscillation can be observed in Figures 4.33 and 4.34.

From the pattern of the cable oscillation, it seems that OP oscillation for the inclined cable is quite influenced by the 2nd OP mode because the 1st QS and the 2nd QS had opposite directions. While the OP oscillation of the horizontal cable, the 1st QS and 2nd QS are more in-line, this means that the 1st OP mode had more influence in the oscillation.

In short, for the case of the horizontal cable, OP occurs after IP oscillation reached certain amplitude. For the case of the inclined cable, OP occurs with no significant IP, but as OP grew larger, IP started to show significant amplitudes.

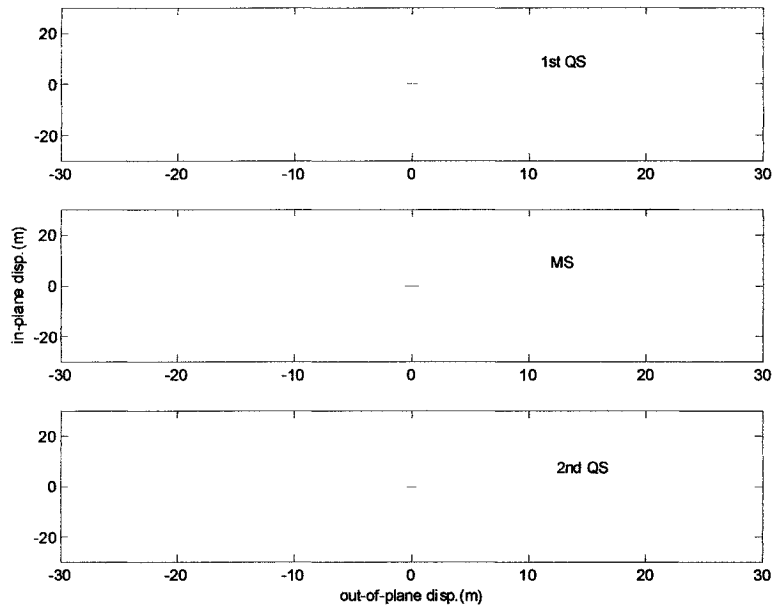

Figure 4.29: Trajectories of 1st QS, MS and 2nd QS points of an inclined cable at $\Omega=1.85\omega_1$, from time=731.21 to 738.80s.

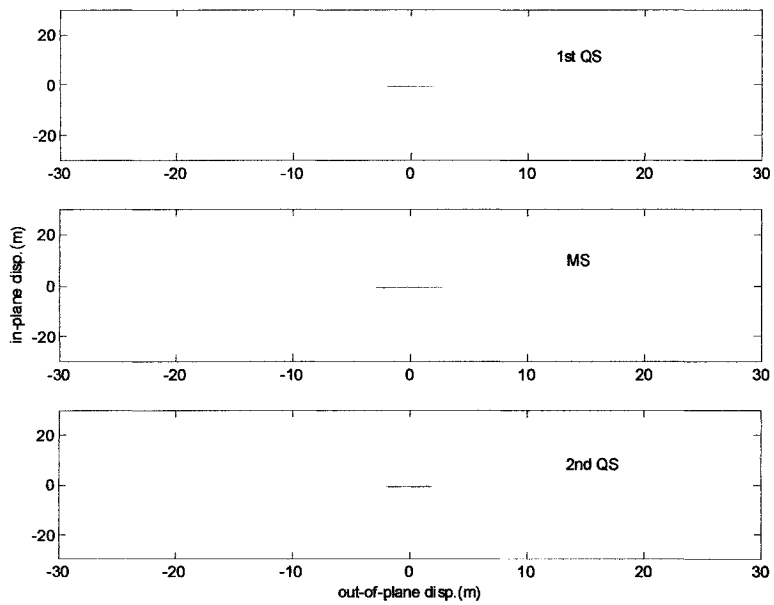

Figure 4.30: Trajectories of 1st QS, MS and 2nd QS points of an inclined cable at $\Omega=1.85\omega_1$, from time=788.18 to 795.78s.

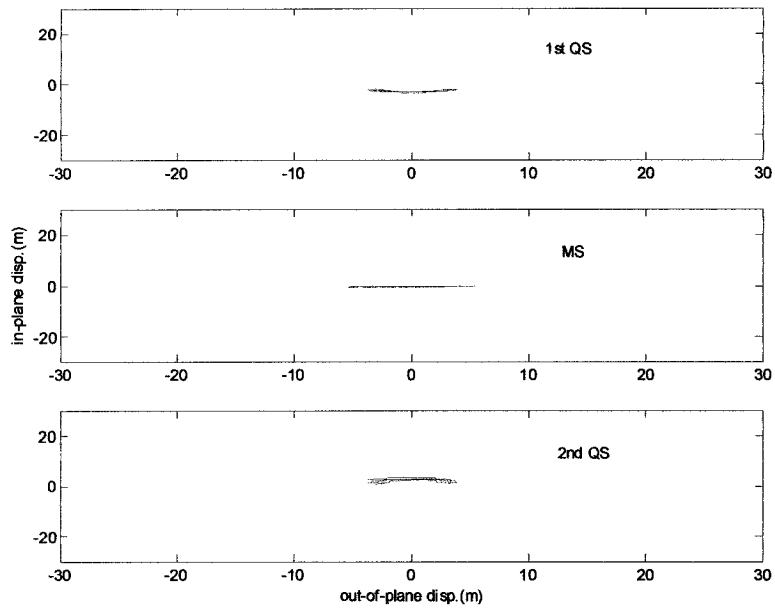

Figure 4.31: Trajectories of 1st QS, MS and 2nd QS points of an inclined cable at $\Omega=1.85\omega_1$, from time=845.16 to 852.76s.

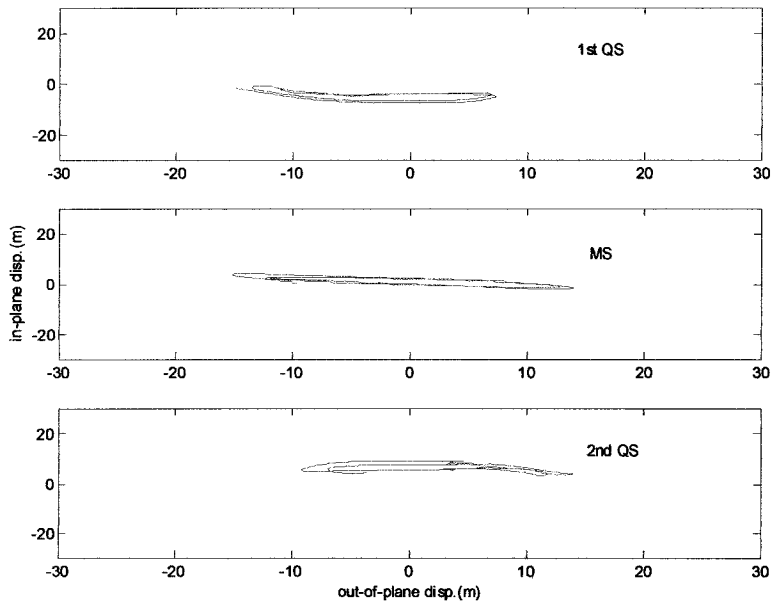

Figure 4.32: Trajectories of 1st QS, MS and 2nd QS points of an inclined cable at $\Omega=1.85\omega1$, from time=875.55 to 883.15s.

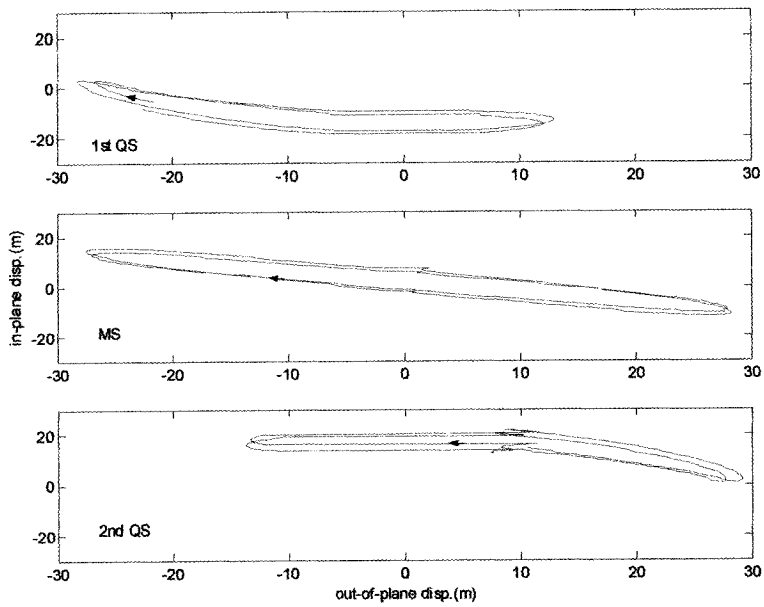

Figure 4.33: Trajectories of 1st QS, MS and 2nd QS points of an inclined cable at $\Omega=1.85\omega_1$, from time=902.14 to 909.74s.

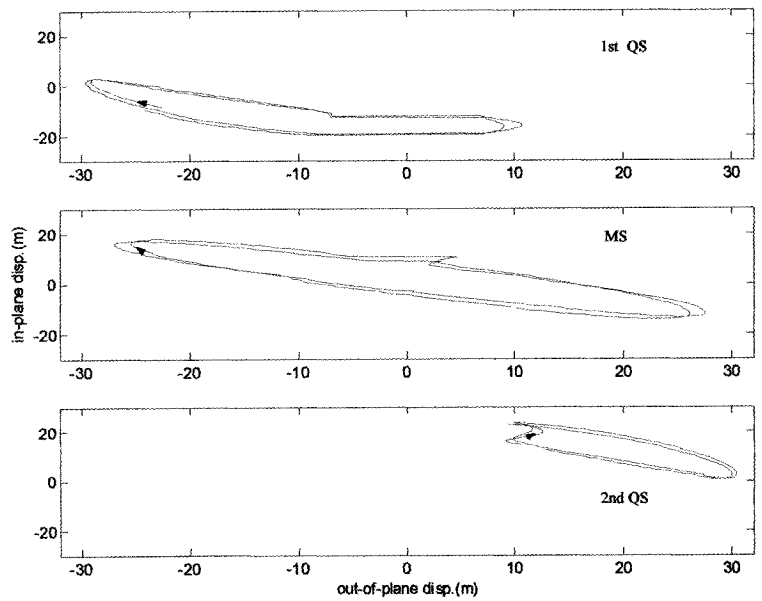

Figure 4.34: Trajectories of 1st QS, MS and 2nd QS points of an inclined cable at $\Omega=1.85\omega_1$, from time=909.74 to 917.33s.

4.6 Instability and phase portrait representation

Using the phase portrait representation, some interesting features about parametric excitation can be found. The phase portrait of MS point for IP parametric excitation was plotted by using the result from section 4.2.2 point 1.a.ii) with $\Omega=2\omega_1$. The plot is shown in Figure 4.35. Several limit cycles are clearly observed, which indicates the instability of the system during oscillation. The shift of the center of the limit cycles can also be observed, the final centre of the limit cycle is shifting below the initial equilibrium. If plotted in 3D orientation, with additional dimension of time, the plot in Figure 4.35 becomes Figure 4.36. It can be seen that the plot forms 3D spherical bulb, first extending then receding with time.

For the OP oscillation of an inclined cable, the from section 4.2.2 point 1.c.ii) with $\Omega=1.85\omega_1$. The plot is shown in Figure 4.37, the velocity and the displacement response are much higher than the IP oscillation. The cause of this characteristic is that the nature of the cable vibrations is completely different, between IP and OP parametric excitations. The 3D plot is shown in Figure 4.38. From this figure, it is clear that before large OP oscillations occurred, practically there is no significant response given by the cable system.

For the OP oscillation of a horizontal cable, shown in Figure 4.39, the result from section 4.2.1 point 3.b with 0.1m of support excitation amplitude. From Figure 4.39, shifts of limit cycles are obvious. The shape of the plot is very irregular. The same irregularity can also be observed from the 3D plot in Figure 4.40.

In conclusion, from Figures 4.35 to 4.40, it is not easy to observe and analyse gainful insight into the behaviour of parametric excitation, especially in the case of OP oscillations. The nature of oscillations of IP case is easier because when large amplitudes in oscillations are happening, they remained in the same plane, the cable plane. In OP oscillation, for each time step in which large OP amplitudes happened, they are not in the cable plane. Therefore, representation in phase portrait gets quite complicated and could be difficult to interpret the behaviour of the system.

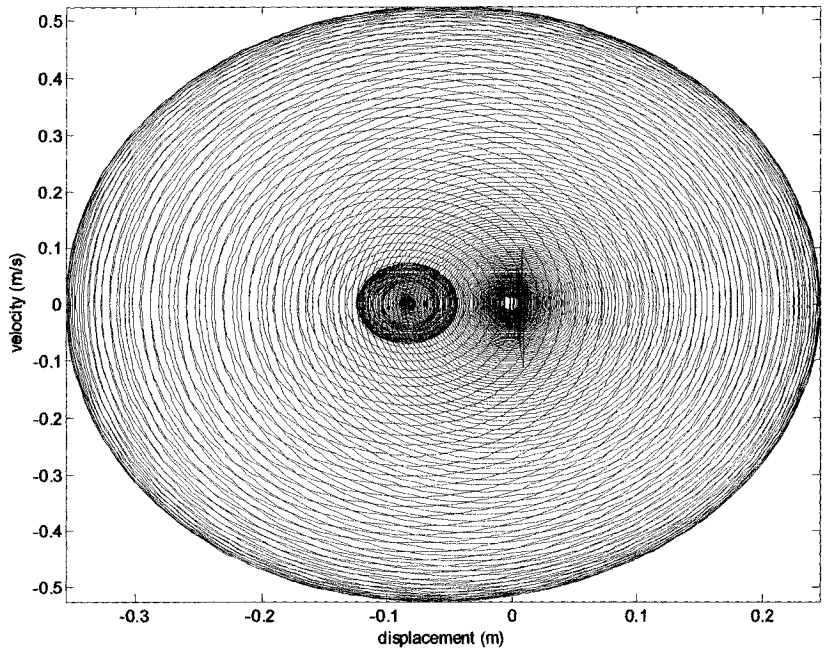

Figure 4.35: 2D Phase portrait of an inclined cable, $\Omega=2\omega_1$

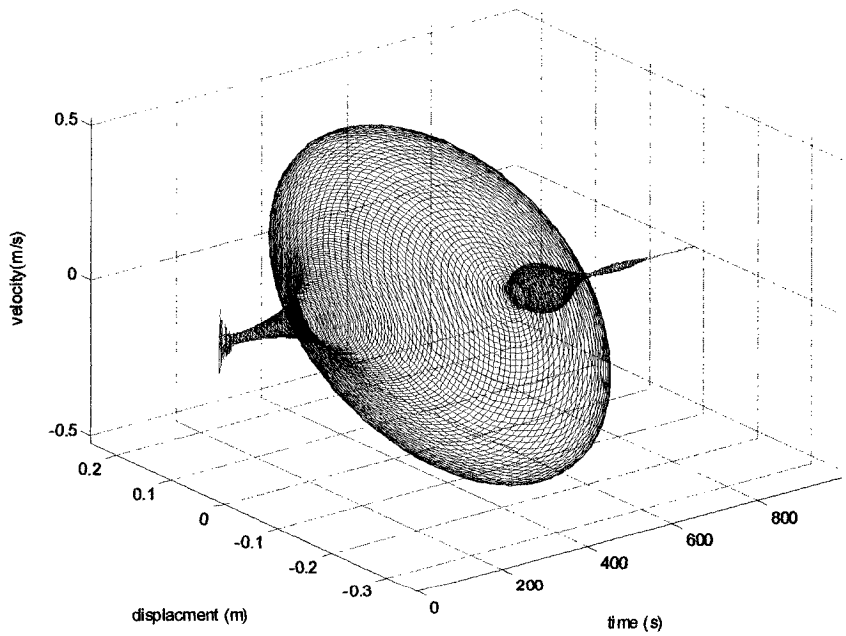

Figure 4.36: 3D Phase portrait of an inclined cable, $\Omega=2\omega_1$

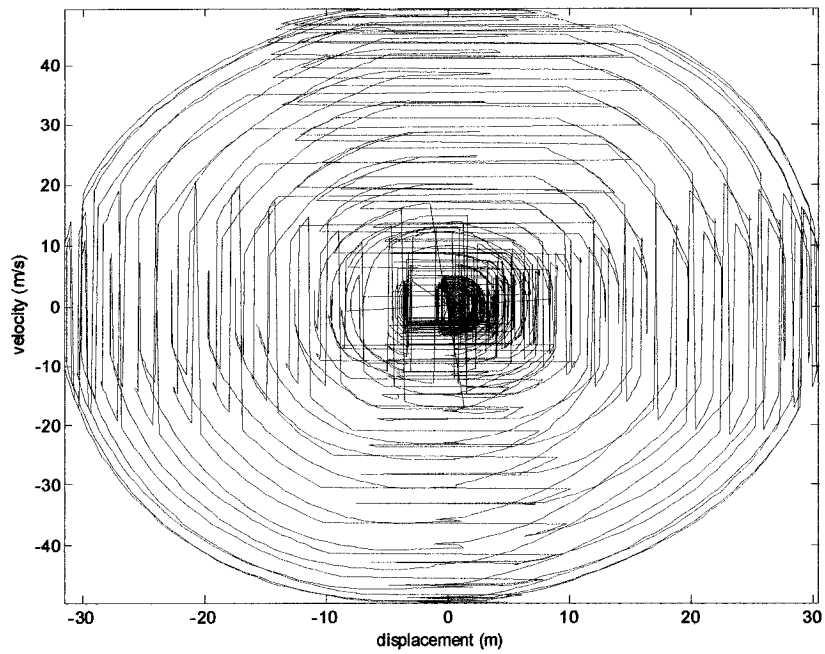

Figure 4.37: 2D Phase portrait of an inclined cable, $\Omega=1.85\omega_1$

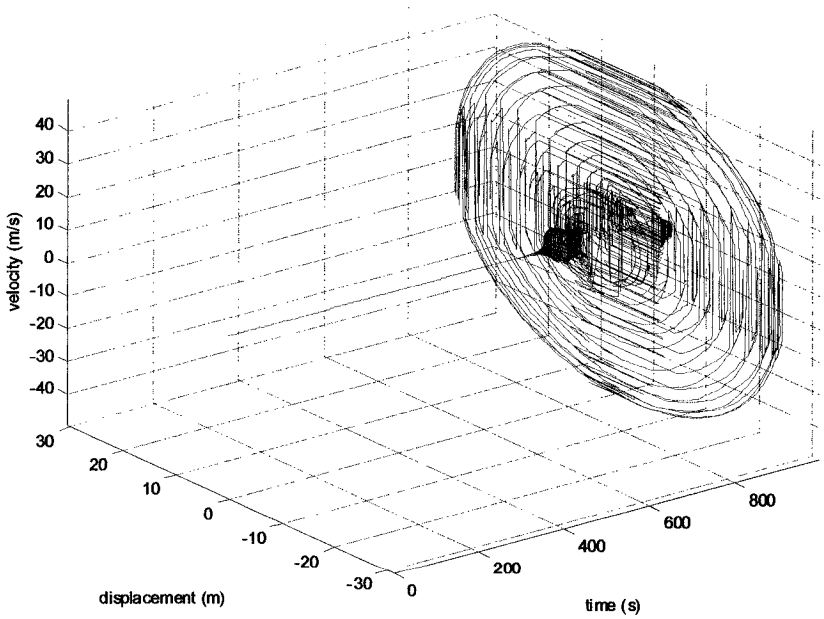

Figure 4.38: 3D Phase portrait of an inclined cable, $\Omega=1.85\omega_1$

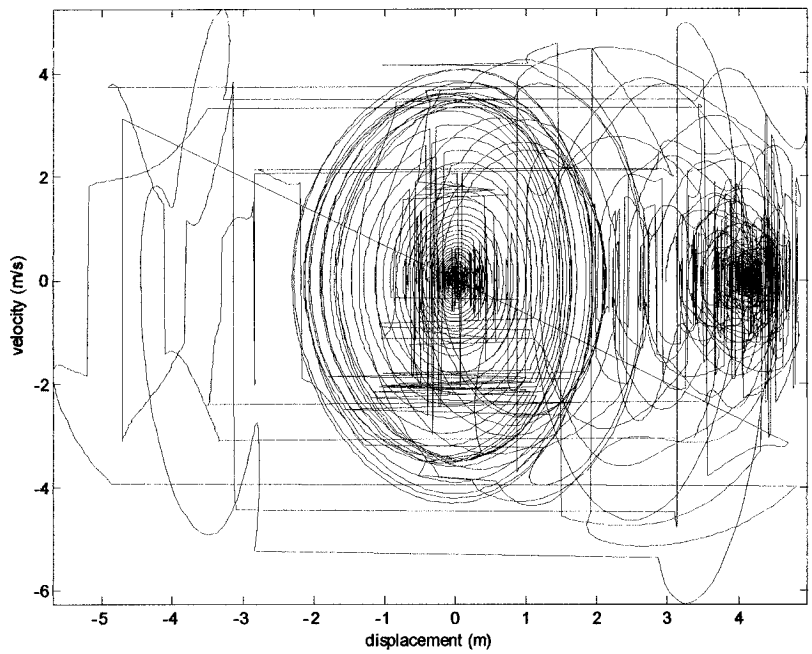

Figure 4.39: 2D Phase portrait of a horizontal cable, $\Omega=2.08\omega_2$

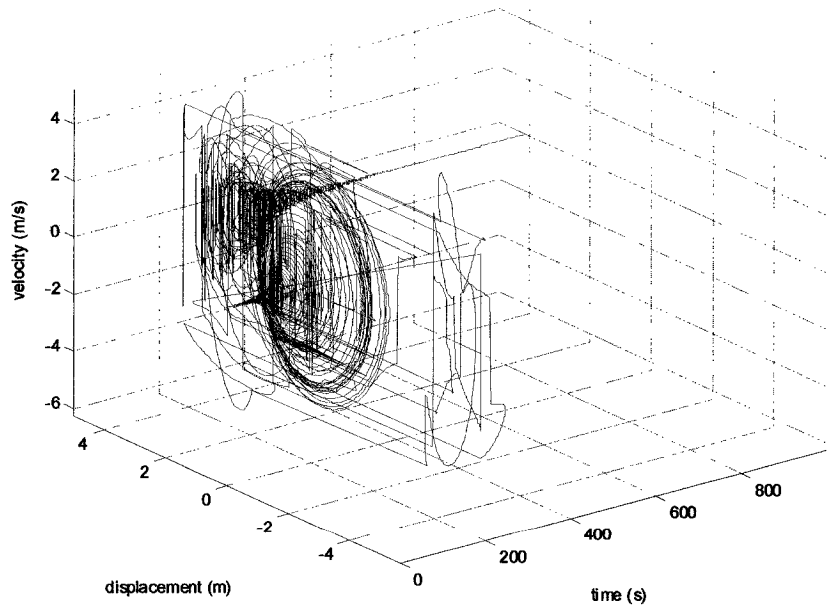

Figure 4.40: 3D Phase portrait of a horizontal cable, $\Omega=2.08\omega_2$

4.7 Bifurcation and chaotic vibration

Parametric excitation of a physical system has long been related to possibility of bifurcation and chaotic vibration. Hence, so is the case of the suspended cable system. The existence of bifurcation and chaotic vibration during parametric excitation definitely shows the loss of stability of the system. Nonetheless, bifurcation and chaotic vibration can happen to an externally excited non-linear system or a self-excited system. The present study was able to validate the possibility of these phenomena for both inclined and horizontal cables.

When the parameters of a system are changed and if some qualitative changes occur in the behaviour of the system, then the system is experiencing bifurcations (Thomsen, 2003). This phenomenon can only occur when the system is structurally unstable. For a structurally stable system, its qualitative properties are retained even if they are slightly perturbed. However, a structurally unstable system does not retain its qualitative properties when it is slightly perturbed.

Chaotic vibration has characteristics of ragged waveform. The recurrent patterns of the vibration are not exactly the same and they repeat at irregular intervals, so the motion is truly non-periodic (Harris and Piersol, 2002). Another typical characteristic of chaotic vibration is that, for repetitive runs with nearly identical initial conditions, the results of the responses of the system are different each time.

The existence of bifurcation and chaotic motion could be predicted analytically. The accuracy of the prediction of bifurcation is good and in some cases, the agreement with experiments has been confirmed (Perkins, 1992). However, for the case of chaotic motion, its existence can be clearly detected only by using numerical models (Harris and Piersol, 2002). The physical model experiment could also realize the existence of chaotic motions. However, there has never been a clear measurement since the results are highly dependent on various physical boundary conditions during an experiment.

A possibility of bifurcation and chaotic vibration was first discussed for the case of horizontal cable with R near the first cross-over of the IP modes by Rao and Iyengar (1991) for the external excitation of the horizontal cable. Zhang and Tang (2002) also

studied the horizontal cables with the same characteristics. Their study was about combination of parametric excitation and external excitation. They discussed about the chaotic vibrations of the horizontal cable.

The existence of the non-planar oscillations definitely proves the existence of bifurcation because the non-planar oscillation will only happen after the IP oscillations bifurcates. Since there have been strong indications that bifurcation can be accompanied by chaotic vibration, the numerical analysis with similar parameters was run at least two times, and every time, the result showed divergence every time, even though the main oscillation behaviour before bifurcation occurs remains the same.

Figure 4.41 showed the divergence between two runs of similar numerical analysis of a cable system, the cable parameters are from section 4.4.1 with $\Omega=1.85\omega_1$. For the characteristic of chaotic vibration that has irregular or ragged waveform. It is difficult, however, to observe the existence of this chaotic motion by looking at the time history response of a system or from a phase portrait.

The evidence of a chaotic vibration would be clear by using the Poincaré section. This method is quite similar to the phase portrait, which shows the functional relationship of velocity and displacement. The difference is, instead of plotting for each time step, the data will be stroboscopically sampled, meaning that it will only plot corresponding data for each cycle according to the natural period of the forced excitation function.

Since the parametric excitation is an autonomous oscillation, there is no natural period for the driving force on which the Poincaré section is based, according to Thomsen (2003), and therefore the natural period should be taken from the excitation function of the system, which is the support excitation. Details of Poincaré section are available at Thompson and Stewart (1987).

The Poincaré section reveals the true behaviour of an oscillation, a periodic motion will result in finite number of points (a periodic motion results in only 2 points, the 1^{st} point is the beginning of a cycle, the 2^{nd} point is at the end of the cycle), an infinite number of points filling up a closed curve correspond to quasi-periodic motion, and infinite number of orderly distributed points (generally) corresponds to chaotic motion.

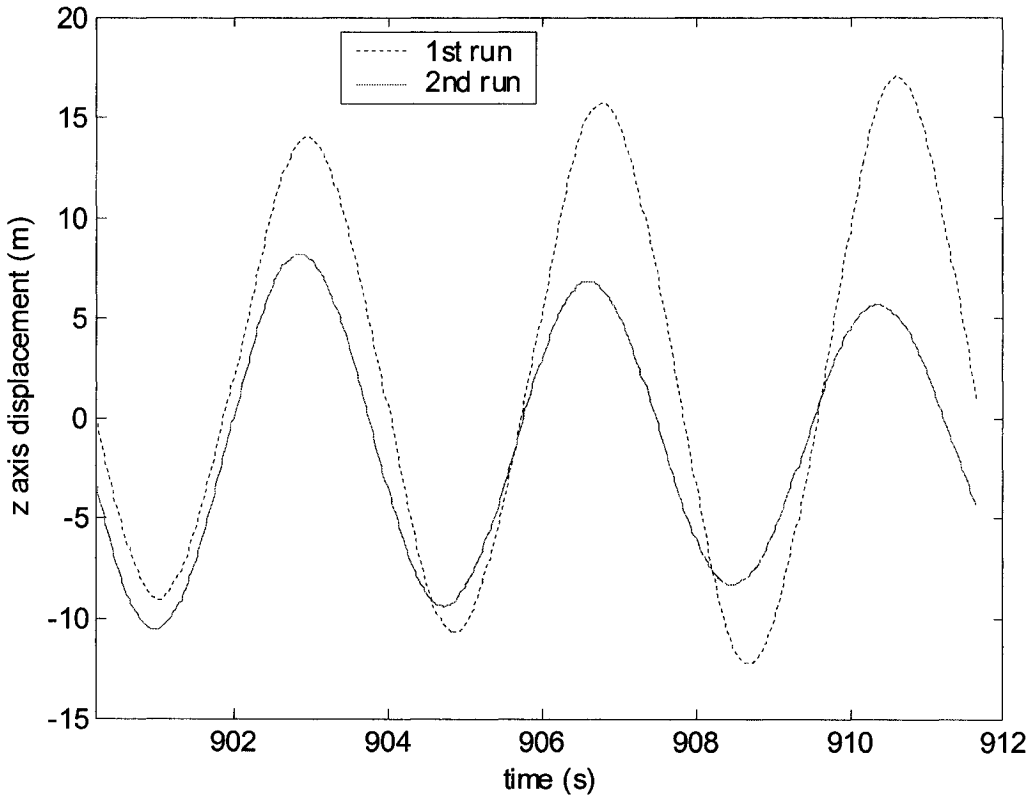

Figure 4.41: Divergence of two runs of a cable system with similar parameters

4.7.1 Chaotic vibration of the horizontal cable

To plot the Poincaré sections, the global coordinates, x, y and z, are combined to get the resultant of the response. After that, velocity and displacement response are plotted for each cycle of the support excitation. For example, for the horizontal cable, using the analysis from section 4.2.1, point 3 with support excitation amplitude=0.1m, the period of the support excitation function is T_p=1.59s, corresponding velocity and displacement are plotted for every T_p up to the total duration of time history record.

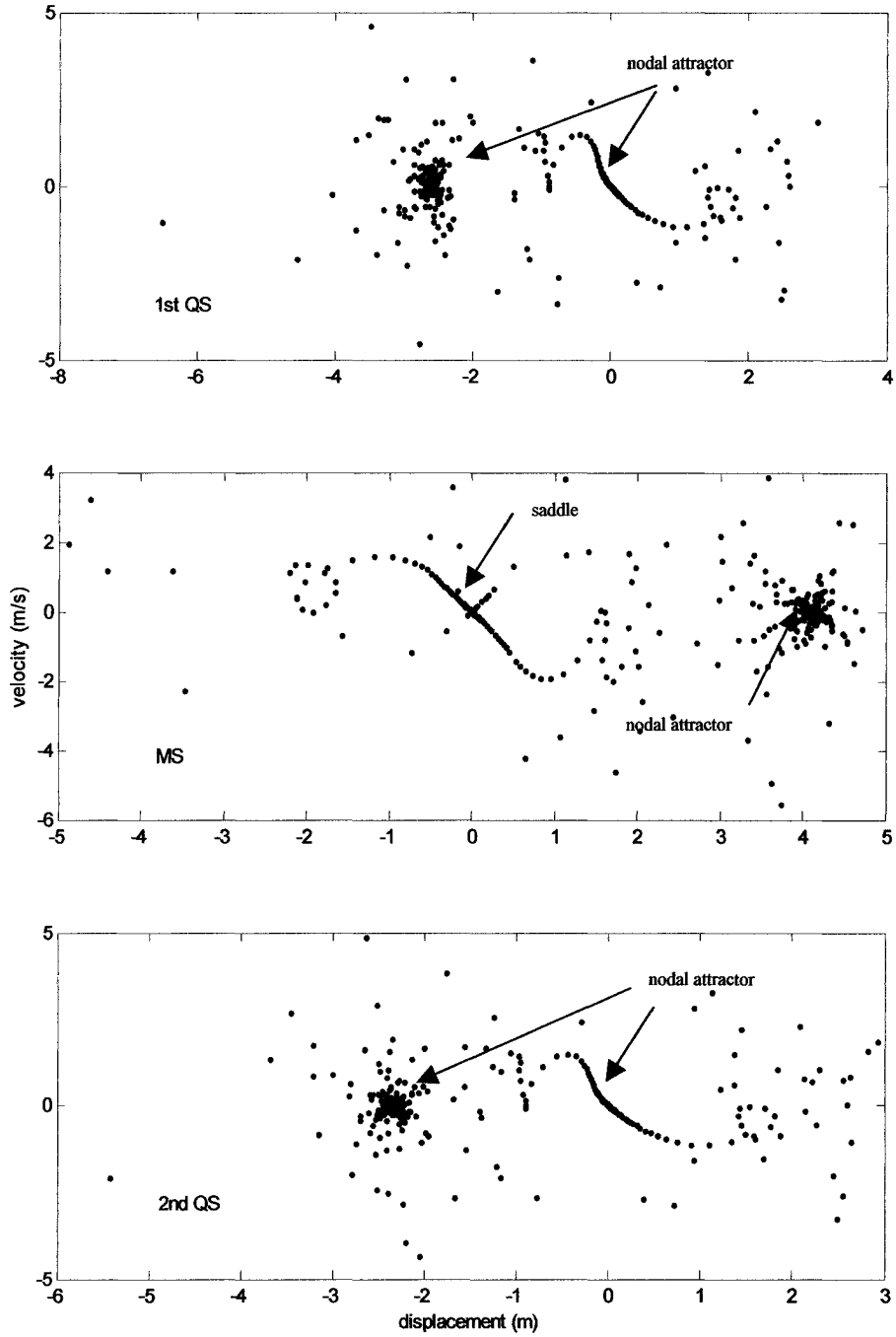

Figure 4.42: Poincaré section of a horizontal cable with $\Omega=2.08\omega_2$

Figure 4.42 shows the Poincaré section of 1st QS, MS and 2nd QS points. From the figure, one can see a very large number of scattered points without a clearly defined pattern. There exist nodal attractors in the 1st QS, MS and 2nd QS and a saddle point in the MS. When the pattern of dots form a nodal attractor, the sequence of the oscillation progresses towards or moves away from a fixed point (Thompson and Stewart, 1987). In Figure 4.42, plots of 1st QS and 2nd QS, one can see that there are 2 nodal attractors. The oscillation moves away from its initial position (at displacement and velocity equal to zero) towards a lower direction but not fixed to one exact point. At 1st and 2nd QS, the final positions hover around at lower positions than the initial positions of the cable configuration. The existence of a saddle means that at first the oscillation progresses towards a fixed point and slows down but then veers away (Thompson and Stewart, 1987). The nodal attractors at MS are positioned above the equilibrium position. Observing from the positions of final nodal attractors, it can be concluded that the horizontal cable sample has an influence of a symmetric mode during its oscillation.

As mentioned before, Zhang and Tang studied (2002) the chaotic motion of the horizontally suspended cable with exactly the same range of R as the present study. In their study, they did not plot any Poincaré section to clarify the existence of the chaotic motion. Though they showed some phase portraits, clear qualitative comparison between their findings and the present study cannot be obtained due to the complexity of the phase portraits.

4.7.2 Chaotic vibration of the inclined cable

The case of the OP oscillation of an inclined cable, which leads to bifurcation and chaotic motion, is plotted into the Poincaré section in which the analysis result from section 4.2.2 point 1.c.ii) with $\Omega=1.85\omega_1$ are used.

Even though the exact cause of this instability cannot be immediately explained, there is an indication of internal resonance between the 1st OP (ω_1) and 2nd OP mode (ω_3), ratio of $\omega_1/\omega_3 = 0.5$ and there is also the effect of external resonance from the 2nd OP mode, $\Omega=0.93\ \omega_3$.

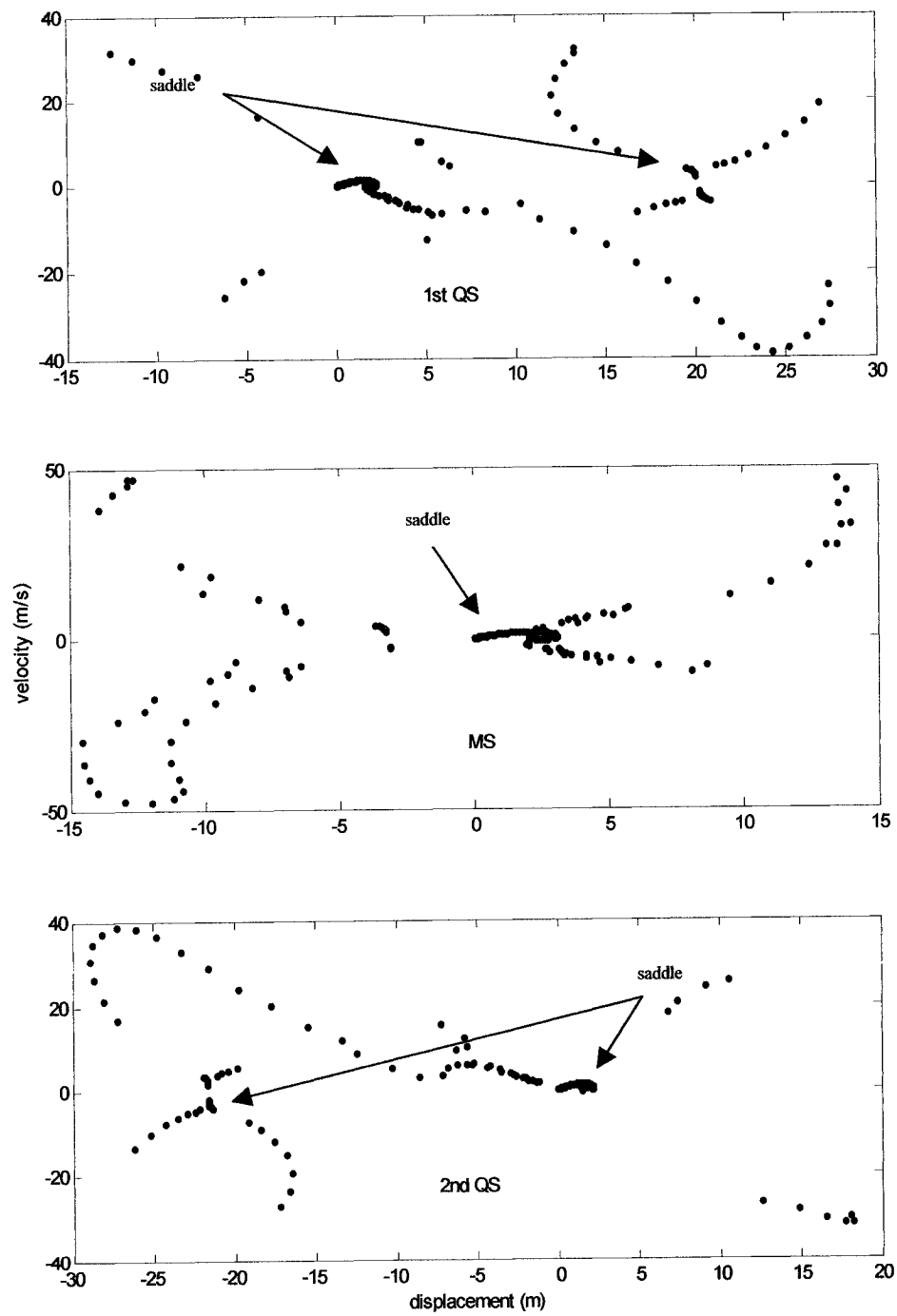

Figure 4.43: Poincaré section of an inclined cable system with $\Omega=1.85\omega_1$

From Figure 4.43, it is observed that the pattern of chaotic motion of an inclined cable is different from the horizontal cable. There exist more saddles and there is no obvious nodal attractor. From Figure 4.43, it can be concluded that the fixed locations of the oscillation are not really obvious. The tendency of the oscillation is such that 1st QS, MS and 2nd QS are veering away after reaching some fixed points. However, every saddle formed at each QS always has an opposite direction corresponding to the other QS and this is an indication that the oscillation is influenced by an asymmetric mode.

The finding of the existence of chaotic motion during a parametric excitation of an inclined cable so far has never been reported anywhere else. Though the indication of the existence of chaotic motion was well known for the non-linear vibration of horizontal cable, as concluded in Cremona (2003), there was no mention of this phenomenon for the case of an inclined cable.

From the present study, it was observed that every existing chaotic motion emerged from the existence of significant OP oscillation. Thus, it can be concluded that the loss of stability due to OP oscillation results in the existence of chaotic motion of the cable system.

4.8 Quasi-periodic vibration

It would be interesting to find out the pattern of the Poincaré section for the IP parametric excitation. As it has been observed, the IP parametric excitation did show instability by having exponential increase in amplitudes until the nonlinearity of the cable system limited the amplitude growth. However, this instability is not a chaotic motion, because if repeated analyses are performed, the same result will be obtained.

To plot the Poincaré section, the analysis result from section 4.2.2 point 1.a.ii) with $\Omega=2\omega_1$ is used. Figure 4.44 shows the Poincaré section of IP parametric excitation for 1st QS, MS and 2nd QS points. From this figure, it can be concluded that IP parametric excitation is a quasi-periodic motion because the plot of the points are filling up a closed curve.

The term quasi-periodic is a type of recurrent motion. As defined by Thompson and Stewart (1987), this phenomenon happens when a periodic motion is modulated in some way by a second motion. The second motion itself is periodic but with a different period. The ratio between the frequencies of the first motion and the second motion is not a ratio of integers. The quasi-periodic is the only instability phenomenon that can be found in two-dimensional orientation, as stated in Thompson and Stewart (1987).

The definitions above definitely agree with the findings from the present study. The incommensurable ratio of the tension oscillation and cable response is obvious as defined briefly in 4.5.2. It is also evident that for the case of IP parametric excitation, the cable response is purely IP that is within two-dimensional orientation.

A study by Zhang and Tang (2002) reported quasi-periodic phenomenon for horizontally suspended cables within similar cable parameters as study by Perkins (1992). Nevertheless, the quasi-periodic phenomenon for inclined suspended cable has never been reported before in previous works related to parametric excitation.

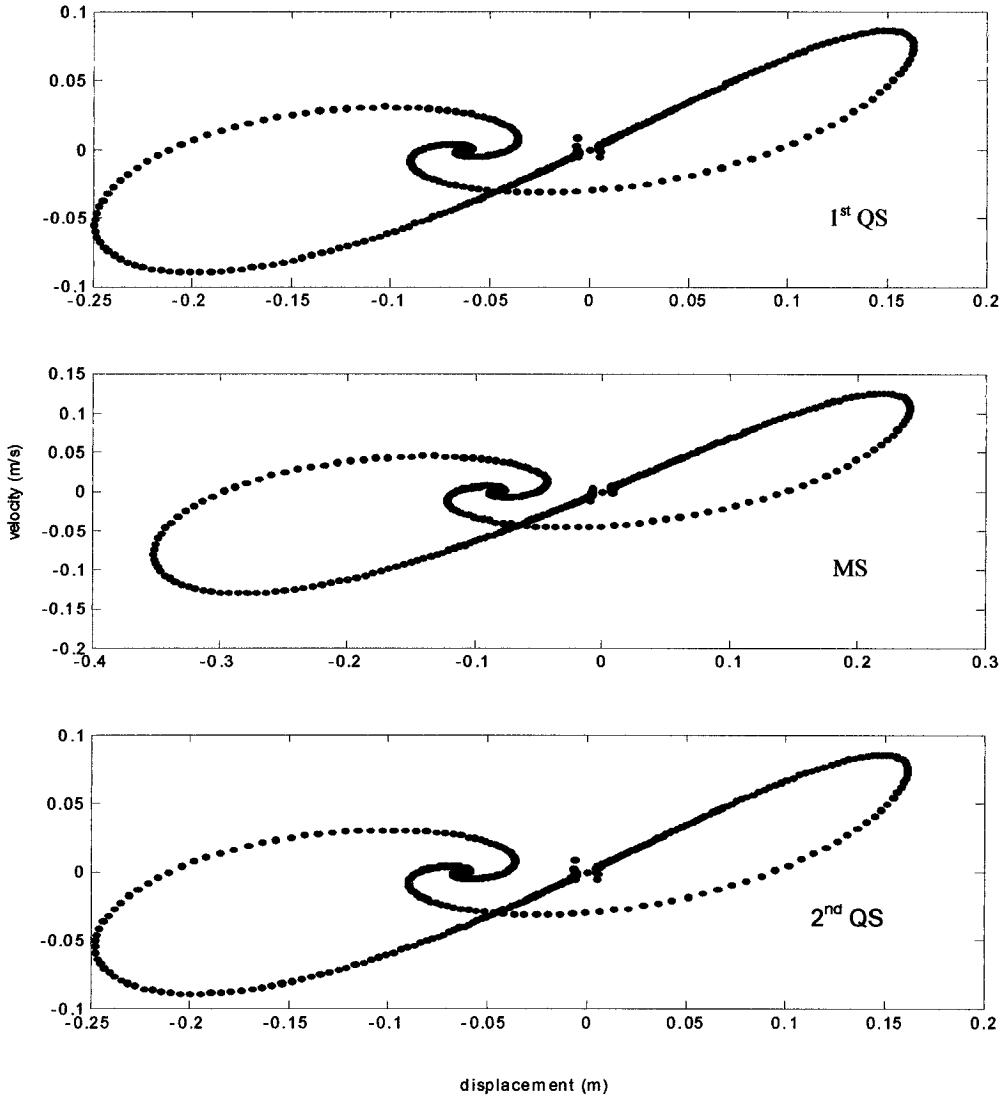

Figure 4.44: Poincaré section of an inclined cable with $\Omega=2\omega_1$

4.9 Summary of Chapter 4

The present study was able to validate:

1. The relationship between various sag-to-span ratio (R) and the first four natural frequencies (1st out-of-plane (OP), 1st in-plane (IP), 2nd OP, 2nd IP) for inclined and horizontal cables.

2. The existence of mode shape transition zones and the difference of the inclined and horizontal cables in the IP mode shape change.
3. The existence of the primary and secondary parametric excitations of the inclined cables and that they are within the 1st and 2nd instability zones.
4. The nature of non-linear parametric excitation response; the growth of response amplitude during parametric excitation, going up until the non-linearity of the system limits further growth.
5. The OP oscillation of the horizontal cable with R near the value of the 1st cross-over of IP modes.

The present study also found:

1. The possibility of coupling between more than two modes for the parametric excitation of the horizontal cable with R near the 1st cross-over value since $\Omega \approx 2\omega_2$ and $\omega_2 \approx \omega_3 \approx \omega_4$.
2. The support amplitude that triggers the parametric excitation has a limit beyond which the parametric excitation does not happen.
3. The OP oscillation of the inclined cable by in-plane excitation.
4. The different development of large amplitude OP oscillation due to the parametric excitation, between the horizontal and the inclined cables, highlights the different mechanism of modal coupling.
5. The existence of bifurcation, chaotic motion and quasi-periodic vibration in the parametric excitation of inclined and horizontal cables.

CHAPTER 5
CONCLUDING REMARKS

5.1 Summary of the present study

The first idea of this study was to develop a model of parametric excitation of the stay-cables with the inclusion of the non-linear terms, that were known to be important and yet have been partially or totally neglected during the previous works. Of course, in doing so, the only appropriate method that could accommodate all of the non-linear terms was the numerical approach.

By representing the suspended cables in a non-linear FE model, assembled from a specifically tailored two-node cable elements with 3D orientation and simulated the support excitation to represent the tension fluctuation, the study was pursued. Through the development of the present study, whenever possible, the results were compared with the previous works in the topic of linear, non-linear cable dynamics and parametric excitation of suspended-cables.

As the present study developed further, some new findings were encountered. Some of them were expected and some others were quite unexpected and yet known to be possible to exist from the fundamental theory of parametric excitation and the previous works.

5.2 Conclusions for the present study

From the present study, the conclusions are as follows:

1. The developed numerical method is able to represent the system linearly as well as non-linearly. By linearizing the system, the natural frequencies and corresponding mode shapes of the suspended cables can be obtained.
2. The cable element developed in the present study is applicable to be assembled either to inclined or horizontally suspended cables. Hence, the FE modeling has more adaptability in application to other cable problems.
3. The present study was able to validate the classical theory of parametric excitation for the inclined suspended cables. The present study found that there

is a limit in excitation amplitude that can trigger the parametric excitation. This is due to the interaction between modes and the change in mode shapes due to the change in cable tension during the parametric excitation.

4. The nature of response amplitude to parametric excitation is verified. The amplitude increases exponentially, and then due to the non-linearity nature, the response amplitude reaches its peak and dies down.
5. The difference in the growth of OP response amplitude growth between the horizontal and inclined cables highlights the possibility of different mode coupling phenomena internal and external resonance.
6. The present study found two forms of instability:
   a. The IP parametric excitation has a quasi-periodic motion. This is a 2D instability
   b. The OP parametric excitation takes place as a result of bifurcation and leads to the chaotic vibration. This is a 3D instability.

5.3 Suggestions for further study

The present study is yet far from complete; there are more subjects that should be covered in a more detailed analysis. Some suggestions for further study are presented here:

1. The present study was able to capture the OP oscillation due to parametric excitation of the inclined suspended cable. This finding was quite new and clear explanation of this phenomenon could not be obtained immediately. This calls for a more refined study in the OP parametric excitation.
2. The study on bifurcation and chaotic vibration can be expanded and be analysed in a more detailed form since these phenomena are also quite new in the study of the suspended cable system.
3. It is desirable to further study on parametric excitation of stay-cables, including the field measurement of the global-local structure interaction.

REFERENCES

1. Abdel-Ghaffar, A.M., Khalifa, M.A., (1992), "Importance of cable vibration in dynamics of cable-stayed bridges," *Journal of Engineering Mechanics*, ASCE, 117(11), 2571-2589.
2. Bathe, K.J., (1996), *Finite Element Procedures*, Prentice Hall, USA
3. Benedettini, F., Rega, G., Allagio, R. (1995), "Non-linear oscillations of a four-degree-of-freedom model of a suspended cable under multiple internal resonance conditions," *Journal of Sound and Vibration*, 182(5), 775-798.
4. Bolotin. V.V. (1964), *Dynamic Stability of Elastic Systems*, Holden Days, USA.
5. Caetano, E.S. (2001), "Indirect excitation of stays on cable-stayed bridges," *Proceedings of the 4th International Symposium on Cable Dynamics*, Montréal, Canada, 129-136.
6. Cai, Y., Chen, S.S. (1994), "Dynamics of elastic cable under parametric and external resonances," *Journal of Engineering Mechanics*, 120(8), 1786-1801.
7. Cartmell, M. (1990), *Introduction to Linear, Parametric and Non-linear Vibrations*, Chapman and Hall, UK.
8. Chopra, A.K., (1995), *Dynamics of Structures: Theory and Application to Earthquake Engineering*, Prentice Hall, USA.
9. Clement, H., Cremona, C. (1996), "Étude mathématique du phénomène d'excitation paramétrique appliqué aux haubans de pont," *Laboratoire Central des Ponts et Chausées, Série Ouvrages d'Art OA 18*, Paris, France.
10. Cremona, C. (2003), "Methods for non-linear cable dynamics," *Proceedings of the 5th International Symposium on Cable Dynamics*, Santa Margherita Ligure, Italy, additional paper.
11. Davenport, AG., Steels, GN. (1965), "Dynamic behaviour of massive guy cables," *Journal of the structural division, Proceeding of ASCE, 91*, ST.2, 43-70.
12. Diana, G., Manenti, A., Cheli, F. (1999), "Cable modelling," *Proceedings of the 3rd International Symposium on Cable Dynamics,* Trondheim, Norway, additional paper.
13. Fujino, Y., Kimura, K. (1997), "Cables and cable vibration in cable-supported bridges," *Proceeding of International Seminar on Cable Dynamics*, Tokyo, Japan, 1-11.

14. Fujino, Y., Warnitchai, P., Pacheco, B.M. (1993), "An experimental and analytical study of auto parametric resonance in a 3DOF model of cable-stayed beam," *Nonlinear Dynamics*, 4, 111-138.
15. Gimsing, N.J. (1997), "Cable Supported Bridges," John Wiley and Sons, USA.
16. Hagedorn, P. (1981), *Non-linear Oscillations*, Clarendon Press, UK.
17. Hagedorn, P., Schäfer, B., (1980), "On non-linear free vibrations of an elastic cable," *International Journal of Non-linear Mechanics*, 15, 333-340.
18. Harris, C.M., Piersol, A.G. (2002), *Harris' Shock and Vibration Handbook*, McGraw-Hill, USA.
19. Humar, J.M. (2002), *Dynamics of Structures*, Balkema, Netherland.
20. Irvine, H.M. (1981), *Cable Structures*, The MIT Press, USA.
21. Jean, P.D., Baker, J.R., Smith, S.W., Li, J. (2003), "Phased development of non-linear finite element simulations of deck-excited response of sagged bridge stay-cables, *Proceedings of the 5th International Symposium on Cable Dynamics*, Santa Margherita Ligure, Italy, 173-180.
22. Kovács, I., Leonhardt, A. (1982), "Zur frage der Seilschwingungen und der Seildämpfung, *Die Bautechnik*, 10, 325-332.
23. Lee, C.L., Perkins, N.C. (1992), "Non-linear oscillations of suspended cables containing a two-to-one resonance," *Non-linear dynamics*, 3, 465-490.
24. Lilien, J.L., Pinto da Costa, A. (1994), "Vibration amplitudes caused by parametric excitation of cable stayed structures," *Journal of Sound and Vibration*, 174(1), 69-90.
25. Lorenzo, R., Macdonald, J.H.G (2003), "Experimental validation of a simplified cable-stayed bridge model exhibiting auto-parametric resonance," *Proceedings of the 5th International Symposium on Cable Dynamics*, Santa Margherita Ligure, Italy, 157-164.
26. Luongo, A., Rega, G., Vestroni, F. (1984), "Planar non-linear free vibrations of an elastic cables," *Journal of Non-linear Mechanics*, 19(1), 39-52.
27. Luongo, A., Rega, G., Vestroni, F. (1987), "Letters to the editor on Large-amplitude vibrations of cables," *Journal of Sound and Vibration*, 116(3), 573-575.
28. Macdonald, J.H.G (2001), "Susceptibility of inclined bridge cables to large amplitude vibrations considering aerodynamic and structural damping," *Proceedings of the 4th International Symposium on Cable Dynamics*, Montréal, Canada, 243-249.

29. McLachlan, N.W. (1951), *Theory and application of Mathieu's functions*, Oxford Clarendon Press, UK.
30. Nafyeh, A.H., Balachandran, B. (1989), "Modal interactions in dynamical and structural systems," *Applied Mechanics Review*, 42(11), Part 2, S175-S201.
31. Nafyeh, A.H., Mook, D.T. (1979), *Non-linear Oscillations*, John Wiley and Sons, USA.
32. Nielsen, S.R.K., Kirkegaard, P.H. (2002), "Super and combinatorial harmonic response of flexible elastic cables with small sag," *Journal of Sound and Vibration*, 251(1), 79-102.
33. Oh, J. (2004), *Dynamics characteristics of inclined cable*, MASc. Thesis, University of Ottawa.
34. Perkins, N.C. (1992), "Modal interactions in the non-linear response of elastic cables under parametric/external excitation," *International Journal of Non-linear Mechanics*, 27(2), 233-250.
35. Pinto da Costa, A., Martins, J., Lilien, J.L. (1994), "Parametric excitation of cables of cable stayed bridges," *Proceedings of the International Conference on Cable Stayed Bridges*, Deauville, France, 475-482.
36. Pinto da Costa, A., Martins, J., Lilien, J.L. (1996), "Oscillations of bridge stay cables induced by periodic motions of deck and/or towers," *Journal of Engineering Mechanics*, 122(7), 613-622.
37. Rao, V.G., Iyengar, R.N. (1991), "Internal resonance and non-linear response a cable under periodic excitation," *Journal of Sound and Vibration*, 149(1), 25-41.
38. Rega, G., Vestroni, F., Benedettini, F. (1984), "Parametric analysis of large amplitude free vibrations of a suspended cable," *Journal of Solids Structures*, 20(2), 95-105.
39. Srinil, N., Rega, G., Chucheepsakul, S. (2003), "Non-linear interactions in 3D free vibrations of horizontal and inclined sagged cables," *Proceedings of the 5th International Symposium on Cable Dynamics*, Santa Margherita Ligure, Italy, 77-84.
40. Sun, B.N., Wang, Z.G., Ko, J.M., Ni, Y.Q. (2003), "Parametrically excited oscillation of stay cable and its control in cable-stayed bridges," *Journal of Zhejiang University Science*, 4(1), 13-20.

41. Takahashi, K., Konishi, Y. (1987a), "Non-linear vibrations of cables in three dimensions, Part I: Non-linear free vibrations," *Journal of Sound and Vibration*, 118(1), 69-84.
42. Takahashi, K., Konishi, Y. (1987b), "Non-linear vibrations of cables in three dimensions, Part II: OP vibrations under IP sinusoidally time-varying load," *Journal of Sound and Vibration*, 118(1), 85-97.
43. Tanaka, H. (2000), *Cable vibrations*, IMAC Project Workplan WP1.
44. Tanaka, H. (2003), "Aerodynamics of cables," *Proceedings of the 5th International Symposium on Cable Dynamics*, Santa Margherita Ligure, Italy, 11-25.
45. Thompson, J.M.T, Stewart, H.B. (1987), *Non-linear Dynamics and Chaos*, John Wiley and Sons, UK.
46. Thomsen, J.J. (2003), *Vibrations and Stability*, Springer-Verlag, Gemany.
47. Uhrig, R. (1993), "On kinetic response of cables of cable-stayed bridges due to combined parametric and forced excitation, *Journal of Sound and Vibration*, 165(1), 185-192.
48. Virlogeux, M. (1998), "Cable vibrations in cable-stayed bridges," *Bridge Aerodynamics*, (ed. Larsen, A.), Balkema, Netherland, 213-233.
49. Xu, Y.L., Zhan, S., Ko, J.M., Yu, Z. (1999), "Experimental study of vibration mitigation of bridge stay cables," *Journal of Structural Engineering*, 125(9), 977-986.
50. Yamaguchi, H. (1997), "Fundamentals of cable dynamics," *Proceeding of International Seminar on Cable Dynamics*, Tokyo, Japan, 81-94.
51. Yamaguchi, H., Fujino, Y. (1998), "Stayed cable dynamics and its vibration control," *Bridge Aerodynamics* (ed. Larsen, A.), Balkema, Netherland, 235-253.
52. Zhang, W., Tang, Y. (2002), "Global dynamics of the cable under combined parametrical and external excitations," *International Journal of Non-Linear Mechanics*, 37, 505-526.

APPENDIX A

Solving the Mathieu's Equation

The standard form of the Mathieu's equation is given by:

$$\ddot{q} + c_1\dot{q} + \omega_1^2(1 - 2a \cdot \cos\Omega t)q = 0 \tag{A.1}$$

Solution for period 2T, with $T=2\pi/\Omega$ can be written in the form:

$$q(t) = \sum_{k=1,3,5}^{\infty}\left(a_k \sin\frac{k\Omega t}{2} + b_k \cos\frac{k\Omega t}{2}\right) \tag{A.2}$$

where a_k and b_k are to be determined by substituting terms of (A.2) to (A.1).

For k=1:

By using the first term of (A.2):

$$q = \sin\frac{\Omega t}{2} \tag{A.3}$$

$$\dot{q} = \frac{\Omega}{2}\cos\frac{\Omega t}{2} \tag{A.4}$$

$$\ddot{q} = -\frac{\Omega^2}{4}\sin\frac{\Omega t}{2} \tag{A.5}$$

By substituting (A.3), (A.4) and (A.5) to (A.1) and dividing each term with ω_1^2, the following equation can be obtained:

$$\frac{-\Omega^2}{4\omega_1^2}\sin\frac{\Omega t}{2} + \frac{\Omega}{2\omega_1^2}c_1 \cdot \cos\frac{\Omega t}{2} + \sin\frac{\Omega t}{2} - 2a \cdot \cos\Omega t \cdot \sin\frac{\Omega t}{2} = 0$$

$$\left(1 + a - \frac{\Omega^2}{4\omega_1^2}\right)\sin\frac{\Omega t}{2} + \frac{\Omega}{2\omega_1^2}c_1 \cdot \cos\frac{\Omega t}{2} - a \cdot \sin\frac{3\Omega t}{2} = 0 \tag{A.6}$$

Similarly, by using the second term of (A.2):

$$q = \cos\frac{\Omega t}{2} \tag{A.7}$$

$$\dot{q} = -\frac{\Omega}{2}\sin\frac{\Omega t}{2} \tag{A.8}$$

$$\ddot{q} = -\frac{\Omega^2}{4}\cos\frac{\Omega t}{2} \tag{A.9}$$

By substituting (A.7), (A.8) and (A.9) to (A.1) and dividing each term with ω_1^2, the following equation can be obtained:

$$\frac{-\Omega^2}{4\omega_1^2}\cos\frac{\Omega t}{2}-\frac{\Omega}{2\omega_1^2}c_1\cdot\sin\frac{\Omega t}{2}+\cos\frac{\Omega t}{2}-2a\cdot\cos\Omega t\cdot\cos\frac{\Omega t}{2}=0$$

$$\left(1-a-\frac{\Omega^2}{4\omega_1^2}\right)\cos\frac{\Omega t}{2}-\frac{\Omega}{2\omega_1^2}c_1\cdot\sin\frac{\Omega t}{2}-a\cdot\cos\frac{3\Omega t}{2} \qquad (A.10)$$

For k=3:

In using 1st term of (A.2):

$$q=\sin\frac{3\Omega t}{2} \qquad (A.11)$$

$$\dot{q}=\frac{3\Omega}{2}\cos\frac{3\Omega t}{2} \qquad (A.12)$$

$$\ddot{q}=\frac{-9\Omega^2}{4}\sin\frac{3\Omega t}{2} \qquad (A.13)$$

By substituting (A.11), (A.12) and (A.13) to (A.1) and dividing each term with ω_1^2, the following equation can be obtained:

$$\frac{-9\Omega^2}{4\omega_1^2}\sin\frac{3\Omega t}{2}+\frac{3\Omega}{2\omega_1^2}\cos\frac{3\Omega t}{2}+\sin\frac{3\Omega t}{2}-2a\cdot\cos\Omega t\cdot\sin\frac{3\Omega t}{2}=0$$

$$-a\cdot\sin\frac{\Omega t}{2}+\left(1-\frac{9\Omega^2}{4\omega_1^2}\right)\sin\frac{3\Omega t}{2}+\frac{3\Omega}{2\omega_1^2}\cos\frac{3\Omega t}{2}-a\cdot\sin\left(\frac{5\Omega t}{2}\right)=0 \qquad (A.14)$$

By continuing the substitution of the following terms and arranging the linear equations in a matrix form, equations (2.9), (2.11) and (2.12) in Chapter 2 can be obtained.

The second instability zone was also obtained using the same method.

APPENDIX B

Alphabetical list of functions developed using Matlab for Non-linear 3D cable analysis

- CABDATA : Provide cable data, contain cable's basic data (E, A, Lc, R0, mass, θ, nel), initial horizontal tension of cable, coordinates of cable and element's angle of inclination in static geometric configuration.
- DAMCAB : Form Rayleigh damping matrix for a certain set of modes and damping value from given mass matrix, stiffness matrix at initial static configuration.
- DCEXC : Calculate changes in geometric configuration of cable due to excitation at deck.
- DIFSAG : If a different sag analysis of a cable is of interest, this function should be applied in combination with CABDATA.
- DISINIT : Apply initial displacement to the cable system, if an amplitude at a certain point is given.
- FINDSAG : Calculates variation of sag due to change in ratio L to lh produced by DCEXC or PYEXC and due to change in horizontal tension produced by RLLALP.
- FNAFREQ : Calculates a set of first natural frequencies and mode shapes.
- FUNGAMEL : Calculates element's angle of inclination.
- GEOPOST : Calculates cable's coordinates, specifically for one set of data.
- HETALP : Calculates horizontal tension of a cable if sag-to-span ratio (R) is known.
- HORIEXC : Calculate changes in geometric configuration of horizontal cable due to support excitation.
- HORITEN : Calculates cable element's tension and orientation angle for each time step for horizontal cable, works in conjunction with HORIEXC, RLLALP, FINDSAG and XYCOR.
- KNOWTEN : Calculates the approximate value of R for a given H.
- LOC3D : Form local tangent stiffness of cable element.

- NEWCT : Post process function that produces displacements, velocities and accelerations from support's excitation for the inclined cable.
- NEWCTHR : Post process function that produces displacements, velocities and accelerations from support's excitation for the horizontal cables.
- NEWMASS : Assembles mass matrix of cable system.
- NEWMODNR : Applies Newton-Raphson Iteration Procedure to minimize error during numerical calculation using NWMRCGM.
- NEWTANG : Assembles tangent stiffness of cable system in global 3D orientation, works with TRR3D and LOC3D
- NWMRCGM : Applies Newmark Non-linear Numerical method to calculate displacements, velocities and accelerations.
- PLOPOCARE : Plots Poincaré sections of quarter-span and mid-span points.
- PLOTHIS : Plots time history record of displacements of a point.
- PLOTNODE : Plots result of time history analysis of QS points and MS point as OP oscillations.
- PLUSMIN : Calculates resultant of displacement and velocity
- PPLANE : Plots time history analysis of a point as phase-plane diagram.
- PYEXC : Calculates changes in geometric configuration of cable due to excitation at pylon.
- RLLALP : Finds value of α and calculates H for each time step, works in conjunction with DCEXC or PYEXC.
- TRR3D : Forms 3D transformation matrix from local to global orientation
- UPLOW : Finds minimum and maximum displacements of a point.
- VARYTENA : Calculates cable element's tension and orientation angle for each time step, works in conjunction with DCEXC or PYEXC, RLLALP, FINDSAG and XYCOR.
- WRAPALL : Post function which produces essential data to perform complete analysis.
- XYCOR : Calculates cable's coordinates for each time step, works in conjunction with DCEXC and PYEXC.

APPENDIX C

Listing of functions developed using Matlab

```
% BASICDT Basic data needed for cable analysis
% ============================================
% [E,A,R,nel,ggm,Lc,mass]=feval(@basicdt);
% ============================================
% E = modulus of elasticity (Pa)
% A = cable cross section area (m2)
% R = sag to span ratio
% nel = number of elements
% ggm = inclination angle of cable system (rad)
% Lc = cable length (m)
% mass = mass/unit length (kg/m)

function [E,A,R,nel,ggm,Lc,mass]=basicdt;
E=190e9;

A=153e-4;

R=8.96917e-3;

nel=12;

gdeg=17.5;

ggm=gdeg/360*2*pi;

Lc=440;

mass=133;
```

```
% CABDATA data of cable
% There are two forms:
% ====================================================
% 1. [E,A,R,nel,ggm,Lc,mass]=feval(@cabdata);
% 2. [E,A,R,mass,nel,Lc,H0,Ten,Xc,Yc,GM]=feval(@cabdata);
% ====================================================
% E = modulus of elasticity (N/m2)
% A = cable cross section area (m2)
% R = sag to span ratio
% mass = mass per unit length (kg/m)
% nel = number of elements
% ggm = inclination angle of cable system (rad)
```

```
% Lc = length of cable (m)
% H0 = horizontal cable tension (N)
% Xc and Yc = cable plane geometric coordinates (m)
% GM = angle of inclinations of cable elements (rad)
% nvl = variation of data in interest
% nvl could be nel, R, E etc.

function [op1,op2,op3,op4,op5,op6,op7,op8,op9,op10,op11]=cabdata,

[E,A,R,nel,ggm,Lc,mass]=feval(@basicdt);

if nargout==7,
   op1=E;   op2=A;   op3=R;
   op4=nel; op5=ggm; op6=Lc;
   op7=mass;
elseif nargout==11,

   [H0,Xc,Yc]=feval(@geopost,nel,R,ggm,Lc,mass);

   GM=feval(@fungamel,Xc,Yc);

   Ten=H0*sec(GM);

   op1=E;   op2=A;   op3=R;
   op4=mass; op5=nel; op6=Lc;
   op7=H0;  op8=Ten; op9=Xc;
   op10=Yc; op11=GM;
end
```

```
% DAMCAB Find damping matrix of cable system
% ==========================================
% C=feval(@damcab,nmod,tsi)
% ==========================================
% C = damping matrix (N.s/m)
% nmod = first n modes taken in the analysis
% tsi = damping ratio of cable (%)

function [wn,C]=damcab(nmod,tsi,M,K0)
si=tsi/100;
[ems,wn]=feval(@fnafreq,nmod,K0,M);

% w1 = first frequency for Rayleigh damping
% w2 = second frequency for Rayleigh damping
w1=wn(1);
w2=wn(nmod);

% a1 and a0 = factors to determine Rayleigh damping
a0=si*2*w1*w2/(w1+w2);
a1=2*si/(w1+w2);
```

```
C=a0*M+a1*K0;

---------------------------------------------------------------------------------------------------

% DCEXC Change of cable tension if deck is moving periodically
% ========================================================
% [Llh,Teta,Lc,wgt]=feval(@dcexc,am,Omg,dt,Ts);
% ========================================================
% Llh = ratio L to lh to find H
% Teta = inclination angle of cable (rad)
% Lc = length of cable (m)
% wgt = weight of cable per unit length (N/m)
% am = amplitude pylon's excitation (m)
% Omg = frequency of pylon's excitation (rad/s)
% dt = time step (s)
% Ts = duration of excitation (s)

function [Llh,Teta,Lc,wgt]=dcexc(am,Omg,dt,Ts);

% Initial data
[E,A,R0,nel,gm0,Lc,mass]=feval(@cabdata);
wgt=mass*9.81;
[alp,lh0,H0]=feval(@hetalp,R0,gm0,Lc,wgt);
lv0=lh0*tan(gm0);

% Function of excitation
% dt = time step (s)
% lts = time (s)
lts=0:dt:Ts;

% amt = excitation amplitude of deck (m)
amt=-am*(cos(Omg*lts)-1);

% dxc = inclination angle of deck (rad)
% will change inclination angle of cable
dxc=2*asin(0.5*amt/lh0);
% lvt = vertical length of cable (m)
% dlh = change in horizontal length of cable (m)
% lht = horizontal length of cable (m)
lht=lh0*cos(dxc);
dlv=lh0*sin(dxc);
lvt=lv0-dlv;
Teta=atan(lvt./lht);
Llh=Lc./lht;

---------------------------------------------------------------------------------------------------

% DIFSAG Analyse effect of sag for a stay cable
% ============================================
% [RM,MH0,WN,mxr]=feval(@difsag,RM,nmod);
```

```
% ============================================
% RM = Range of R (sag to span ratio)
% MH0 = Initial horizontal tensions (N)
% WN = Four lowest natural frequencies (rad/s)
% mxr = maximum of wn2/wn1
% nmod = number of modes

function [RM,MH0,WN,mxr]=difsag(RM,nmod);

lrm=length(RM);
MH0=zeros(1,lrm);
WN=zeros(nmod,lrm);
[E,A,R,nel,ggm,Lc,mass]=feval(@cabdata);
M=feval(@newmass,mass,nel,Lc);
u0=zeros(3*(nel-1),1);
Dvi=zeros(nel,1);
for zx=1:lrm,
   R=RM(zx);
   [H0,Xc,Yc]=feval(@geopost,nel,R,ggm,Lc,mass);
   GM=feval(@fungamel,Xc,Yc);
   Ten=H0*sec(GM);
   [K0,F0]=feval(@newtang,E,A,Lc,Ten,GM,Dvi,u0);
   [ems,wn]=feval(@fnafreq,nmod,K0,M);
   ems=1e3.*ems;
   feval(@plotems,ems,R,nel);
   MH0(1,zx)=H0;
   WN(:,zx)=wn;
end
rwn=(WN(2,:)./WN(1,:))';
TR=[RM' rwn];
[vwn lwn]=max(rwn);
mxr=TR(lwn,:);
figure; plot(RM,WN);

% sub-function to plot 1st four mode shapes
function plotems(ems,R,nel),
ms1=1; ms2=2; ms3=3; ms4=4;
ns1=num2str(ms1); ns2=num2str(ms2);
ns3=num2str(ms3); ns4=num2str(ms4);
nmr=num2str(R);
nex=nel+1;
tmr=['R=' nmr];
figure('Name',tmr);
for xy=1:4,
   nxy=num2str(xy);
   tms=zeros(nex,1);
   tms(2:nel,1)=ems(3:3:end,xy)+ems(1:3:end,xy)-ems(2:3:end,xy);
   subplot(2,2,xy); plot(tms);
   axis tight; title(['R=' nmr '-'   'mode' '(' nxy ')']);
end
```

```
% DISINIT Initial displacement of cable
% ====================================
% U0=feval(@disinit,nel,amf,nof,dax)
% ====================================
% U0 = initial displacements (m)
% nel = number of elements
% amf = given amplitude at node nof (m)
% nof = number of node where amf is applied
% dax = axis where displacement is applied
% dax = 1 for x, 2 for y, 3 for z

function U0=disinit(nel,amf,nof,dax);
nstep=nel-1;
node=nel+1;
nlim=nof-1;
U=zeros(nstep,1);
U0=zeros(3*nstep,1);
for qq=1:nlim,
   U(qq,1)=qq/nlim*amf;
end
for qz=nof:nstep,
   U(qz,1)=(node-qz-1)/(nel-nlim)*amf;
end
if dax==1,
   for xz=1:nstep,
      U0(3*xz-2,1)=U(xz,1);
   end
elseif dax==2,
   for xy=1:nstep,
      U0(3*xy-1,1)=U(xy,1);
   end
else
   for xq=1:nstep,
      U0(3*xq,1)=U(xq,1);
   end
end
```

```
% FINDSAG Value of sag for static configuration
% ============================================
% sag=feval(@findsag,lhr,alp,teta)
% ============================================
% sag = lowest point from chord line (m)
% lhr = horizontal projection of cable (m)
% alp = value found to get H
% teta = inclination angle of cable

function sag=findsag(lhr,alp,teta),
```

```
C1=asinh(alp*tan(teta)/sinh(alp))-alp;
sag=0.5*lhr/alp*((asinh(tan(teta))-C1)*tan(teta)-sec(teta)+cosh(C1));
```

```
% FNAFREQ Frequencies and mode shapes
% ====================================
% [ems,wn]=feval(@fnafreq,nmod,K0,M)
% ====================================
% ems = first n mode shapes
% wn = first n natural frequencies (rad/s)
% nmod = number of modes
% K0 = static equilibrium stiffness matrix (N/m)
% M = mass matrix (kg)

function [ems,wn]=fnafreq(nmod,K0,M);

% ef = complete set of mode shapes
% wf = full matrix of complete eigen values
[Ems,wf]=eigs(K0,M,nmod,'sm');

[wn,lwn]=sort(diag(sqrt(wf)));

for xz=1:nmod,
   ln=lwn(xz);
   ems(:,xz)=Ems(:,ln);
end
```

```
% FUNGAMEL Inclination angle of cable element
% ============================================
% GM=feval(@fungamel,Xc,Yc)
% ============================================
% GM = inclination angles of cable elements (rad)
% Xc = cable plane x axis coordinates (m)
% Yc = cable plane y axis coordinates (m)

function GM=fungamel(Xc,Yc),
[nrw,ncl]=size(Xc);
nel=nrw-1;
GM=zeros(nel,ncl);
for qz=1:nel,
   dx=Xc(qz+1,:)-Xc(qz,:);
   dy=Yc(qz+1,:)-Yc(qz,:);
   GM(qz,:)=atan(dy./dx);
end
```

```
% GEOPOST Geometric configuration of cable
```

```
% Combined with function HETALP will obtain:
% ==========================================
% [H0,Xc,Yc]=feval(@geopost,nel,R,teta,L,mass)
% ==========================================
% H0 = horizontal cable tension (N)
% Xc = cable plane x coordinates (m)
% Yc = cable plane y coordinates (m)
% nel = number of cable elements
% R = sag to span ratio (dimensionless)
% teta = inaclination angle of cable (rad)
% L = cable length (m)
% mass = cable mass per unit length (kg/m)


function [H0,Xc,Yc]=geopost(nel,R,teta,L,mass),
% grav = gravity (m/s^2)
grav=9.81;

% nnode = number of nodes
nnode=nel+1;

% wgt = weight per unit length
wgt=mass*grav;

Lel=L/nel;
[alp,lh,H0]=feval(@hetalp,R,teta,L,wgt);
Xc=zeros(nnode,1);
Yc=Xc;
C1=asinh(alp*tan(teta)/sinh(alp))-alp;
for zz=2:nnode,
   Xc(zz,1)=H0/wgt*(asinh(wgt*Lel/H0+sinh(wgt*Xc(zz-1,1)/H0+C1))-C1);
   Yc(zz,1)=H0/wgt*(cosh(wgt*Xc(zz,1)/H0+C1)-cosh(C1));
end

-----------------------------------------------------------------------------------------------------

% HETALP find value of H, lh, and alp
% ===================================
% [alp,lh,H]=feval(@hetalp,R,teta,L,wgt)
% ===================================
% alp = value needed to obtain H (dimensionless)
% lh = horizontal projection of cable chord (m)
% H = cable horizontal tension (N)
% H and alpha are also needed to calculate
% cable geometric coordinates
% R = sag to span ratio (dimensionless)
% teta = inclination angle of cable (rad)
% L = cable length (m)
% wgt = cable weight per unit length (N/m)

function [alp,lh,H]=hetalp(R,teta,L,wgt),
```

```
% al = starting guess to find value of alp
% options = setting for fzero function
% it is important to set options = optimset
% when there are other arguments passed through the function
% else than the value wanted to be obtained
al=0.01; options=optimset;
alp=fzero(@funalp,al,options,R,teta);
lh=sqrt(L^2*alp^2/((sinh(alp))^2+alp^2*(tan(teta))^2));
H=wgt*lh/(2*alp);

% ----------Subfunction "FUNALP"
% Function of alpha, R and teta
function falp=funalp(al,R,teta),
C1=asinh(al*tan(teta)/sinh(al))-al;
falp=-R+1/(2*al)*((asinh(tan(teta))-C1)*tan(teta)-sec(teta)+cosh(C1));
```

```
% LOC3D Local stiffness of 3D cable element
% Allowing cable movement in 3D
% ============================================
% [Kc,Fc,tt1,tt2]=feval(@loc3d,E,A,Ten,Lel,ulc)
% ============================================
% Kc = local element stiffness (N/m)
% Fc = local nodal forces (N)
% tt1 and tt2 = incremental inclination angle (rad)
% E = modulus of elasticity (N/m2)
% A = cable cross section (m2)
% Ten = cable tension (N)
% Lel = cable element length (m)
% ulc = local nodal displacements (m)

function [Kc,Fc,tt1,tt2]=loc3d(E,A,Ten,Lel,ulc),

% Cable coordinate at local axes
% x0 = cable local coordinates at static equilibrium
x0=[0 0 0 Lel 0 0]';

% xt = cable coordinates at time t
xt=x0+ulc;

% Lnew = new length (m)
% dx1, dx2, dx3 = delta for each axes 1,2,3
dx1=xt(4,1)-xt(1,1);
dx2=xt(5,1)-xt(2,1);
dx3=xt(6,1)-xt(3,1);
dx12=sqrt(dx2^2+dx1^2);
Lnew=sqrt(dx1^2+dx2^2+dx3^2);
% tt1 and tt2 are orientation angle at time t
tt1=atan(dx2/dx1);
tt2=atan(dx3/dx12);
```

```
% Assemble stiffness of a cable element

% Kl = linear part of the local stiffness
% k1,...,k6 = elements of Kl
fl=E*A*Lnew^2/Lel^3;
k1=(cos(tt1))^2*(cos(tt2))^2;
k2=sin(tt1)*cos(tt1)*(cos(tt2))^2;
k3=cos(tt1)*sin(tt2)*cos(tt2);
k4=(sin(tt1))^2*(cos(tt2))^2;
k5=sin(tt1)*sin(tt2)*cos(tt2);
k6=(sin(tt2))^2;
Kl=fl*[k1 k2 k3 -k1 -k2 -k3
   k2 k4 k5 -k2 -k4 -k5
   k3 k5 k6 -k3 -k5 -k6
   -k1 -k2 -k3 k1 k2 k3
   -k2 -k4 -k5 k2 k4 k5
   -k3 -k5 -k6 k3 k5 k6];

% Knl = nonlinear part of the local stiffness
fnl=Ten/Lnew;
Knl=fnl*[1 0 0 -1 0 0
   0 1 0 0 -1 0
   0 0 1 0 0 -1
   -1 0 0 1 0 0
   0 -1 0 0 1 0
   0 0 -1 0 0 1];
Kc=Kl+Knl;

Fc=Ten*[-cos(tt1)*cos(tt2)
   -sin(tt1)*cos(tt2)
   -sin(tt2)
   cos(tt1)*cos(tt2)
   sin(tt1)*cos(tt2)
   sin(tt2)];
```

```
% NEWMASS Mass matrix for cable system
% in global 3D axes
% ======================================
% M=feval(@newmass,mass,nel,Lc)
% ======================================
% M = mass matrix (kg)
% mass = unit mass per length (kg/m)
% nel = number of elements
% Lc = length of cable (m)

function M=newmass(mass,nel,Lc);
% nnode = number of nodes
% mc = element local mass matrix
```

```
% mbc = global mass matrix before BC
Lel=Lc/nel;
nnode=nel+1;
mc=mass*Lel/2*eye(6);
mbc=zeros(3*nnode);
for zq=1:nel,
   for xu=1:6,
      for xv=1:6,
         gnr=(zq-1)*3+xu;
         gnc=(zq-1)*3+xv;
         mbc(gnr,gnc)=mbc(gnr,gnc)+mc(xu,xv);
      end
   end
end
% M = mass matrix after BC
% BC are at node 1 and node end
M=mbc(4:3*nel,4:3*nel);
M=sparse(M);
```

```
% NEWMODNR Modified Newton-Raphson iteration
% To minimize error in non-linear numerical
% analysis using Newmark Method
% ============================================
% du=feval(@newmodnr,ui,fsi,dpci,kci,ki)
% ============================================
% du = increment of displacements (m)
% ui = displacements at step i (m)
% fsi = nodal point forces at step i (N)
% dpci = increment of external force (N)
% kci = total stiffness (N/m)
% ki = tangent stiffness (N/m)

function du=newmodnr(ui,fsi,dpci,kci,ki);

% 1.0 Initialize data
% step identification: 1=j-1, 2=j, 3=j+1
u1=ui;
fs1=fsi;
fs2=fsi;
dr2=dpci;

% 2.0 Calculations for each iteration
% 2.1
du2=inv(kci)*dr2;
dv=du2;
sdu=dv;
perr=inv(dpci'*sdu)*dr2'*du2;
while perr>1e-16,
   % 2.2
```

```
   u2=u1+du2;
   % 2.3
   dfs2=fs2-fs1+(kci-ki)*du2;
   fs3=fs2+ki*du2;
   % 2.4
   dr3=dr2-dfs2;
   du3=inv(kci)*dr3;
   dv=sdu;
   sdu=dv+du3;
   % 3.0 Repetition for the next iteration
   perr=inv(dpci'*sdu)*dr3'*du3;
   u1=u2; du2=du3; dr2=dr3; fs1=fs2; fs2=fs3;
end
du=sdu;
```

```
% NEWTANG Assemble tangent stiffness
% and nodal forces of 3D cable elements
% ================================================
% [KT,FT,DVI,DGM]=feval(@newtang,E,A,Lc,Ten,GM,Dvi,u);
% ================================================
% KT = global 3D stiffness matrix after BC (N/m)
% FT = global 3D nodal forces after BC (N)
% DVI and DGM = incremental inclination angle (rad)
% E = modulus of elasticity (Pa)
% A = area of cable section (m2)
% Lc = cable length (m)
% Ten = cable tension of cable elements at time t (N)
% GM = inclination of cable elements at time t (rad)
% Dvi = increment of out-of-plane inclination angle (rad)
% u = global 3D displacement at time t (m)

function [KT,FT,DVI,DGM]=newtang(E,A,Lc,Ten,GM,Dvi,u);

% nel = number of elements
% Lel = length of cable elements (m)
% nnode = number of nodes
% ngl = number of DOF before BC
nel=length(GM);
Lel=Lc/nel;
nnode=nel+1;
ngl=3*nnode;
U=zeros(ngl,1);
U(4:nel*3)=u;
KG=zeros(ngl);
FG=zeros(ngl,1);
DVI=zeros(nel,1);
DGM=DVI;
for xy=1:nel,
   xa=(xy-1)*3+1;
```

```
   xb=(xy-1)*3+6;
   % U global for each element
   uel=U(xa:xb,1);
   gm=GM(xy);
   dvi=Dvi(xy);
   Tel=Ten(xy);
   % Transformation to local axes
   Tr=feval(@trr3d,gm,dvi);
   % U local for each element
   ulc=Tr*uel;
   [ktlc,ftlc,dvi,dgm]=feval(@loc3d,E,A,Tel,Lel,ulc);
   DVI(xy)=dvi;
   DGM(xy)=dgm;
   % Transformation back to global 3D
   ktgb=Tr'*ktlc*Tr;
   ftgb=Tr'*ftlc;
   FG(xa:xb,1)=FG(xa:xb,1)+ftgb(1:6,1);
   for xu=1:6,
      for xv=1:6,
         gnr=(xy-1)*3+xu;
         gnc=(xy-1)*3+xv;
         % KG and FG without bc
         KG(gnr,gnc)=KG(gnr,gnc)+ktgb(xu,xv);
      end
   end
end
KT=KG(4:nel*3,4:nel*3);
KT=sparse(KT);
FT=FG(4:nel*3,1);
```

```
% NWMRCGM apply Newmark numerical method
% to non-linear system using implicit integration
% also known as Constant Average Acceleration Method
% ====================================================
% [U,UD1,UD2]=feval(@nwmrcgm,M,C,K0,Lc,u0,ud10,Ptt,Tten,TGM,dt,Ts)
% ====================================================
% U = displacements of nodes (m)
% UD1 = velocity of nodes (m/s)
% UD2 = acceleration of nodes (m/s2)
% M = mass matrix (kg)
% C = damping matrix (N.s/m)
% K0 = stiffness matrix at static equilibrium (N/m)
% u0 = initial displacements (m)
% ud10 = initial velocity (m/s)
% Ptt = function of external force (N)
% Tten = function of tension change (N)
% TGM = set of inclination angle of elements (rad)
% dt = time step (s)
% Ts = time span (s)
```

```
function [U,UD1,UD2]=nwmrcgm(M,C,K0,E,A,Lc,u0,ud10,Ptt,Tten,TGM,dt,Ts);
% nel = number of elements
% orientation of node is internal nodes
% imid = mid-span node where displacement is recorded
% orientation of numbering is internal node after BC
% dfa & dfb number of dof at node imid at global 3D
lk=length(K0);
lu0=length(u0);
[nrg,ncg]=size(TGM);
nel=nrg;
imid=nel/2;
dfa=(imid-1)*3+1;
dfb=(imid-1)*3+3;

% 1.0 Initial Calculations
% 1.1 Solve for ud20 (initial acceleration)
ud20=inv(M)*(Ptt(:,1)-C*ud10-K0*u0);

% 1.2 Select dt
% dt is chosen based on degree of non-linearity
% value of dt can be assessed by trial and error

% 1.3 Calculate aa and bb
aa=4/dt*M+2*C;
bb=2*M;

% 2.0 Calculations for each time step ii
% reminder:
% at t=0 second, ii=1
% du(ii)=u(ii+1)-u(ii)
% Input for point 2 is Kii,uii,ud1ii and ud2ii
Tts=0:dt:Ts;
[nts,lts]=size(Tts);
[ntp,ltp]=size(Ptt);
[ntn,ltn]=size(Tten);
[nrg,lcg]=size(TGM);

% U=zeros(3,lts+1);
U=zeros(lu0,lts+1);
UD1=U; UD2=U;

if ltp<=lts,
   Ptt(:,ltp+1:lts+1)=0;
end
if ltn<=lts,
   for xu=ltn+1:lts,
      Tten(:,xu)=Tten(:,1);
   end
end
if lcg<=lts,
```

```
   for xt=ltn+1:lts,
      TGM(:,xt)=TGM(:,1);
   end
end

u=u0;
% U(:,1)=u0(dfa:dfb,1);
U(:,1)=u0;
ud1=ud10;
% UD1(:,1)=ud10(dfa:dfb,1);
UD1(:,1)=ud10;
ud2=ud20;
% UD2(:,1)=ud20(dfa:dfb,1);
UD2(:,1)=ud20;

% Incremental angle at t=0;
Dgm=zeros(nel,1);
Dvi=Dgm;

for ij=1:lts,
   % 2.1 Effect of forces
   dpt=Ptt(:,ij+1)-Ptt(:,ij);
   Ten=Tten(:,ij);
   dpc=dpt+aa*ud1+bb*ud2;

   % 2.2 Determine the tangent stiffness matrix
   %     and nodal point forces
   GM=TGM(:,ij)+Dgm;

   [Kt,Fs,DVI,DGM]=feval(@newtang,E,A,Lc,Ten,GM,Dvi,u);

   % DVI and DGM will be used for next time step
   Dvi=DVI;
   Dgm=DGM;

   % 2.3 Total stiffness
   Kc=Kt+2/dt*C+4/(dt^2)*M;

   % 2.4 du = increment of displacement
   % Solve du using modified Newton-Raphson iteration
   du=feval(@newmodnr,u,Fs,dpc,Kc,Kt);

   % 2.5 dud1 = increment of velocity
   dud1=2/dt*du-2*ud1;

   % 2.6 dud2 = increment of acceleration
   dud2=4/(dt^2)*du-4/dt*ud1-2*ud2;

   % 2.7 uu, uud1, uud2
   uu=u+du; uud1=ud1+dud1; uud2=ud2+dud2;
   ik=ij+1;
```

```
   % U(:,ik)=uu(dfa:dfb,1); UD1(:,ik)=uud1(dfa:dfb,1); UD2(:,ik)=uud2(dfa:dfb,1);
   U(:,ik)=uu; UD1(:,ik)=uud1; UD2(:,ik)=uud2;
   u=uu; ud1=uud1; ud2=uud2;
end
```

```
% PYEXC Change of cable tension if pylon is moving periodically
% ================================================
% [Llh,Teta,Lc,wgt]=feval(@pyexc,am,Omg,dt,Ts)
% ================================================
% Llh = ratio L to lh to find H
% Teta = inclination angle of cable (rad)
% Lc = length of cable (m)
% wgt = weight of cable per unit length (N/m)
% am = amplitude pylon's excitation (m)
% Omg = frequency of pylon's excitation (rad/s)
% dt = time step (s)
% Ts = duration of excitation (s)

function [Llh,Teta,Lc,wgt]=pyexc(am,Omg,dt,Ts);

% Initial data
[E,A,R0,nel,gm0,Lc,mass]=feval(@cabdata);
wgt=mass*9.81;
[alp,lh0,H0]=feval(@hetalp,R0,gm0,Lc,wgt);
lv0=lh0*tan(gm0);

% Function of excitation
% dt = time step (s)
% lts = time (s)
lts=0:dt:Ts;

% amt = excitation amplitude of pylon (m)
amt=-am*(cos(Omg*lts)-1);

% dxc = inclination angle of pylon (rad)
% will change inclination angle of cable
dxc=2*asin(0.5*amt/lv0);
% lvt = vertical length of cable (m)
% dlh = change in horizontal length of cable (m)
% lht = horizontal length of cable (m)
lvt=lv0*cos(dxc);
dlh=lv0*sin(dxc);
lht=lh0-dlh;
Teta=atan(lvt./lht);
Llh=Lc./lht;
```

```
% RLLALP Find alpha and H if ratio of cable length
```

```
% to horizontal projection (Lc/lh) and inclination
% angle of cable are known
% ================================================
% [alp,H]=feval(@rllalp,RL,teta,Lc,wgt)
% ================================================
% alp = unknown factor to find H
% H = horizontal cable tension (N)
% RL = ratio of Lc to lh
% teta = inclination angle of cable (rad)
% Lc = length of cable (m)
% wgt = weight of cable per unit length (N/m)

function [alp,H]=rllalp(RL,teta,Lc,wgt);
% al = starting guess to find value of alp
% options = setting for fzero function
% it is important to set options=optimset
al=0.01;
options=optimset;
lh=Lc/RL;
alp=abs(fzero(@funalpha,al,options,RL,teta));
H=wgt*lh/(2*alp);



% ----------subfunction "FUNALPHA"
% Function of alpha,RL and teta
function flp=funalpha(al,RL,teta)
flp=-RL^2+(sinh(al)/al)^2+(tan(teta))^2;

-----------------------------------------------------------------------------------------------------------

% TRR3D Transformation from 3D local to 3D global
% ================================================
% Tr=feval(@trr3d,gm,dvi)
% ================================================
% Tr = transformation matrix of a cable element
% gm = inclination of cable at cable plane (rad)
% dvi = increment of out-of-plane angle (rad)

function Tr=trr3d(gm,dvi);
% vi = angle between axis x and cable plane
% vi is taken as 0.25*pi

vi0=0.25*pi;
vi=vi0+dvi;
ta=cos(vi)*cos(gm);
tb=sin(vi)*cos(gm);
tc=sin(gm);
td=-sin(vi);
te=cos(vi);
tf=0;
```

```
tg=-cos(vi)*sin(gm);
th=-sin(vi)*sin(gm);
ti=cos(gm);
Tr=[ta tb tc 0 0 0
   td te tf 0 0 0
   tg th ti 0 0 0
   0 0 0 ta tb tc
   0 0 0 td te tf
   0 0 0 tg th ti];
```

```
% VARYTENA Change of tension of cable
% when pylon or deck is having periodic excitation
% ================================================
% 1. [GM,Tel]=feval(@varytena,am,Omg,dt,Ts,nel,opt)
% 2. [GM,Tel,MH]=feval(@varytena,am,Omg,dt,Ts,nel,opt)
% 3. [GM,Tel,MH,Sag]=feval(@varytena,am,Omg,dt,Ts,nel,opt)
% 4. [GM,Tel,MH,Sag,Llh]=feval(@varytena,am,Omg,dt,Ts,nel,opt)
% 5. [GM,Tel,MH,Sag,Llh,Teta]=feval(@varytena,am,Omg,dt,Ts,nel,opt)
% ================================================
% GM = inclination of cable's elements (rad)
% Tel = tension for each element (N)
% MH = horizontal tension (N)
% Sag = sag of cable (m)
% Llh = ratio L to lh
% Teta = inclination angle of cable (rad)
% am = amplitude of pylon's movement (m)
% Omg = frequency of the movement (rad/s)
% dt = time step (s)
% Ts = duration of movement (s)
% nel = number of elements
% opt = options of movement's source:
% opt = 1 for movement of pylon
% opt = 2 for movement of deck

function [p1,p2,p3,p4,p5,p6]=varytena(am,Omg,dt,Ts,nel,opt),

% [Llh,Teta,MH,GM,Tel]=varytena(am,Omg,Ts,nel,opt)
if opt==1,
   [Llh,Teta,Lc,wgt]=feval(@pyexc,am,Omg,dt,Ts);
elseif opt==2,
   [Llh,Teta,Lc,wgt]=feval(@dcexc,am,Omg,dt,Ts);
end

clh=length(Llh);
MH=zeros(1,clh);
Alp=MH; Sag=MH;
Tel=zeros(nel,clh);
for xz=1:clh,
   RL=Llh(xz);
```

```
   lhr=Lc/RL;
   teta=Teta(xz);
   [alp,H]=feval(@rllalp,RL,teta,Lc,wgt);
   sag=feval(@findsag,lhr,alp,teta);
   MH(1,xz)=H;
   Alp(1,xz)=alp;
   Sag(1,xz)=sag;
end
[Xc,Yc]=feval(@xycor,nel,Alp,MH,Teta,wgt,Lc);
GM=feval(@fungamel,Xc,Yc);

for yx=1:clh,
   tel=MH(yx)*sec(GM(:,yx));
   Tel(:,yx)=tel;
end

if nargout==2,
   p1=GM; p2=Tel;
elseif nargout==3,
   p1=GM; p2=Tel; p3=MH;
elseif nargout==4,
   p1=GM; p2=Tel; p3=MH;
   p4=Sag;
elseif nargout==5,
   p1=GM; p2=Tel; p3=MH;
   p4=Sag; p5=Llh;
elseif nargout==6,
   p1=GM; p2=Tel; p3=MH;
   p4=Sag; p5=Llh; p6=Teta;
end
```

```
% XYCOR Cable plane's coordinates of cable elements
% ================================================
% [Xc,Yc]=feval(@xycor,nel,alp,H,teta,wgt,Lc)
% ================================================
% Xc and Yc = cable plane's coordinates (m)
% nel = number of elements
% alp = alpha to find H
% H = Horizontal tension of cable (N)
% teta = iclination angle of cable (rad)
% wgt = weight of cable per unit length (N/m)
% Lc = length of cable (m)

function [Xc,Yc]=xycor(nel,alp,MH,Teta,wgt,Lc)
% Lel = length of element (m)
% nnode = number of total nodes
% lts = number of time steps
lts=length(Teta);
Lel=Lc/nel;
```

```
nnode=nel+1;
Xc=zeros(nnode,lts);
Yc=Xc;
C1=asinh(alp.*tan(Teta)./sinh(alp))-alp;
for zz=2:nnode,
   Xc(zz,:)=MH./wgt.*(asinh(wgt*Lel./MH+sinh(wgt*Xc(zz-1,:)./MH+C1))-C1);
   Yc(zz,:)=MH./wgt.*(cosh(wgt*Xc(zz,:)./MH+C1)-cosh(C1));
end
```